Dissertation zur Erlangung des Doktorgrades der

Fakultät für Chemie und Pharmazie

der Ludwig-Maximilians-Universität München

Combinatorial optimization of nucleic acid carriers for folate-targeted delivery

Dongsheng He

aus

Chongqing, China

2016

Erklärung

Diese Dissertation wurde im Sinne von § 7 der Promotionsordnung vom 28. November 2011 von Herrn Prof. Dr. Ernst Wagner betreut.

Eidesstattliche Versicherung

Diese Dissertation wurde eigenständig und ohne unerlaubte Hilfe erarbeitet.

München, 15.04.2016

.....……

Dongsheng He

Dissertation eingereicht am 19.04.2016

1. Gutachter: Prof. Dr. Ernst Wagner

2. Gutachter: Prof. Dr. Wolfgang Frieß

Mündliche Prüfung am 18.05.2016

Dedicated to My Family

In memory of my grandfather

古今之成大事业、大学问者，必经过三种之境界：

“昨夜西风凋碧树，独上高楼，望尽天涯路。”此第一境也。

“衣带渐宽终不悔，为伊消得人憔悴。”此第二境也。

“众里寻他千百度，蓦然回首，那人却在，灯火阑珊处。”此第三境也。

——王国维《人间词话》

Throughout the ages of all those who have been highly successful in great ventures and in the pursuit of learning must of necessity have (successively) experienced three kinds of "ching-chieh".

"Last night the west wind shrivelled the green-clad trees,
Alone I climb the high tower
To gaze my fill along the road to the horizon."
expresses the first state of (ching)

"My clothes grow daily more loose, yet care I not.
For you am I thus wasting away in sorrow and pain."
expresses the second state.

"I sought her in the crowd a hundred, a thousand times.
Suddenly with a turn of the head (I saw her),
That one there where the lamplight was fading."
expresses the third state.

——„Jen-chien Tz'u-hua" by Wang Kuo-wei
translated by Adele Austin Rickett

Table of Contents

1 Introduction

1.1 Nucleic acid therapy：opportunities and challenges

Since the first evidence that genetic information is carried by deoxyribonucleic acid (DNA) was presented in 1944,[1] the description of double helix structure of DNA by Watson and Crick,[2] as well as the illustration of central dogma,[3] the related molecular biology has been intensively investigated, changing and enriching our understanding about basis of life. The completion of Human Genome Project and latter continuous efforts to decrypt human genome provide us enormous information about genes, and also help us to identify disease related genes. [4] Nowadays, many diseases are known to be caused by genetic defects, such as inherited single gene disorders (like Huntington's chorea[5], or cystic fibrosis[6]), or acquired disorders such as in cancer. Gene therapy provides an option for the treatment of these genetic disorders and other severe diseases by genetically modification of the target cells.[7] Although the first documented heritable gene transfer was performed with mammalian cells over 50 years ago,[8] the first officially approved gene transfer into humans was conducted in 1989[9]. Currently, there are over 2000 approved clinical trials worldwide completed or still ongoing.[10] After decades of development, China first approved a gene therapy product Gendicine for the treatment of head- and neck squamous cell carcinoma in 2003,[11] and finally in 2012, Glybera became the first gene therapy product approved by European Medicines Agency.[12]

The initial approach of gene therapy was carried out by substituting defective genes with therapeutic DNA delivered into the nucleus.[7] The first gene therapy human clinical trial approved by the US FDA for the treatment of severe combined immune deficiency (SCID) was proceeded under this strategy.[13] With increasing knowledge of the biological role of RNA, in addition to the application of therapeutic DNA, the delivery of RNA has also been widely involved. In contrast to the delivery of DNA which require intracellular location into nucleus, direct transfer of messenger RNA (mRNA) into cytosol provides another approach to code protein products. Additionally, the option of suppressing pathogenic gene expression have been established. Antisense oligonucleotides, which specific complementary bind to the target mRNA, suppress the translation of target mRNA by either steric-blocking or mRNA degrading. Furthermore, the discovery of RNA interference (RNAi) provide as a novel approach to suppress a specific gene. Based on the classic gene silencing strategy of using single stranded oligonucleotides, double-

stranded RNA (dsRNA) with over 30 base pairs was first discovered to be able to mediate suppression of a specific gene in C. elegans.[14] The latter attempt successfully achieved effective silencing of target genes in mammalian cells via application of the shorter small interfering RNA (siRNA) without immune responses.[15] RNAi based therapy offers as a remarkable approach for sequence-specific suppression of gene expression. Other nucleic acid types, such as micro RNA (miRNA), polyinosinic-polycytidylic acid (poly(I:C)), splice-switching oligonucleotides (SSOs), as well as aptamers have also been extensively investigated as tools for gene therapy.

Despite these dramatic achievements in seeking novel strategies for gene therapy, one inherent week point is the biological instability of naked therapeutic nucleic acid. A variety of chemical nucleic acid modifications focusing on the improvement of stability, therapeutic potency, as well as reduced immunogenicity, have been developed. Commonly chemical modifications include 2'-O-methyl or 2'-fluoro RNA, 2'-O, 4'-C-methylene bridges (locked nucleic acid, LNA), phosphorothioate or phosphorodiamidate morpholino oligomers (PMOs) and peptide nucleic acid (PNA).

Although the variety of different nucleic acid forms provides us a wide range of therapeutic options, the efficient targeted delivery of therapeutic nucleic acids into the affected patient cells remains the main challenge. Therefore, the availability of an efficient and safe delivery vehicle is a crucial factor for success.

1.2 Conquering barriers: non-viral nucleic acid carriers

Despite remarkable progress in gene therapy have been made over the past few decades, the development of appropriate therapeutic nucleic acid delivery systems with high efficiency and biocompatibility remains a challenge to be conquered. Learning from nature, viruses provide us excellent examples for transfer of nucleic acid into targeted cells. Nowadays, the majority of gene therapy studies are using recombinant viral vectors like adeno-associated vectors, retroviral vectors and lentiviral vectors. Originated from natural virus, these viral vectors obtained by replacing most of the virus genome with therapeutic gene exhibit high transfection efficiency. However, some disadvantages of viral carriers such as immunogenicity, limited loading capacity, risk of insertional mutagenesis, and difficulties in optimization of production and upscale have hindered them from being the ideal commonly applicable nucleic acid delivery carrier. A subclass of non-viral carriers, known as synthetic "artificial viruses" provide an option for the development of nucleic

acid delivery systems with high efficiency and low toxicity. Currently, their transfection efficiency is relatively low as compared to the viral vectors. However, non-viral carriers possess the advantages of low immunogenicity, high biocompatibility, possibilities for further optimization with multi-functional groups and good potential for scale-up manufacturing.

Since a successful nucleic acid based therapy requires successful delivery of the therapeutic nucleic acid into the target cell. The nucleic acid delivery systems need to protect the payload from various extracellular and intracellular barriers (**Figure 1. 1**), and reach the final targeting site. Generally, an ideal carrier needs to 1) compact the cargo into nanoparticles with suitable particle size to protect from nucleases and clearance from kidney; 2) bear surface shielding domains to limit the interaction with serum proteins and mediate effective and selective cellular uptake; 3) efficiently escape from intracellular endo-lysosomal pathway; and 4) transfer the cargo to the target intracellular site.

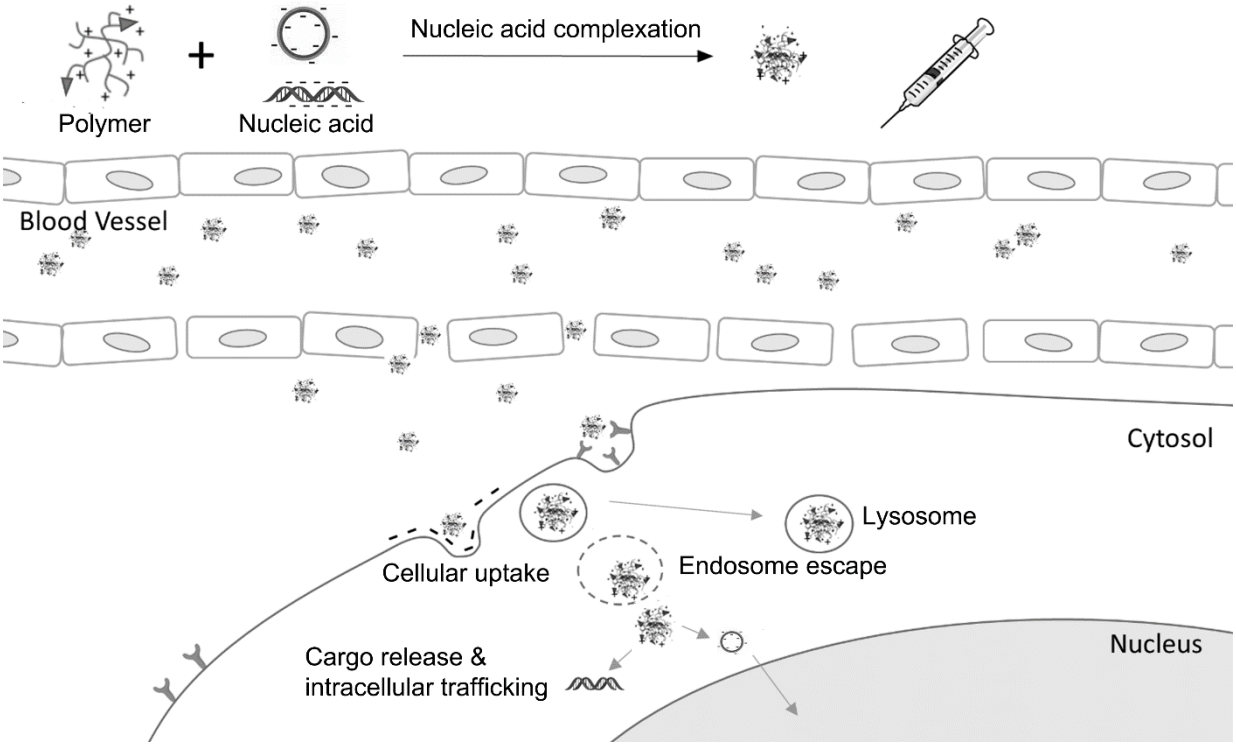

Figure 1.1 Systemic nucleic acid delivery pathway.

1.2.1 Nucleic acid complexation

As nucleic acids are enzymatically degradable in the blood and tissues, carriers need to compact them into stable complexes, to protect them from being degraded by nucleases and cleared from the blood stream. Because of the negatively charged nature of nucleic

acid, most non-viral vectors, like cationic lipid, polyethyleneimine (PEI) and dendrimer, facilitate the complexation with the cargo through electrostatic interaction. The stability of the formed complexes is another critical issue to be mastered. Besides manipulating the charge density of the carrier, enhanced complex stability could be achieved via the introduction of crosslinking domains and hydrophobic domains. For systemic delivery of nucleic acid, the particle size of complexes also plays a crucial role. While particles with smaller size are rapidly cleared form the kidney, complexes with an appropriate size lead to an extended circulation time, which is beneficial for an improved bio distribution and pharmacokinetic profile.

1.2.2 Targeted intracellular accumulation

Many non-viral vectors form nucleic acid complexes with a net positive charge, increase the unspecific interaction with undesired cell membrane and proteins, leading to a reduced delivery of the payload into the targeted cells. The incorporation of shielding domains might solve this problem. Hydrophilic polymers such as polyethylene glycol (PEG), have been used to coat the surface of polyplexes, resulted in reduced unspecific interactions with blood component during circulation. [16, 17] Other polymers, like poly-N-(2-hydroxypropyl)methacrylamide (pHPMA) and hydroxyl ethyl dextran (HES) [18] have also been used for this purpose.

To enable subsequent accumulation of the therapeutic payload at the target tissue, different passive and active targeting attempts have been involved. In the case of tumor directed nucleic acid delivery, accumulation at the target tumor tissue has been obtained based on the enhanced permeability and retention effect (EPR), because of the more leaking vascular endothelium in tumors[19]. Here again the influence of particle size on the delivery pathway is illustrated. To facilitate intracellular entry, polyplexes must initially associate with the cell surface, either through electrostatic interactions, physical concentration via adsorption, or by ligand–receptor mediated pathways. By the use of specific targeting ligands, it is possible to allow binding to specifically expressing or over expressing receptors on the target cell surface.[20] Enhanced specific cellular uptake has been achieved by the use of transferrin, folate, RGD, GE11, cMet and other targeting ligands. The use of active targeting ligand also help to combat with the PEG-dilemma in the case of PEGylated formulations. After successful cellular uptake, the nucleic acid complexes usually reside in internal vesicles (endolysosomes) facing next challenges.

1.2.3 Endosomal escape

The next delivery task is the escape of polyplexes from the degradative endolysosomal pathway, to prevent lysosomal degradation of the payload and deliver it safely to their targeting site into either the nucleus or cytosol. This can be achieved through several strategies. Similar to PEI, several carriers with intrinsic pH-specific buffering capacity could facilitate endosomal escape through the so-called proton sponge effect.[21] Like for several lipid-based systems, this escape from the endo-lysosomal pathway can also be promoted by destabilization of the endosomal membrane. Additionally, chemical motifs such as histidine [22, 23] and imidazole groups [24] which enhance the buffer capacity at the endosomal pH, can be incorporated to achieve successful endosomal escape.

As an alternative to the proton sponge mechanism, endosomal escape was mediated by fusogenic peptides, including amphipathic sequences and/or peptides with high content of basic amino acids[25], such as Tat[26], melittin[27, 28], influenza virus-derived INF peptides[29, 30], KALA[31] and others.[32, 33] This kind of peptides can interact with the endosomal lipid membrane and lead to their disruption.[25] Several fusogenic peptides were used in combination with cationic peptides, polymers, or other gene delivery carriers.

1.2.4 Intracellular trafficking and cargo release

After successfully escape from endosome, further transportation to the final target site of action is dependent on the type of nucleic acid. While siRNA and miRNA only need to locate in the cytosol, pDNA has to be urther transported all the way into the nucleus. This has been demonstrated to preferentially happen during the cell division process when the nuclear envelope dissolves.[34] Attempts have been made through conjugating short nuclear localization signals (NLS) peptide to DNA for a targeted active transport through the nuclear pore complex.[35-37] It has also been suggested that some cationic polymers may have a nuclear-localizing effect because of their positive charge. While the transport of polyplexes into the nucleus is still not clearly understood and requires further optimization at several stages,[38] studies have shown that it seems to be advantageous to use pDNA polyplexes for nuclear transfer.[39, 40]

Another critical issue is the cargo release. As we mentioned in the nucleic acid compaction, the complexes need to be stable enough to help them be able to transport to the action site. However, at the target site, the high stability of the complexes might hinder the release of the cargo, thus lead to reduced transfection efficiency. In this case, the formed

complexes need to find a balance between a sufficient extracellular stability and fast cargo release at the final stage. The bio-inspired redox sensitive strategy which commonly facilitated as the incorporation of bioreducible disulfide linkage presents a successful example.[41] Relatively stable complexes was formed via the formation of disulfide linkage in the extracellular conditions, while in the final cytosol, with the help of approximately 100 to 1000 fold glutathione, the fast reduction also contribute to the fast release of the cargo.[42] This strategy also shows the benefits for the biocompatibility of the delivery system.

1.3 Sequence-defined materials for nucleic acid delivery

Within the class of polymeric delivery systems, polyethylenimine (PEI) has been the most investigated cationic carrier for pDNA delivery, it presents a gold standard for pDNA transfection. PEI has a very high density of amino groups, beneficial for both stable pDNA complex (‘polyplex’) formation, and also possesses buffering capacity to mediate endosome escape of polyplexes into the cytosol.[21, 43] Many efforts have been undertaken to optimize PEI based delivery systems, introducing biodegradable linkages, and/or attaching targeting and shielding functions.[44-46] However, the polydispersity and heterogeneities of such multifunctional structures presents a big problem for further development. Specific modifications in defined numbers at different polymer sites are difficult to achieve. Such a heterogeneous nature of PEI and also other related polymeric materials such as poly(L-lysine) is hardly compatible for reproducible manufacturing of components as needed for clinical studies.

This fundamental drawback has been calling for more defined polymeric materials for gene delivery.[47] A precise chemistry is not only useful for the site-specific modification that is required to develop a defined multi-functional vector, but also important for obtaining the structure-activity relationships needed for further optimization. Thus, several synthetic strategies have been utilized to obtain better defined cationic polymeric materials. These include improved polymerization chemistries such as controlled radical polymerization, providing a narrow polymer size-distribution. Defined block copolymers, optionally also with defined ligation sites, can be obtained.[48-50] Alternatively, step-wise synthesis of precise dendrimers[51] has been utilized to obtain defined cationic polymeric materials. Recently also solid-phase assisted synthesis of peptides and polymers has been introduced.[52] These sequence-defined carriers can be applied for nucleic acid delivery.

1.3.1 Dendrimers

Dendrimers are globular macromolecules with well-defined, highly branched three-dimensional architecture, generated by precise step-wise introduction of branching points onto a core molecule. [53] With monodispersity and high density of multivalent functional surface groups, they exhibit attractive properties as precise nucleic acid delivery platform.[54]

Polyamidoamine (PAMAM) dendrimers (**Figure 1.2A**) [51]have high density of amines which can be partially protonated at physiological pH to complex with nucleic acid, while the large numbers of secondary and tertiary amines at the interior act as “proton sponge” to mediate efficient endosome escape.[55] With pioneering studies proving that PAMAM can mediate high transfection efficiency, [56, 57] considerable optimization in the aspects of biocompatibility, polyplex formation, endosomal escape, and targeted delivery has been made. [57] With reduced surface charge density including partial acetylation or PEGylation,a reduced inherent cytotoxicity was obtained.[58] Via introducing L-lysines and L-arginines as surface modification, improved polyplex formation as well as cellular interaction was demonstrated. [59] Enhanced endosomal escape with the integrate of histidine residues lead to an effective delivery of pDNA.[60] Many other efforts manipulating the dendrimer surface charge and hydrophobicity, including the introduction of hydrophobic phenylalanine,[61] leucine,[61] or alkyl lipid[62] residues all showed encouraging results. Recently, a fluorination approach of PAMAM dendrimers via reacting with perfluoro acid anhydrides formed fluorinated dendrimers with low toxicity and significant improved transfection efficacy in several cell lines at extremely low N/P ratios, which is comparable or superior to commercial agents Lipofectamine 2000 and SuperFect.[63] Another important topic, the targeted delivery of nucleic acid, has also been introduced into PAMAM dendrimers. Targeting moieties such as biotin,[64] transferrin,[65] folic acid,[66] lactose,[67] and peptides[68, 69] were investigated. In several cases successful targeted *in vivo* gene transfer was reported.

Poly(propylenimine) (PPI) dendrimers (**Figure 1.2B**),[53] just like PAMAM, can compact nucleic acid via electrostatic interactions with the positively charged protonated amino groups, while the residual amines provide endosomal buffering.[70] Researchers have utilized amino acids like arginine[71], galactose[72], transferrin[73], oligoethylenimine[74] and other modules to modify PPI dendrimers, resulting in improved transfection efficiency with reduced cytotoxicity, and optionally also receptor targeting. For example, transferrin-

conjugated PPI G3 was used in pDNA polyplexes for systemic delivery in A431 tumor-bearing mice. Gene expression was predominantly observed in the tumor tissue, with long-term therapeutic antitumoral effects was exhibited upon a therapeutic tumor necrosis-α (TNF-α) expressing pDNA treatment.[73]

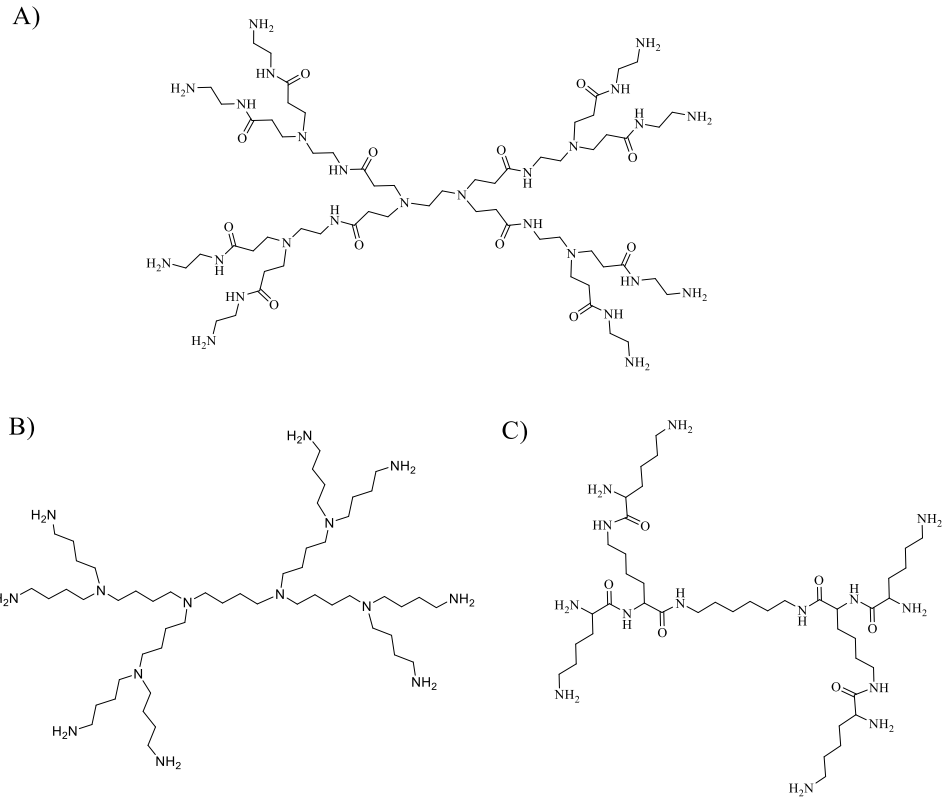

Figure 1.2 Chemical structure of three typical dendrimers. A) PAMAM (G1) dendrimer. B) PPI dendrimer (DAB8). C) Poly(L-lysine) dendrimer (G2).

Poly(L-lysine) dendrimers (DPL, **Figure 1.2C**) [75] also show their potential as effective nucleic acid carriers. Similarly, variations of the terminal residue with arginines demonstrated as an efficient way to enhance gene transfer.[76] With regard to optimize the synthesis of higher generation DPL, Luo *et al*.[77] utilized a click chemistry strategy and obtained arginine grafted dendrimers with higher transfection efficiency than branched PEI (25 kDa). DPLs have also been successfully used for receptor-targeted gene transfer to the brain.[78-80] The peptidic ligands T7 targeting the transferrin receptor,[78] angiopep-2 targeting the LDL receptor-related protein LRP1,[79] or a bacterial protein derived peptide targeting the laminin receptor,[80] have been used as PEG-DPL conjugates for pDNA polyplex formation. Successful *in vivo* gene delivery into brain and brain tumors was reported.

1.3.2 Peptide based carriers

Peptide based nucleic acid carriers have several favorable platform characteristics. They can condense nucleic acid through electrostatic interaction with the help of the natural amino acids lysine, arginine, or ornithine providing positive charges,[81] and also achieve many other transfer functions such as endosomal escape, bioreversible polyplex stabilization, or receptor-targeted delivery. Amongst the key advantages of peptide carriers are the sequence-defined structure and the monodispersity obtained by solid-phase assisted peptide synthesis (SPPS), which are beneficial for establishing precise structure-activity relationship studies.

Oligolysine peptides consisting defined length of lysine provide an alternative to the heterogeneous poly-(L-lysine). The precise structure also makes it possible to perform site-specific modification. Studies have shown that oligolysine containing 13 or more lysine monomers are able to compact pDNA,[82] and a peptide containing 18 lysines is able to from stable polyplexes with pDNA protecting them from degradation.[83] Coupling a trimeric galactoside-containing ligand to an oligolysine of 19 monomers resulted in an asialoglycoprotein receptor targeted carrier which mediated efficient gene transfer in HepG2 cells in the presence of endosomotropic chloroquine.[84][94] A defined Lys_{30} terminally modified with PEG was used in pDNA polyplexes in human clinical studies for expressing the CFTR gene in the airway epithelium of cystic fibrosis patients.[85]

To further improve the stability of DNA complexes, cross-linking strategies have been developed. Cysteine has been introduced into the peptide sequence to form bioreversible disulfide bonds through oxidation.[86] McKenzie *et al*. investigated modifications of Trp-Lys_{20} peptide by substitution one to four of the lysines with cysteines. The peptide with two terminal cysteines showed the highest transfection efficiency.[87] Similar transfection efficiency was achieved with shortened lysine chains consisting of only four lysines and two terminal cysteines.[87] Read *et al*. prepared a bioreducible polylysine analog by oxidative polymerization of Cys-Lys_{10}-Cys ($CK_{10}C$). In the presence of either chloroquine of the cationic lipid DOTAP efficient pDNA gene transfer was observed which was far more effective than analogous studies with a nonreducible standard poly(L)lysine.[88]

In order to achieve more efficient endosomal escape, histidine-rich or fusogenic peptide domains were incorporated. The histidine-containing oligolysine sequence CHK_6HC was found to possess a 10-fold higher transfection efficiency than the control peptide without

histidine.[87] Analogously, bioreducible polymers based on oxidation of $CH_3K_3H_3C$ and $CH_6K_3H_6C$ demonstrated improved activity over C-K_{10}-C based polymers.[89] The group of Mixson developed a series of branched oligopeptides containing nucleic acid binding lysines and endosomal-buffering histidines. They discovered that different peptide sequences were needed for optimized pDNA and for siRNA delivery.[90, 91] Lu and colleagues used solid-phase assisted peptide synthesis for inserting defined oligoamines such as triethylene tetramine into histidine and terminal disulfide-forming cysteine containing peptides, which were subsequently oxidized into polymers used for nucleic acid delivery.[92]

1.3.3 Sequence-defined oligoaminoamide carriers

Solid phase synthesis (SPS), introduced by Merrifield in 1963, are widely used to synthesize sequence defined oligopeptide. This method also provides an option to introduce artificial building blocks with proper functional groups to the SPS process, and enables a stepwise assemble of sequence defined polymeric product. Hartmann *et al*. successfully modified the classical approach, and obtained sequence-defined linear poly(amidoamines) (PAA).[52, 93-98] Optionally, disulfide moiety [93], PEG [52, 93, 94], novel chiral building blocks [97], as well as building blocks allowing asymmetrical branching [98] have been introduced into the syntheses of multifunctional PAAs.

Schaffert *et al*. introduced a set of novel artificial amino acids comprising repeats of the 1,2-diaminoethane motif derived from the classic gene carrier polyethylenimine (PEI). Such artificial oligoamino acids (**Figure 1.3 A**), like glutaryl-triethylene tetramine (Gtt), glutaryl-tetraethylene pentamine (Gtp), succinoyl-tetraethylene pentamine (Stp) [99] and succinoyl-pentaethylene hexamine (Sph) [100], are fully compatible with the standard Fmoc-based SPS. In combination with natural α-amino acids, they were applied in SPS to generate sequence-defined cationic oligomers for nucleic acid delivery, provide excellent nucleic acid binding ability, endosomal buffering capacity, and an option of site-specific positioning of multiple functionalities.[101] Continuous efforts have been taken to optimize this type of cationic oligomers for nucleic acid delivery, resulted in a library of over 1000 sequence defined oligomers as potential nucleic acid carriers (**Figure 1.3 B**).

Starting from the basic linear oligomers, i-shape, U-shape as well as T-shape olgiomers have been synthesized.[101] Additionally, three arm[101, 102], four arm[100], and even five arm[100] structure could be obtained. Scholz *et al*.[103] developed a library of comb-

like oligomers using oligolysine as the backbone which was modified with one out of four different artificial oligoamino acids at the lysine ε-amino groups (for example see oligomer *552* in **Figure 1.3B**). Results showed clear differences between the comb and linear oligomers as pDNA carriers, and comb-like Stp containing structures was found an overall advantage compared to the linear oligomers in the aspect of buffering capacity, cellular uptake, and transfection efficiency.

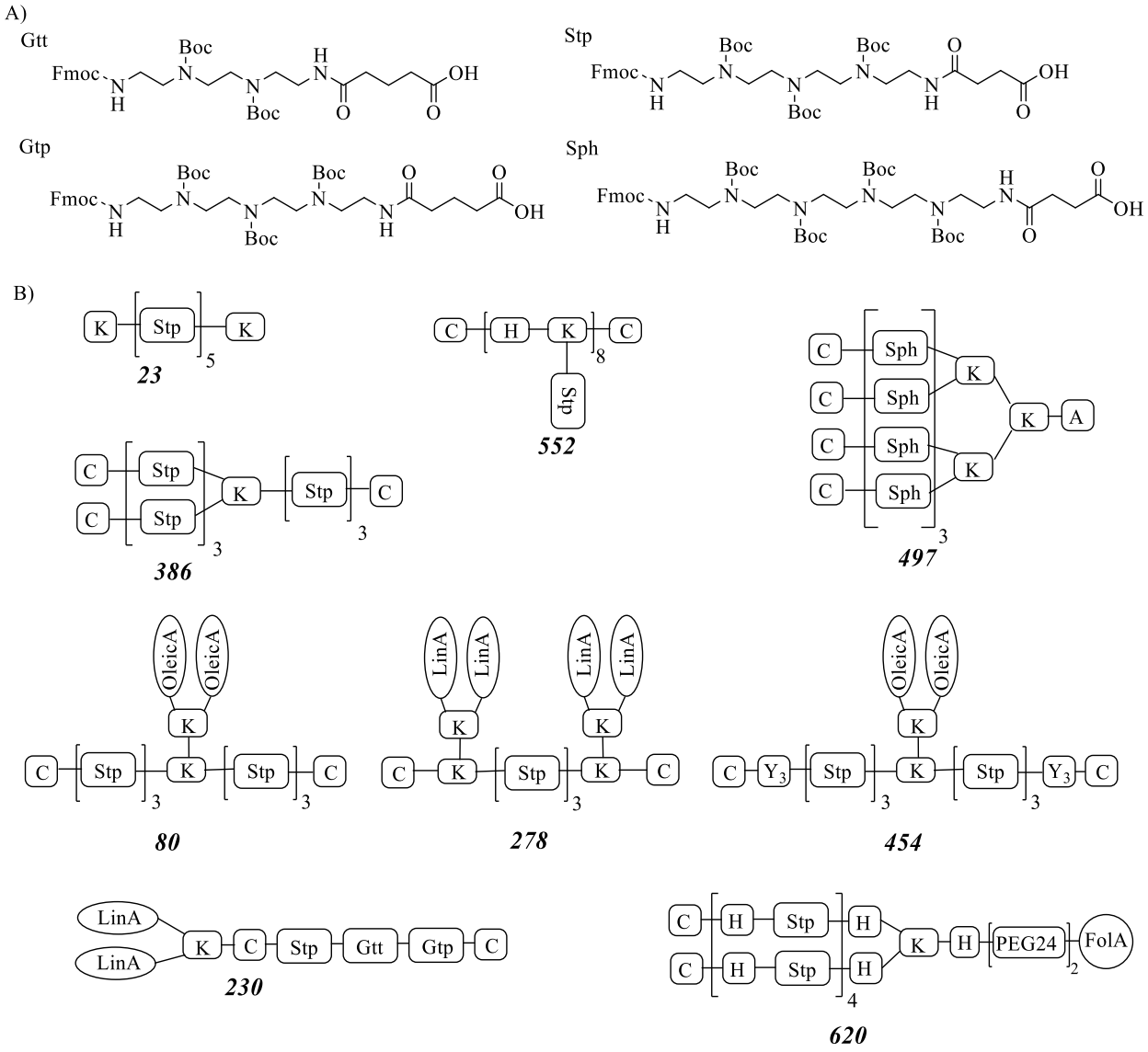

Figure 1.3 Sequence-defined oligomers. A) Artificial oligoamino acid building blocks. B) Exemplary oligomer structures (N-terminus left, C-terminus right). Linear structures (such as *23*), three-arm (*386*), four-arm structures (*497*), lipid containing oligomers (*80*, *230*, *278*), comb structures (*552*), tyrosine-containing structures (*454*), and receptor-targeted and histidine-containing structures (*620*) were designed. C, cysteine; K, lysine; H, histidine; A, alanine; Y, tyrosine; LinA, linolic acid; OleicA, oleic acid; FolA, folic acid; PEG24, monodisperse polyethylene glycol consisting of 24 ethylene glycol units.

The integration of small chemical motifs into the oligomers enables generation of multifunctional carriers for nucleic acid delivery. In this case, fatty acid have been

incorporated for hydrophobic stabilization of polyplexes, as well as manipulating endosomal escape.[104] Another stabilizing modification was achieved by the integration of tyrosine trimers (see **Figure 1.3B**, oligomer *454*). A combination of terminal oligotyrosines and cysteines was favorable for forming stable polyplexes, and exhibited an enhanced transfection efficiency in most cases.[105] Alternatively, twin disulfide forming units have also been investigated for the redox sensitive polyplexes stabilization and dissociation.[106] Lächelt *et al.* focused on the fine-tuning of endosomal buffering capacity with a library of sequence-defined oligomers containing different building blocks with and without histidine. The result reveal that building blocks with even numbers of protonatable amine groups exhibited higher total endosomal buffer capacity than those with odd numbers. In addition, the introduction of buffering histidines increased the buffer capacity, and resulted in a further improvement of gene transfer efficiency both *in vitro* and *in vivo*.[23]

This SPS-based oligomer platform also enable assemble of oligomers for receptor-targeted delivery. Martin *et al.* [107] first utilized peptide B6 and c(RGDfK) as targeting ligands, for binding the transferrin receptor or $\alpha_v\beta_3$ integrin, respectively. Effective specific gene transfection could be achieved only in combination with endosomolytic agent chloroquine. The introduction of buffering histidines into the backbone of the targeting oligomers (see for example **Figure 1.3B**, oligomer *620*), resulted a targeted and high transfection efficiency in the absence of chloroquine.[23] Unlike the mentioned stepwise SPS strategy, native chemical ligation chemistry provides an interesting option for a site-specific converting non-targeted oligomers into folate targeting PEGylated oligomers.[108] The application of other targeting ligands like a cMet binding peptide [109], GE11 [110], Angiopep-2 [111], transferrin [112] all provided interesting results essential for future optimization. Recent progress in the co-formulation of two different oligomers achieved *in vitro* dual targeting effects [110], efficient *in vivo* gene expression in combination of cMet targeted oligomer with 3-arm histidine integrated oligomer[109], and remarkably brain targeted siRNA delivery with Angiopep-2 bearing PEGylated 2-arm oligomer with lipo-oligomer 49 [111].

1.4 Aims of the thesis

The current thesis focuses on the combinatorial optimization of oligomers with precise molecular structure and site-specific modification in the development of multifunctional carriers for nucleic acid delivery.

The first aim of the thesis was combinatorial optimization of sequence-defined oligo(ethanamino)amides for folate receptor-targeted pDNA and siRNA delivery. For this purpose, a library of sequence-defined oligomers comprising the artificial polyamino acids Stp and Sph for nucleic acid complexation, monodisperse polyethylene glycol (PEG) for surface shielding, and folic acid for receptor-specific cellular uptake, in combination of alternating different topologies of branched cationic oligomers, optionally containing endosomal buffering histidines and/or hydrophobic tyrosine trimers had to be designed and synthesized in order to systematically evaluate their properties in pDNA and siRNA delivery. The ligand-dependency of the nucleic acid transfer by comparing with analogous folate-free oligomers had to be included. The findings of this study should provide identified different beneficial modules for the delivery of pDNA and siRNA and structure activity relationships for further optimization of targeted oligomers.

The second aim was to provide an alternative efficient option to obtain a multifunctional targeting carrier by combination of two different oligomers for the formulation of therapeutic siRNA polyplexes. For this purpose, siRNA polyplexes in combination with folate-PEG-containing oligomers (for FR targeting and shielding of surface charges) and a 3-arm oligomer (for optimizing particle size and stability) at various molar ratios had to be formulated to optimize the physicochemical properties of polyplexes. Therefore an easy conjugation strategy had to be developed for uni-directional fast coupling between the two types of oligomer. These targeted combinatorial polyplexes (TCP) had to be systematically evaluated in order to find an optimal siRNA polyplex formulation.

The final aim was to investigate branched fatty acid containing oligomers for nucleic acid delivery. For this purpose, a library of fatty acid containing oligomers with different cationic branches had to be synthesized in order to evaluate their potential as nucleic acid carriers. The influence of different cationic branches on the delivery of pDNA and siRNA should be identified.

2 Materials and Methods

2.1 Chemicals and reagents

2-Chlorotrityl chloride resin, all Fmoc or Boc protected α-amino acids, peptide grade dimethylformamide (DMF), N,N-diisopropylethylamine (DIPEA), piperidine and trifluoroacetic acid (TFA) were purchased from Iris Biotech (Marktredwitz, Germany). Benzotriazol-1-yl-oxy-tris-pyrrolidino-phosphonium hexafluorophosphate (Pybop) and syringe microreactors were obtained from Multisyntech GmbH (Witten, Germany). 1-Hydroxy-benzotriazole (HOBt), triisopropylsilane (TIS), tris(2-carboxyethyl)phosphine (TCEP), 5,5'-dithio-bis(2-nitrobenzoic acid) (DTNB), 1,8-diazabicyclo[5.4.0]undec-7-ene (DBU), 3,6-dioxa-1,8-octanedithiol (DODT), dimethylsulfoxide (DMSO) and 3-(4,5-dimethylthiazol-2-yl)-2,5-diphenyltetrazolium bromide (MTT) were purchased from from Sigma-Aldrich (Munich, Germany), hydrazine from Merck (Darmstadt, Germany), and 25% ammonia solution from Carl Roth (Karlsruhe, Germany). N^{10}-(trifluoroacetyl) pteroic acid was obtained from Niels Clauson-Kaas A/S (Farum, Denmark), and Fmoc-N-amido-dPEG$_{24}$-acid from Quanta Biodesign (Powell, USA). All other solvents and small molecular reagents were obtained in high quality (analytical or HPLC grade). Acetonitrile (ACN, HPLC grade) was obtained from VWR (Darmstadt, Germany), deuterium oxide (D_2O) from Euriso-Top (Saint-Aubin Cedex, France), dichloromethane (DCM) from Bernd Kraft (Duisburg, Germany), n-hexane and methyl-tert-butyl ether (MTBE) from Brenntag (Mülheim/Ruhr, Germany). Ninhydrin, phenol, potassium cyanide (KCN), sodium hydroxide (NaOH), Hydrochloric acid solution (HCl, 1M) were purchased from Sigma-Aldrich (Munich, Germany). Water was used as purified, deionized water. Cell culture media, fetal bovine serum (FBS) and antibiotics were purchased from Life Technologies (Darmstadt, Germany), glucose from Merck (Darmstadt, Germany), and HEPES from Biomol GmbH (Hamburg, Germany). Luciferase cell culture lysis buffer and D-luciferin sodium were obtained from Promega (Mannheim, Germany). pCMVLuc pDNA was obtained in purified form from Plasmid Factory (Bielefeld, Germany). pDNA Cy5-labeling kit was obtained from Mirus Bio (Madison, WI, USA). Ready to use siRNA duplexes were obtained from Axolabs GmbH (Kulmbach, Germany): siGFP (sense: 5'-AuAucAuGGccGAcAAGcAdTsdT-3'; antisense: 5'-UGCUUGUCGGCcAUGAuAU dTsdT-3'; small letters: 2'-methoxy; s: phosphorothioate) for silencing of eGFPLuc; siCtrl (sense: 5'-AuGuAuuGGccuGuAuuAGdTsdT-3'; antisense: 5'-

CuAAuAcAGGCcAAuAcAU dTsdT-3'). Peptide modified sequences siGFP-Inf7 (sense: Inf7-ss-C6-5'-AuAucAuG GccGAcAAGcAdTsdT-3'; antisense: 5'-UGCUUGUCGGCcAUGAuAUdTsdT-3') and its control siCtrl-Inf7 (sense: Inf7-ss-C6-5'-AuGuAuuGGccuGuAuuAGdTsdT-3'; antisense: 5'-CuAAuAcAGGCcAAuAcAUdTsdT-3') were synthesized as published. [113]

2.2 Oligomer synthesis methods

2.2.1 Synthesis of polyamino acid building blocks

The cationic building blocks Stp(Boc_3)-Fmoc and Sph(Boc_4)-Fmoc were synthesized as described before.[99, 100] Generally, starting with selective protection of the primary amines of TEPA (for Stp(Boc_3)-Fmoc) or PEHA (for Sph(Boc_4)-Fmoc) and the secondary amines by ethyl trifluoroacetate and di-tert butyl dicarbonate respectively, followed with deprotection of the primary amines with NaOH, the building block could be obtained by asymmetric functionalization of the terminal primary amine with Fmoc-Osu and succinic anhydride.

2.2.2 Resin loading

2.2.2.1 Loading of 2-chlorotrityl resin

The desired amount of 2-chlorotrityl chloride resin (chloride loading 1.6 mmol/g) was placed in a syringe reactor and preswelled in dry DCM (10 mL/g resin) for 30 min, the DCM was discarded subsequently. A solution containing 0.4 eq mmol Fmoc-amino acid and 0.8 eq mmol DIPEA in dry DCM (10 mL) were added per gram resin and incubated for 1 h at RT. After disposal of the reaction mixture, the resin was incubated with a mixture of DCM/MeOH/DIPEA (10 mL/g resin; 80/15/5 v/v/v) for 30 min at RT to cap residual reactive chloride functions. The resin was washed 5 times with DCM (10 mL/g resin) and part of the resin was separated for the loading determination. The rest resin was washed 3 times with DMF (10 mL/g resin) and treated 5 times for 10 minutes with 20 % piperidine in DMF. Finally, the resin was washed 3 times with DMF, 3 times with DCM, 3 times with n-hexane and dried under vacuum. In general, by this procedure resin loadings between 0.2 and 0.3 mmol/g were achieved. To avoid aggregation of the highly branched four-arm oligomers, a very low loaded resin have been obtained by using decreased amount of Fmoc-amino acid (0.2 eq), resulted in a very low resin loading around 0.1 mmol/g.

2.2.2.2 Loading determination

For resin loading determination, an exact amount (about 10 mg) of vacuum-dried resin were react with 1 mL of 20 % piperidine in Eppendorf reaction tubes for 1 h at RT under shaking. After vortex and centrifugation, 25 µl of the supernatant were diluted with 975 µl DMF. A solution of 20% piperidine in DMF acted as a blank. The absorption was measured at 301 nm using a Genesys 10S UV-VIS spectrophotometer (Thermo Scientific, Dreieich, Germany), and the resin loading was calculated using the following formula.

$$Loading = FS\left(\frac{mmol}{g}\right) = \frac{1000 \cdot A}{m \cdot \varepsilon \cdot D}$$

A: Absorbance; m: resin mass in mg; ε: molar extinction coefficient = 7800 L/(mol*cm); D: dilution factor (in this example: D=0,025)

2.2.3 Standard solid-phase synthesis conditions

2.2.3.1 General SPS process

SPS represent as a sequential repeated process of coupling and deprotection. For a general Fmoc based SPS, the resin was incubated with a 4-fold excess of the appropriate pre-activated Fmoc amino acid identified by the target oligomer sequence for 1 h at RT. The pre-activation of Fmoc amino acid was carried out with an equimolar of HOBt, PyBOP and two fold molar DIPEA. Fmoc deprotection was normally carries out by 10 min incubation with 20% piperidine in DMF for several times. Kaiser test was performed to determine the presence of free amines after each coupling and deprotection step.[114] In case of an unexpected result of the Kaiser test, the last coupling respectively deprotection step was repeated. After assembly of the full sequence, the desired product was cleaved from the resin and purified by SEC.

2.2.3.2 Kaiser test

Kaiser test was used to qualitatively determine the presence of free amines.[114] A small amount of sample of DCM washed resin was transferred to an Eppendorf reaction tube. One drop of each 80 % (w/v) phenol in EtOH, 5 % (w/v) ninhydrin in EtOH and 20 µM potassium cyanide (KCN) in pyridine were added. The tube was incubated at 99 °C for 4 min under shaking. The presence of free amines was indicated by a blue colored resin beads and solution (positive Kaiser test), while the remained colorless resin beads and light yellow solution indicate the absence of free amines (negative Kaiser test).

2.2.3.3 Oligomer cleavage

The assembled conjugates was cleaved off the resin by incubation with TFA/DODT/TIS/H2O 94:1:2.5:2.5 (10 mL/g resin) for 90 min. The filtered cleavage solution was collected in a round-bottom flask and the resin was washed 3 times with TFA, 3 times with DCM (10 mL/g resin). The combined solution was concentrated under reduced pressure to a final volume of approximately 1 mL and added dropwise to a pre-cooled 50 mL MTBE/n-hexan (1/1 v/v) mixture, given out the precipitated crude product. After centrifugation for 15 min at 4000 RCF and 4 °C, the supernatant was discarded and the precipitate was dried with nitrogen.

2.2.4 Oligomer synthesis

2.2.4.1 Synthesis of three-arm oligomers

The three arm oligomer *386* and *689* were synthesized as described before.[101, 109] Generally, 2-Chlorotrityl chloride resin preloaded with Fmoc-Cys(Trt)-OH was used to step-wisely coupled with building block Fmoc-Stp(Boc_3)-OH, Fmoc-His(Trt)-OH, Fmoc-Lys(Fmoc)-OH and Boc-Cys(Trt)-OH according to the required sequence under the general SPS procedure.

2.2.4.2 Synthesis of PEGylated two- and four-arm oligomers with FolA ligands

2-Chlorotrityl chloride resin preloaded with Fmoc-Lys(ivDde)-OH was used for the synthesis of PEGylated structures with ligands. The protected artificial oligoamino acid building block Fmoc-Stp(Boc_3)-OH or Fmoc-Sph(Boc_4)-OH and protected α-amino acids Fmoc-His(Trt)-OH, Fmoc-Tyr(OtBu)-OH, Fmoc-Lys(Fmoc)-OH and terminal Boc-Cys(Trt)-OH were coupled stepwise to the deprotected α-amine of the preloaded Lys using 4 eq amino acid, 4 eq HOBt, 4 eq PyBop and 8 eq DIPEA in DCM/DMF and 1 h incubation time. The equivalents were calculated according to the free amines generated after the Fmoc deprotection. Fmoc deprotection was accomplished by 4 x 10 min incubation with 20% piperidine in DMF and twice with 20% piperidine in DMF containing 2% DBU for 5 min. After each coupling and deprotection step the resin was washed three times with DMF and DCM, and a Kaiser test was performed. In case of an unexpected result of the Kaiser test, the last coupling respectively deprotection step was repeated. The ivDde group of the C-terminal lysine was removed by treating the resin 20-30 times with 2% hydrazine in DMF, the deprotection process was monitored by checking absorption of the reaction solution at 290 nm. Subsequently, at the deprotected ε-amine

of the C-terminal lysine a precise bifunctional Fmoc-N-amido-dPEG$_{24}$-acid was attached followed by coupling of Fmoc-Glu-OtBu and N^{10}-(Trifluoroacetyl)pteroic acid in case of the folic acid targeted oligomers or substitutes in case of the controls. Couplings of the PEG-ligand segment were carried out under the same conditions as described above. For the folic acid containing oligomers, a deprotection of the trifluoroacetyl-group of pteroic acid was carried out using 25% aqueous ammonia solution/DMF (1:1) four times for 30 min. After each deprotection cycle, the resin was washed with DMF. After completion of the reaction, the resin was washed with DMF, DCM and n-hexane and dried in vacuo. The crude product was purified by SEC after cleavage.

2.2.4.3 Synthesis of TNB-modified oligomers

To generate corresponding TNB-modified oligomers, the unmodified oligomers were dissolved in deionized water, and treated with 10 eq of TCEP solution for 30 min in order to make sure that they are fully converted into the reduced thiol form, followed with adding of 10 eq DTNB stock solution (5 mM DTNB in 100 mM potassium phosphate buffer solution, pH 7.2 containing 0.1 mM EDTA), and reacted for another 2 h at room temperature. The reaction solution was then purified by SEC according to the general procedure described in **2.2.5.1**.

2.2.4.4 Synthesis of branched oleic acid containing oligomers

2-Chlorotrityl chloride resin preloaded with Fmoc-Lys(ivDde)-OH was used for the synthesis of branched oligomers containing oleic acid. The assembly of the branched cationic backbone was carried out using the general SPS procedure, building block Fmoc-Stp(Boc$_3$)-OH, Fmoc-Lys(Fmoc)-OH and terminal Boc-Cys(Trt)-OH. After deproctection of ivDde, Fmoc-Lys(Fmoc)-OH and oleic acid were step-wisely coupled. The crude product was purified by SEC after cleavage.

2.2.4.5 Synthesis of PEGylated targeted oleic acid containing oligomers

2-Chlorotrityl chloride resin preloaded with Dde-Lys(Fmoc)-OH was used for the synthesis of PEGylated targeted oligomers containing oleic acid. Specifically, the assembly started with the coupling of PEG$_{24}$ chain. After finishing assembly of the folic acid (or glutamic acid) ligand, the lysine α-Dde protection group was removed to continue the synthesis of the Stp backbone analogously as described in general SPS process.

2.2.5 Oligomer purification and analytical characterization

2.2.5.1 Size-exclusion chromatography

All oligomers were purified by size exclusion chromatography using an Äkta purifier system (GE Healthcare Bio-Sciences AB, Uppsala, Sweden) based on a P-900 solvent pump module, a UV-900 spectrophotometrical detector, a pH/C-900 conductivity module, a Frac-950 automated fractionator, a Sephadex G-10 column and 10 mM hydrochloric acid solution / acetonitrile 7:3 as solvent. The corresponding fractions were collected and lyophilized.

2.2.5.2 ^{1}H-NMR

^{1}H NMR spectra were recorded using a Jeol JNMR-GX 400 (400 MHz) or JNMR-GX 500 (500 MHz) without TMS as internal standard. All chemical shifts were calibrated to the residual proton signal of the solvent and are reported in ppm. Data are reported as s = singlet, d = doublet, t = triplet, m = multiplet. The spectra were analyzed using MestreNova (Ver. 9.0.1, MestReLab Research).

2.2.5.3 RP-HPLC

The purity of the oligomers was analyzed by RP-HPLC using a Waters HPLC system equipped with a Waters 600E multisolvent delivery system, a Waters 996 PDA detector and a Waters 717plus autosampler. As indicated, the compounds were analyzed using a Waters Sunfire C18 or Xbridge C18 column (5 µm, 4.6 x 150 mm) and a water/acetonitrile gradient (95:5 – 0:100) containing 0.1 % TFA. For the detection the extinction at 214 nm was monitored.

2.2.6 Buffer capacity of oligomers by alkalimetric titrations

The oligomer sample, containing 15 µmol protonable amines, was diluted in a total volume of 3.5 mL NaCl solution (50 mM) and the pH was adjusted to 2 by addition of hydrochloric acid. Afterwards, a back titration with 0.05 M NaOH was performed with an automatic titration system (Titrando 905 from Metrohm, Germany) equipped with a Biotrode pH electrode (METROHM GmbH & Co. KG, Filderstadt, Germany), until a pH of 11 was reached. To distinguish oligomer and solvent effects, a control titration of 50 mM sodium chloride solution without oligomer was performed. Volume differences (ΔV) between defined pH values were determined. Total endolysosomal buffer capacity C in the pH range between 5 and 7.4 was calculated according to the following formula:

$$C_{\text{pH 5}-\text{pH 7.4}} = \frac{[\Delta V(\text{Sample})_{\text{pH 5}-\text{pH 7.4}} - \Delta V(\text{NaCl})_{\text{pH 5}-\text{pH 7.4}}] \cdot 50\ \text{mM}}{15\ \mu\text{moles}} \cdot 100\%$$

2.3 Polyplex formation and biophysical analysis

2.3.1 Polyplex formation

2.3.1.1 General pDNA and siRNA polyplex formation

pDNA or siRNA and oligomers at indicated nitrogen/phosphate (N/P) ratios were separately diluted with equal volumes of 20 mM HEPES buffered 5% glucose pH 7.4 (HBG). Only protonatable nitrogens were considered in the N/P calculations. The N/P ratio was calculated according to the cationic amine groups (N number) of the Stp and Sph building blocks and N-terminal first amine of cysteine residues to anionic phosphate groups (P number) in pDNA or siRNA. Here the amines of the imidazole group in Histidine were not taken into account when calculating the N numbers, as they are not protonated at pH 7.4. The polycation solution was added to the nucleic acid, mixed by rapid pipetting and incubated for 40 min at RT under air exposure to led oxidative disulfide formation.

2.3.1.2 Formation of targeted combinatorial siRNA polyplexes (TCP)

siRNA polyplexes for transfections were prepared (unless otherwise mentioned) as follows: at the indicated N/P ratios, 500 ng of siRNA was diluted in 10 µL of 20 mM HEPES buffered 5% glucose pH 7.4 (HBG), and the calculated amount of the two oligomers for the designated [TNB-modified oligomer / unmodified mercapto-form of oligomer] molar ratio, were separately diluted in 5 µL of HBG. The solution of the first TNB-modified oligomer was added to the siRNA solution and mixed by rapid pipetting (at least 5 times) to obtain 15 µL of binary siRNA polyplex solution. After 30 min in the closed Eppendorf reaction tube at room temperature, the solution of the second oligomer was added to the siRNA polyplex solution, to obtain 20 µL of siRNA polyplexes solution in total. The solution was placed for further 40 min at room temperature for disulfide formation. Unless indicated differently (**Figure 6.6** only), the same TCP siRNA mixing sequence was applied.

TCP polyplex calculations. Calculations of the individual two oligomers used at N/P 16 in formation of TCPs at indicated molar ratios were made as follows. Protonatable nitrogens (N) for the applied oligomers in the current work were calculated excluding histidine Ns (defined as unprotonated at pH 7.4): N=29 for *386/769*, N=29 for *689/770*, N=68 for *709/873*, N=34 for *717/874.* The required molar amine amounts of oligomers at

N/P 16 were calculated, which are 24.88 nmol nitrogens (N) for 500 ng siRNA (in transfection). For size measurements 10µg siRNA were used, corresponding to 498 nmol N.

For the following calculation of the molar amount of each oligomer, general formulas were applied as follows:

1) $N/P_{total} = 16 = N/P_a + N/P_b$ ("a" and "b" to stand for the two oligomers).
2) Total molar amount of nitrogen $M_{total}=N_a*M_a+ N_b*M_b$, here N stands for the number of protonatable nitrogens, while M stands for the molar amount.
3) The molar ratio of oligomers $M_a/M_b=R_a/R_b$. R stands for the ratio of each oligomer (1:1 in the majority of cases).
4) Calculation of the molar amount of each oligomer: $M_a=16*M_{total}*N_a/(N_a+N_b*R_b/R_a)$, and $M_b=16*M_{total}*N_b/(N_a*R_a/R_b+N_b)$.
5) The individual N/P ratio for each oligomer (at $N/P_{total} = 16$): $N/P_a=16*N_a/(N_a+N_b*R_b/R_a)$, and $N/P_b=16*N_b/(N_a*R_a/R_b+N_b)$.

As an example of TCP1 *386/873* at molar ratio 40:60, the individual N/P for *386* is 16*29/(29+68*60/40)=3.5, for *873* it is 16*68/(29*40/60+68)=12.5, and the molar amount M for *386* is 24.88*29/(29+68*60/40)=5.45 nmol for 500 ng siRNA.

Depending on the selected molar ratios and TCPs, the final molar ratios of thiol SH /TNB will differ. At oligomer molar 1:1 ratio, SH/TNB are 3:4 for TCP1, 2:3 for TCP2, 4:3 forTCP3, and 3:2 for TCP4.

2.3.2 Ethidium bromide compaction assay

A Cary Eclipse spectrophotometer (Varian, Germany) was used for the quantification of ethidium bromide (EtBr) fluorescence at the excitation wavelength λex = 510 nm and emission wavelength λem = 590 nm. pDNA polyplexes were incubated with 2 µg pDNA and the oligomer at N/P 12 in 200 µL HBG for 40 minutes. siRNA polyplexes were incubated with 5 µg siRNA and the oligomer at N/P 20 in 200 µL HBG for 40 minutes. Before the measurement 800µL of EtBr solution (c = 0.4 µg/mL) was added. 200 µL HBG buffer with 800µL of EtBr solution (c = 0.4 µg/mL) was used as blank. 200µL of nucleic acid solution (2µg pDNA or 5µg siRNA) + 800µL of EtBr solution (c = 0.4 µg/mL) was assigned to 100%. The fluorescence intensity of EtBr measured after 3 minutes of incubation was determined in relation to the 100% value. Triplicates were measured.

2.3.3 Electrophoretic mobility shift assay

A 1% (w/v) agarose gel for pDNA analyses and a 2.5% (w/v) agarose gel for siRNA analyses were prepared by dissolving agarose in TBE buffer (Trizma base 10.8 g, boric acid 5.5 g, disodium EDTA 0.75 g, and 1 L of water). After adding of GelRed™ (Biotium, Hayward, U.S.A.), the agarose gel was formed in the electrophoresis unit. Polyplexes containing 200 ng pDNA or 500 ng siRNA were formed and placed into the sample pockets after adding of 4 µL loading buffer (6 mL of glycerine, 1.2 mL of 0.5 M EDTA, 2.8 mL of H_2O, 0.02 g of bromophenol blue). Electrophoresis was performed at 120 V for 80 min in case of pDNA polyplexes and for 40 min in case of siRNA polyplexes.

2.3.4 Particle size and zeta potential

Particle size and zeta potential of polyplexes were measured by dynamic laser-light scattering (DLS) using a Zetasizer Nano ZS (Malvern Instruments, Worcestershire, U.K.). Polyplexes containing 10 µg of nucleic acid in a total volume of 50 µL were further diluted 1:20 with 20mM HEPES pH 7.4 buffer before measuring in a folded capillary cell (DTS1060 or DTS1070). For size measurements, each sample was measured 3 times with 10 subruns at 25 °C. Zeta potentials were calculated by the Smoluchowski equation, each samples was measured 3 times with 10 to 30 subruns at 25 °C.

2.4 Cell culture

All cell culture work was carried out by Katharina Müller, Ana Krhac Levacic, Dian-Jang Lee, and Dr. Petra Kos (Pharmaceutical Biotechnology, LMU).

Mouse neuroblastoma cells Neuro2a WT cells and Neuro2a/eGFPLuc cells were cultured in Dulbecco's modified Eagle's medium. Human KB WT cells and KB/eGFPLuc cells were cultured in folate free RPMI-1640 medium. Both medium were supplemented with 10% fetal bovine calf serum (FBS), 4 mM stable glutamine, 100 U/mL penicillin, and 100 µg/mL streptomycin at 37 °C in 5% CO_2. Cells were collected by using a trypsin-EDTA (0.25%) solution and the cell suspension was seeded at the required concentration for each experiment.

2.4.1 Luciferase gene transfer

For folate targeted polyplexes, KB cells were seeded in 96-well plates with 8000 KB cells/well 24 h before pDNA transfection. Before treatment, the cell culture medium was

replaced with 80 µL fresh medium containing 10% FBS. Polyplexes containing 200 ng pCMVLuc formed at different protonatable nitrogen/phosphate (N/P) ratios in a total volume of 20 µL HBG were added to each well and incubated at 37 °C. Medium was replaced 45 min after transfection by fresh medium or chloroquine (0.1 mM) containing medium. After 4 h incubation at 37 °C, medium was changed again by fresh medium, and cells were further cultured for 24 h after initial transfection. For non-targeted pDNA polyplexes containing 200 ng pCMVLuc formed at different protonatable nitrogen/phosphate (N/P) with branched fatty acid containing oligomers, the luciferase gene transfer experiments were performed with 10000 Neuro2a WT cells/well. Alternatively, after adding the polyplexes, the cells were further cultured for 24 h at 37 °C without medium change.

Cells were treated with 100 µL cell lysis buffer. Luciferase activity was measured using a luciferin-LAR buffer solution and a Centro LB 960 plate reader luminometer (Berthold Technologies, Bad Wildbad, Germany). Transfection efficiency was evaluated as relative light units (RLU) per well. All experiments were performed in quintuplicates.

2.4.2 Metabolic activity of pDNA transfected cells (MTT assay)

To detect metabolic activity of pDNA transfected cells, the transfection experiments were performed as described in ***2.4.1***. After 24 h of initial transfection, 10 µl of MTT (5 mg/ml) was added to each well and incubated for 2 h at 37 °C for the formation of the dark purple formazane product. After removal of unreacted dye and medium, the 96-well plates were stored at −80 °C for at least one hour. Then 100 µL DMSO per well were added to dissolve the purple formazan product. The absorbance was measured at 590 nm with 630 nm as the reference wavelength, using microplate reader (Tecan Spectrafluor Plus, Tecan, Switzerland). The relative cell viability (%) related to control wells treated only with 20 µL HBG was calculated as ([A] test/[A] control) × 100%. All experiments were performed in quintuplicates.

2.4.3 Gene silencing with siRNA

For folate targeted polyplexes, gene silencing experiments were performed in KB/eGFPLuc cells. Polyplexes were formed with the unmodified siRNA against eGFP for silencing the eGFPLuc fusion protein, its control sequence siCtrl, and the lytic peptide modified Inf7-siGFP, with its control sequence Inf7-siCtrl. Cells were seeded in 96-well plates with 4000 KB/eGFPLuc cells/well 24 h before siRNA silencing. The cell culture

medium was replaced with 80 µL fresh medium containing 10% FBS before treatment. Polyplexes containing 200 ng siRNA formed at different protonatable nitrogen/phosphate (N/P) ratios in a total volume of 20 µL HBG were added to each well and incubated at 37 °C. 45 min after transfection medium was replaced by fresh medium, and cells were further cultured for 48 h after initial transfection. For non-targeted polyplexes, experiments were performed with polyplexes containing 500 ng siGFP or siCtrl in 5000 Neuro2A/eGFPLuc cells respectively, cells were further cultured for 48 h after initial transfection. Luciferase activity was determined as described above. The relative light units (RLU) were presented as percentage of the luciferase gene expression obtained with buffer treated control cells. All experiments were performed in triplicates.

2.4.4 Flow cytometry

Cellular internalization. KB WT or KB/eGFPLuc cells were seeded into 24-well plates coated with collagen at a density of $5*10^4$ cells/well. After 24 h, culture medium was replaced with 400 µL fresh growth medium. pDNA polyplexes (N/P 12, for oligomers #29-32 and #35-42 polyplexes were formed at N/P 3) containing 1 µg pDNA (including 20% Cy5-labeled pDNA) or siRNA polyplexes (N/P 12) containing 1.35 µg siRNA (including 20% Cy5-labeled siRNA) in 100 µL HBG were added to each well and incubated at 37 °C for 45 min. Afterwards, cells were washed with 500 µL PBS containing 500 IU of heparin on ice for 15 min to remove any polyplexes sticking to the cell surface. After an additional PBS washing step, cells were detached with trypsin/EDTA and resuspended in PBS with 10% FBS. Cellular internalization of the polyplexes was measured by excitation of Cy5 at 635 nm and detection of emission at 665 nm. Cells were appropriately gated by forward/sideward scatter and pulse width for exclusion of doublets. DAPI (4',6-diamidino-2-phenylindole) was used to discriminate between viable and dead cells. Data were recorded by Cyan™ ADP flow Cytometer (Dako, Hamburg, Germany) using Summit™ acquisition software (Summit, Jamesville, NY, USA) and analyzed by FlowJo® 7.6.5 flow cytometric analysis software. All experiments were performed in triplicates.

2.5 Statistical analysis

Results are presented as mean ± standard deviation (SD). The number of replicates is indicated in the corresponding methods section.

3 Results

3.1 Combinatorial optimization of sequence-defined oligo(ethanamino)-amides for folate receptor-targeted pDNA and siRNA delivery

As discussed in the introduction section, successful gene therapy strategies require efficient and safe delivery methods for the transfer of therapeutic nucleic acids into the target cells. An ideal nucleic acid carrier has to overcome many extracellular and intracellular barriers. Integrated functional microdomains may accomplish these different tasks, including nucleic acid complexation, nanoparticle shielding and targeting, cellular uptake, endosomal escape and nucleic acid release at the intracellular target site.[115-118] Polymeric materials, like polyethylenimine (PEI), dendrimers, chitosan, or others have been widely investigated as nucleic acid carriers.[119-126] However, heterogeneity and polydispersity of polymers remain critical issues that have to be carefully considered in structure-activity relationship assessments, manufacturing, and in clinical studies. Therefore, polymers with precise molecular structure and site-specific modification [49, 52, 95, 96] are preferred in the further development of multifunctional carriers for gene delivery.

Our group has developed sequence-defined cationic oligomers by solid-phase assisted synthesis using artificial amino acids as building blocks comprising repeats of the 1,2-diaminoethane motif.[99-102, 104] The diaminoethane motif was previously discovered as a key chemical structure providing PEI and related transfection polymers an excellent nucleic acid binding and endosomal buffering capacity.[21, 55, 123, 124, 127-129] The artificial oligoamino acids, such as succinoyl-tetraethylene pentamine (Stp) and succinoyl-pentaethylene hexamine (Sph), were used in combination with natural α-amino acids and other building blocks to assemble sequence-defined oligoamino amides with different topologies and multiple functional domains.[23, 103, 105, 109, 113, 130-131] Previous studies by several groups showed that histidines can provide additional pH-buffering via the protonation of imidazole groups, facilitating endosomal escape.[22, 23, 109, 132, 133] Insertion of hydrophobic amino acids such as tyrosine enhanced the stability as well as endosomal escape of polyplexes.[105, 134-137] For the targeted delivery of nucleic acids to the site of action, shielding domains such as polyethylene glycol (PEG) to minimize unspecific interactions [138-141] and targeting ligands to mediate specific cellular binding

and uptake can be incorporated. In this respect, multiple functionalizations of oligomers may meet the requirements to overcome the multiple barriers of gene delivery.[124, 142, 143]

For this purpose, we designed and synthesized a library of forty-two sequence-defined oligomers comprising the artificial polyamino acids Stp and Sph for nucleic acid complexation, monodisperse polyethylene glycol (PEG) for surface shielding, and folic acid for receptor-specific cellular uptake. Two topologies of branched cationic oligomers (two-arms, four-arms) based on Stp or Sph monomers, optionally containing endosomal buffering histidines and/or hydrophobic tyrosine trimers were designed and systematically evaluated for properties in pDNA and siRNA delivery. We also focused on the ligand-dependency of the nucleic acid transfer by comparing with analogous folate-free oligomers.

3.1.1 Design and synthesis of folate targeted sequence-defined oligomers

The starting point of the current study was oligomer *356*, a branched two-arm cationic domain of Stp units linked with a PEG segment and a FolA ligand (see **Figure 3.1**) as folic acid receptor-specific nucleic acid carrier.[113] This precise oligoamino amide sequence consists of folate linked with a chain of twenty-four ethylene glycol monomers, a branching α,ε-amidated lysine, and two arms of each four Stp units followed by a terminal cysteine unit. Within polyplexes, the terminal cysteines provide stabilization by disulfide crosslinks and were found strictly required for stable polyplex formation and transfection.[113] The high PEG content (24 ethylene glycol units in comparison to 24 protonatable aminoethane units) negatively affects the endosomolytic property and the nucleic acid compaction process. For *356* pDNA polyplexes, the addition of lysosomotropic chloroquine is required for efficient gene transfer. In siRNA transfections, modification of siRNA with the endosomolytic Inf7 peptide [29, 144] was critically required for gene silencing. With regard to nucleic acid compaction, the high PEG content of *356* and related two-arm oligomers prevents intermolecular nucleic acid compaction, resulting in very small unimolecular siRNA complexes on the one hand,[113] and loosely compacted pDNA complexes on the other hand.[107] The latter could be overcome by reducing the PEG content of polyplexes.[109] Four-arm oligomers (without PEG but with double number of Stp or Sph units) had been found as very effective pDNA compacting carriers.[23, 100]

Topology	Sequence	No.
2-arm 	C-Stp$_4$-K-(PEG$_{24}$-FolA)-Stp$_4$-C	356
	K-(PEG$_{24}$-Acetate)-K-(Sph$_3$-C)$_2$	#1
	K-(PEG$_{24}$-FolA)-K-(Sph$_3$-C)$_2$	#2
	K-(PEG$_{24}$-Acetate)-K-(Sph$_4$-C)$_2$	#3
	K-(PEG$_{24}$-FolA)-K-(Sph$_4$-C)$_2$	#4
2-arm-H 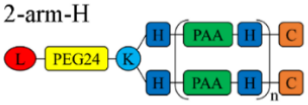	K-(PEG$_{24}$-E)-K-[(H-Stp)$_3$-H-C]$_2$	#5
	K-(PEG$_{24}$-FolA)-K-[(H-Stp)$_3$-H-C]$_2$	#6
	K-(PEG$_{24}$-E)-K-[(H-Stp)$_4$-H-C]$_2$	#7
	K-(PEG$_{24}$-FolA)-K-[(H-Stp)$_4$-H-C]$_2$	#8
2-arm-Y$_3$ 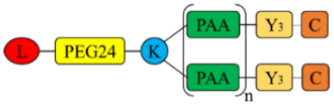	K-(PEG$_{24}$-E)-K-(Stp$_3$-Y$_3$-C)$_2$	#9
	K-(PEG$_{24}$-FolA)-K-(Stp$_3$-Y$_3$-C)$_2$	#10
	K-(PEG$_{24}$-E)-K-(Stp$_4$-Y$_3$-C)$_2$	#11
	K-(PEG$_{24}$-FolA)-K-(Stp$_4$-Y$_3$-C)$_2$	#12
	K-(PEG$_{24}$-E)-K-(Sph$_3$-Y$_3$-C)$_2$	#13
	K-(PEG$_{24}$-FolA)-K-(Sph$_3$-Y$_3$-C)$_2$	#14
	K-(PEG$_{24}$-E)-K-(Sph$_4$-Y$_3$-C)$_2$	#15
	K-(PEG$_{24}$-FolA)-K-(Sph$_4$-Y$_3$-C)$_2$	#16
2-arm-H-Y$_3$ 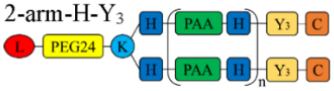	K-(PEG$_{24}$-E)-K-[(H-Stp)$_3$-H-Y$_3$-C]$_2$	#17
	K-(PEG$_{24}$-FolA)-K-[(H-Stp)$_3$-H-Y$_3$-C]$_2$	#18
	K-(PEG$_{24}$-E)-K-[(H-Stp)$_4$-H-Y$_3$-C]$_2$	#19
	K-(PEG$_{24}$-FolA)-K-[(H-Stp)$_4$-H-Y$_3$-C]$_2$	#20
4-arm 	K-(PEG$_{24}$-E)-K-[K-(Stp$_3$-C)$_2$]$_2$	#21
	K-(PEG$_{24}$-FolA)-K-[K-(Stp$_3$-C)$_2$]$_2$	#22
	K-(PEG$_{24}$-E)-K-[K-(Stp$_4$-C)$_2$]$_2$	#23
	K-(PEG$_{24}$-FolA)-K-[K-(Stp$_4$-C)$_2$]$_2$	#24
	K-(PEG$_{24}$-A)-K-[K-(Sph$_3$-C)$_2$]$_2$	#25
	K-(PEG$_{24}$-FolA)-K-[K-(Sph$_3$-C)$_2$]$_2$	#26
	K-(PEG$_{24}$-A)-K-[K-(Sph$_4$-C)$_2$]$_2$	#27
	K-(PEG$_{24}$-FolA)-K-[K-(Sph$_4$-C)$_2$]$_2$	#28
4-arm-H 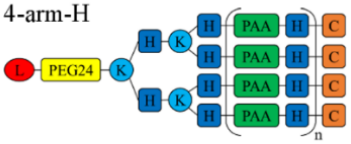	K-(PEG$_{24}$-E)-K-[H-K-((H-Stp)$_3$-H-C)$_2$]$_2$	#29
	K-(PEG$_{24}$-FolA)-K-[H-K-((H-Stp)$_3$-H-C)$_2$]$_2$	#30
	K-(PEG$_{24}$-E)-K-[H-K-((H-Stp)$_4$-H-C)$_2$]$_2$	#31
	K-(PEG$_{24}$-FolA)-K-[H-K-((H-Stp)$_4$-H-C)$_2$]$_2$	#32
	K-(PEG$_{24}$-E)-K-[H-K-((H-Sph)$_3$-H-C)$_2$]$_2$	#33
	K-(PEG$_{24}$-FolA)-K-[H-K-((H-Sph)$_3$-H-C)$_2$]$_2$	#34
4-arm-Y$_3$ 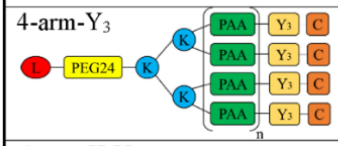	K-(PEG$_{24}$-E)-K-[K-(Stp$_3$-Y$_3$-C)$_2$]$_2$	#35
	K-(PEG$_{24}$-FolA)-K-[K-(Stp$_3$-Y$_3$-C)$_2$]$_2$	#36
	K-(PEG$_{24}$-E)-K-[K-(Stp$_4$-Y$_3$-C)$_2$]$_2$	#37
	K-(PEG$_{24}$-FolA)-K-[K-(Stp$_4$-Y$_3$-C)$_2$]$_2$	#38
4-arm-H-Y$_3$ 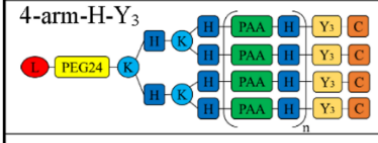	K-(PEG$_{24}$-E)-K-[H-K-((H-Stp)$_3$-H-Y$_3$-C)$_2$]$_2$	#39
	K-(PEG$_{24}$-FolA)-K-[H-K-((H-Stp)$_3$-H-Y$_3$-C)$_2$]$_2$	#40
	K-(PEG$_{24}$-E)-K-[H-K-((H-Stp)$_4$-H-Y$_3$-C)$_2$]$_2$	#41
	K-(PEG$_{24}$-FolA)-K-[H-K-((H-Stp)$_4$-H-Y$_3$-C)$_2$]$_2$	#42

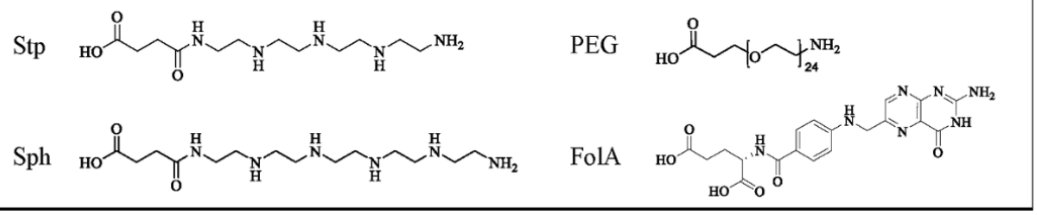

Figure 3.1 Overview of the synthesized PEGylated oligomers, their topologies, sequences, and their numbers within the current manuscript. L stands for the targeting ligand or the corresponding negative control (FolA, folic acid; A, alanine; E, glutamate; acetate); PAA, polyamino acid (Stp, succinoyl-tetraethylene-pentamine; Sph, succinoyl-pentaethylene-hexamine); PEG, polyethylene glycol; K, lysine; H, histidine; Y, tyrosine; C, cysteine. K-(and K-[refer to branchings by α- and ε-amino modification of lysines.

The new library of forty-two oligomers was synthesized using solid-phase assisted synthesis and contained the following systematic variations (**Figure 3.1**): *(1)* the type of artificial oligoamino acid building block (succinoyl tetraethylene pentamine (Stp) containing five nitrogens, or succinoyl pentaethylene hexamine (Sph) containing six nitrogens), *(2)* the topology (two-arm or four-arm cationic core for nucleic acid compaction), *(3)* additional histidines for enhanced endosomal pH-buffering and/or *(4)* terminal tyrosine trimers for enhanced stability of the formed polyplexes. Folic acid was chosen as small molecule targeting ligand due to its high affinity for folate receptors, which are commonly over-expressed on the cell surface of many human cancer types [145, 146]. To investigate the targeting ligand dependency, we incorporated negative control substitutes. For most of the oligomers, we used glutamic acid in the ligand negative control, as the glutamic acid residue is a fragment of folate with the same negative charge. For some oligomers synthesized in an early project phase, we used alanine, similar as in the previous published *356* oligomer study,[113] or acetate (as a small noncharged residue) as alternative negative control ligands. A full list of detailed sequences and the internal library identification number could be find in **Table 6.1**.

3.1.2 Biophysical properties

To investigate the binding behavior of these oligomers with nucleic acids (pDNA or siRNA), agarose gel shift assays of the formed polyplexes were performed (**Figure 3.2**, **6.1**, **6.2**). For pDNA polyplexes, all PEGylated oligomers with a combination of cationic building blocks and terminal cysteines showed effective pDNA binding already at a low N/P of 6, as evidenced by retardation in the agarose gel electrophoresis. This was largely independent from the cationic backbone, histidine and tyrosine trimer modifications (**Figure 3.2A**, **6.1**). Well consistent with the smaller size of siRNA as compared to pDNA,[151] siRNA polyplexes displayed less stability in the agarose gel shift assay (**Figure 3.2B**, **6.2**).

For the majority of oligomers, an N/P ratio of 12 or higher was required for stable nucleic acid complexation indicated by complete retardation in the agarose gels. Interestingly, integration of tyrosine trimers (#9-16, #35-36) did not promote polyplex stability. This observation apparently contradicts our previous studies with non-PEGylated siRNA lipopolyplexes.[105] It can, however, be explained by the presence of PEG in the present oligomers. PEG increases solubility and thus counteracts the hydrophobic interactions of tyrosine trimer domains. On the other hand, insertion of histidines slightly increased the

binding ability of the corresponding oligomers.

The ability of oligomers to complex and compact nucleic acids was further evaluated by an ethidium bromide exclusion assay performed at N/P 12 (**Figure 3.3**). The larger cationic backbone provided by four-arm oligomers resulted in a higher compaction compared to two-arm oligomers. Within each subclass, oligomers with four cationic building blocks per arm bound pDNA slightly better than those with only three building blocks (**Figure 3.3A**). With regard to siRNA, the best compaction (monitored by dye exclusion) was observed by using the basic two-arm (#1-4) and four-arm (#21-28) oligomers without further integration of histidines and tyrosine trimers (**Figure 3.3B**). A tendency towards decreased complexation ability with increased insertion of domains into the cationic backbone was found, especially for the two-arm-H-Y_3 group. These results suggest the cationic charge density of the backbone as most critical point for nucleic acid interaction.

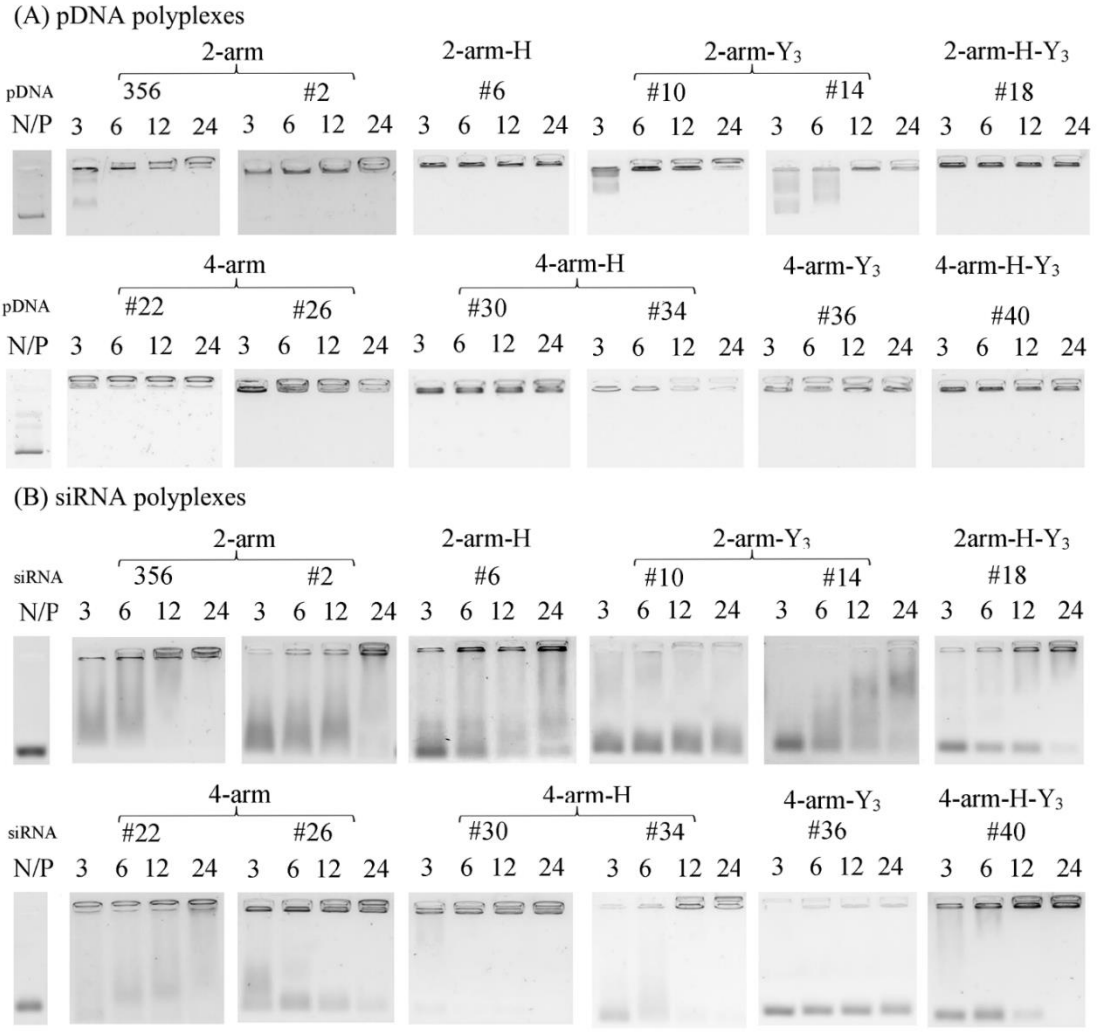

Figure 3.2 Gel retardation assays of selected pDNA (A) or siRNA (B) polyplexes formed in HBG at the indicated different N/P ratios. Left lanes: free pDNA or siRNA, respectively. A full set of data for all oligomers is presented in **Figure 6.1** (pDNA) and **Figure 6.2** (siRNA).

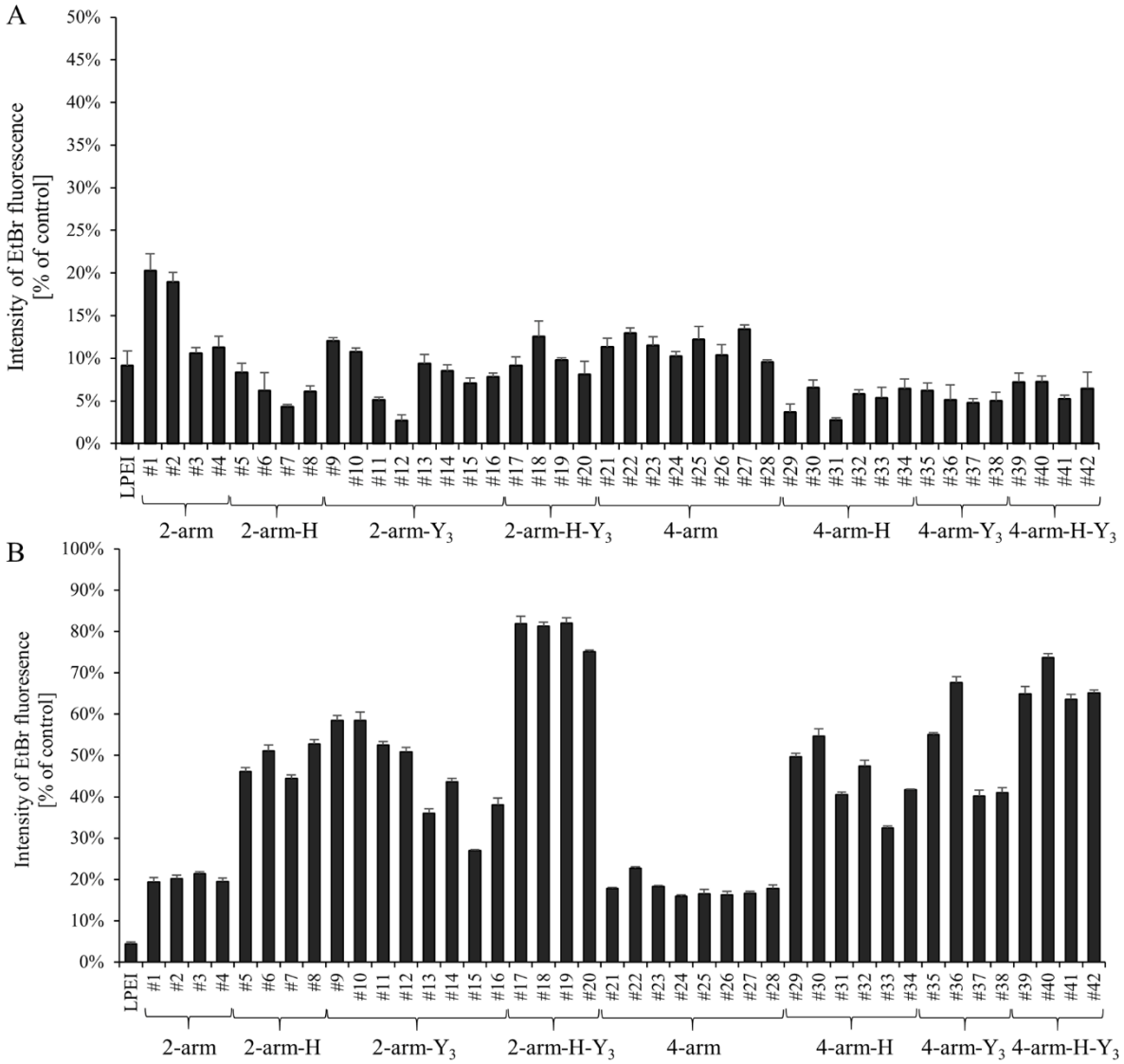

Figure 3.3 Nucleic acid compaction ability of synthesized oligomers as detected by an ethidium bromide exclusion assay. A) pDNA compaction and B) siRNA compaction by different oligomers at N/P 12. Linear 22kDa PEI (LPEI) N/P 6 was used as positive control. The fluorescence intensity of EtBr was determined in relation to the 100% value (samples with only pDNA or siRNA) with a blank solution of HBG buffer. Data were presented as mean + SD (n=3).

Other important biophysical parameters for the evaluation of suitable polyplexes are particle size and zeta potential (**Table 3.1**). pDNA polyplexes (in contrast to small siRNA nanoplexes)[131] can be easily analyzed by dynamic laser light scattering (DLS). Most of the oligomers formed nanoparticles with a Z-average diameter between 100-300 nm and zeta potentials between +5 to +20 mV. However, some FolA conjugates (#10, #12, #14, #16, #18, #20, #30, #32) showed increased size compared to their corresponding control oligomers. Especially for #10 and #12 a low zeta potential and polyplex aggregation with Z-averages above 1000 nm was observed. Apparently the combination of exposed hydrophobic FolA ligands with a reduced electrostatic repulsion between nanoparticles causes colloidal instability and flocculation of polyplexes, which is consistent with other related observations.[148] Oligomers with additional cationic building blocks showed a

slightly higher zeta potential compared to their analogs with less cationic building blocks. Four arm oligomers generally showed a higher zeta potential (between 13- 20 mV) than two-arm oligomers (below 15 mV).

Table 3.1. Particle size (Z-average) and zeta potential of pDNA polyplexes formed at N/P 12 in HBG buffer measured by DLS. Polyplexes were diluted 1:20 with HEPES buffer before measurement. Data were presented as mean ± SD (n=3).

No.	pDNA polyplexes		
	Z-average (nm)	PDI	Zeta potential (mV)
#1	104.6±6.0	0.34±0.06	15.0±0.6
#2	143.4±1.2	0.12±0.01	13.0±0.1
#3	149.0±3.8	0.46±0.01	14.4±0.6
#4	163.7±1.8	0.22±0.03	13.2±0.7
#5	570.6±125.2	0.23±0.04	2.1±0.04
#6	525.1±78.8	0.20±0.01	0.2±0.2
#7	219.9±8.4	0.14±0.03	6.7±0.3
#8	491.9±57.3	0.14±0.03	6.1±0.1
#9	165.1±1.5	0.33±0.3	4.8±0.2
#10	1099±177.2	0.51±0.04	3.2±0.2
#11	156.5±3.0	0.28±0.002	6.5±0.6
#12	1503±42.3	0.54±0.12	6.1±0.4
#13	344.6±59.0	0.54±0.05	6.4±0.6
#14	641.5±133.1	0.20±0.02	6.9±0.8
#15	248.9±40.8	0.50±0.06	8.0±0.1
#16	484.5±68.9	0.18±0.05	8.7±0.3
#17	163.8±10.5	0.10±0.001	5.5±1.2
#18	520.0±75.6	0.13±0.03	6.6±0.2
#19	132.3±1.5	0.12±0.02	8.2±0.1
#20	368.0±48.4	0.11±0.01	10.1±0.6
#21	177.3±3.5	0.37±0.02	13.1±0.9
#22	561.5±29.1	0.34±0.03	14.1±0.3
#23	147.6±0.9	0.25±0.01	15.3±0.8
#24	198.5±1.2	0.13±0.003	17.5±0.5
#25	144.9±2.7	0.45±0.02	15.1±0.6
#26	136.9±0.7	0.09±0.004	15.2±0.5
#27	114.1±1.1	0.35±0.01	17.8±1.5
#28	120.3±2.9	0.12±0.01	20.4±0.5
#29	140.8±0.2	0.31±0.02	14.1±0.5
#30	576.7±146.9	0.27±0.03	13.5±0.3
#31	132.5±2.3	0.24±0.01	14.1±0.4
#32	673.7±94.4	0.28±0.02	14.8±0.3
#33	125.6±2.82	0.39±0.01	13.9±0.4
#34	156.1±4.4	0.10±0.01	16.0±0.6
#35	125.2±4.9	0.15±0.02	14.1±0.6
#36	123.2±2.0	0.12±0.01	17.6±0.2
#37	120.8±2.0	0.16±0.01	15.2±0.2
#38	113.7±1.1	0.12±0.01	19.5±0.6
#39	130.7±1.6	0.26±0.01	15.6±0.7
#40	164.9±2.2	0.13±0.02	19.2±0.9
#41	150.5±1.6	0.30±0.02	16.5±0.5
#42	122.7±2.9	0.13±0.02	20.8±0.2

Next, we investigated the buffer capacity in the physiological pH range between extracellular and endolysosomal environment (between pH 7.4 and pH 5) for selected oligomers using alkalimetric back titration (**Table 3.2**). The two-arm Stp oligomers #5 and #7 modified with histidines exhibited the by far highest buffering capacity. For four-arm oligomers, the highest buffer capacity was found for the histidine containing oligomers #29 and #31.

Table 3.2 Total buffer capacity of selected oligomers between pH 5.0 to 7.4 measured by acidification to pH 2 and back titration with NaOH.

Oligomer	Buffer capacity
#2	21.9%
#4	24.5%
#5	29.5%
#7	29.0%
#21	20.2%
#23	18.3%
#25	19.7%
#27	19.0%
#29	29.1%
#31	25.8%
#33	21.6%

3.1.3 pDNA transfection

The new oligomers (without or with PEG-linked folate as targeting ligand) were used for pDNA transfection of folate receptor-rich KB cells (**Figure 3.4**, **6.3**). Standard transfections with the displayed nonshielding positive control (LPEI polyplexes) include incubation of cells with transfection complexes for a 4 h period longer than in case of targeted polyplexes, to enable sufficient cell binding and uptake. To verify the role of the faster receptor-mediated uptake in the transfection process, [113, 122, 149] KB cells were incubated with the targeted polyplexes for a reduced period of only 45 min, after which the medium containing the non-bound transfection complexes was exchanged. Transfected cells were further incubated for 24 h with fresh media. The transfection results with selected examples of two-arm oligomers (matched pairs with or without folate targeting ligands) are displayed in **Figure 3.4** (the complete set of data is presented in **Figure 6.3**). Every transfection was performed in the absence or 4 h presence of the endolysosomotropic agent chloroquine, which had been previously found to facilitate endosomal escape of entrapped polyplexes.[150] Comparison of transfection levels plus/minus chloroquine provided a measure of different intracellular transport problems for the individual oligomers. Our previously described Stp two-arm oligomer *356* mediated efficient gene transfer only with the help of chloroquine, suggesting that endosomal

escape represented a serious bottleneck which still had to be overcome. Also oligomers substituted with the larger building block Sph (e.g. #2) displayed this strong limitation. An analogous Stp two-arm oligomer with integrated histidines (#6) displayed a greatly improved pDNA transfection efficacy. The transgene expression levels in the absence of chloroquine equaled those of *356* in the presence of chloroquine. The addition of chloroquine further (approximately 10-fold) increased luciferase activity, consistent with our previous studies using different targeting ligands.[23, 109]

The alternative modification of the Stp oligomer *356* with tyrosine trimers (#10) showed very low gene transfer activity with or without chloroquine. In contrast, the Sph oligomer #14 with tyrosine trimers exhibited an enhanced transfection activity as compared to the tyrosine free analog #2; effective gene transfer without chloroquine was observed at N/P 12 and higher. The by far highest transgene expression (approx. 100.000-fold above background) was achieved with the Stp-based FolA-targeted two-arm oligomer (#18) by combined histidine and tyrosine trimer incorporation. Importantly, all negative control analogs lacking the targeting ligand folic acid showed negligible gene transfer activity. Regarding four-arm oligomers (**Figure 3.4B**), a similar tendency could be observed. The basic four-arm Stp oligomer without histidines or tyrosine trimers (#22) could already mediate moderate gene transfer without chloroquine, presumably as a result of the higher molecular fraction with cationic charge. However, chloroquine still significantly improved the transfection efficiency. For oligomer #26 based on Sph, the transfection activity without chloroquine also improved compared to the two-arm analog (#2). After modification with histidines, the transfection efficiency of the targeted oligomers (#30, #34) was greatly improved and similar efficacy could be achieved in transfections without or with chloroquine. Surprisingly, also the non-targeted oligomer #29 was moderately active at low N/P ratio. Consistent with the observation for two-arm oligomers, the modification of four-arm oligomers with tyrosine trimers alone (#35, #36) did not enhance pDNA delivery efficiency. Finally, four-arm oligomers were modified with a combination of histidines and tyrosine trimers. Non-targeted oligomer #39 showed medium gene transfer without chloroquine, and decreased transfection efficiency with chloroquine. The highest transfection activity of all four-arm oligomers could be achieved by oligomer #40 at the low N/P 3, and the transfection efficiency dramatically decreased with increased oligomer amount for toxicity reasons as explained below. Again, the control oligomers lacking the targeting folate showed low transfection efficiency compared to the folate containing oligomers.

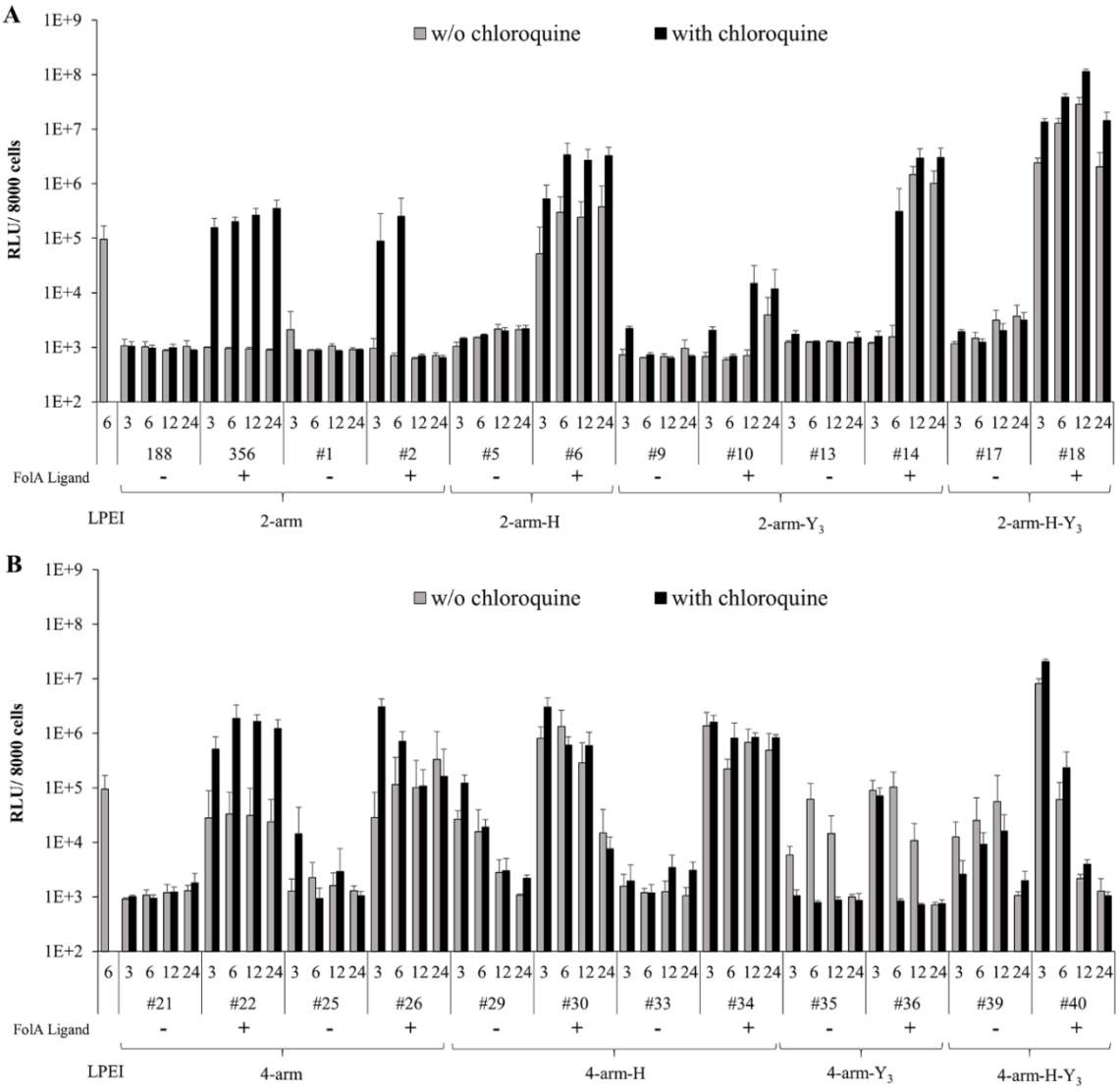

Figure 3.4 Gene transfer in folate receptor expressing KB cells with selected examples of A) two-arm and B) four-arm oligomers. The lane FolA Ligand (- or +) refers to the absence or presence of folate ligand within the indicated oligomer. Luciferase pDNA oligomer polyplexes formed at N/P 3, 6, 12 or 24 were incubated with KB cells for the short period of 45 min, followed by replacement of transfection medium by fresh medium with (black bars) or without (grey bars) chloroquine for 4 h additional incubation before another medium exchange. LPEI polyplexes (at N/P 6, incubation with cells for a 4 h longer period before medium exchange) were set as the positive control. Luciferase activities at 24 h after transfection are presented in relative light units (RLU) as the mean + SD (n=5). A full set of data for all oligomers is presented in **Figure 6.3**. The experiments were performed by Ana Krhac Levacic and Dr. Petra Kos (Pharmaceutical Biotechnology, LMU Munich).

In parallel to the gene transfer studies, metabolic activities of KB cells were evaluated by an MTT assay after transfection with the pDNA polyplexes. Importantly, only the four-arm oligomers containing tyrosine trimers (#35-42) showed obvious toxicity at higher N/P ratios (**Figure 3.5B**), which correlated well with the transfection data. Presumably, the increased hydrophobicity caused by the higher number of tyrosines in four-arm oligomers led to increased cytotoxicity. A slight toxicity could be observed for #32 (four-arm oligomer

containing histidines) at higher N/P of 12 and 24 (**Figure 6.4**). All other tested pDNA polyplexes did not cause toxicity, whereas the 4 h co-incubation with chloroquine triggered a slight reduction of cell viability after transfection (**Figure 3.5A, 6.4**).

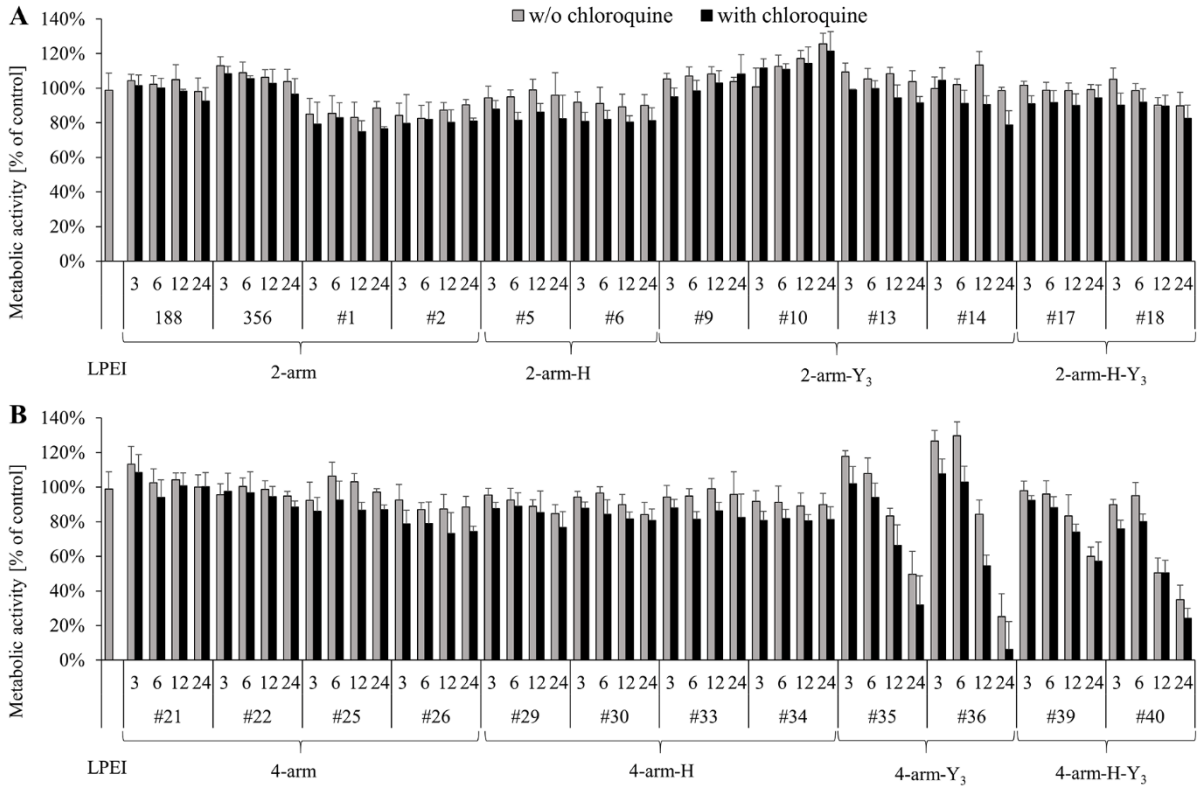

Figure 3.5 Metabolic activities of KB cells after transfection with the pDNA polyplexes as evaluated by an MTT assay. pDNA/oligomer polyplexes formed at N/P 3, 6, 12 or 24 were incubated with KB cells for 45 min, followed by replacement of fresh medium with (black bars) or without (grey bars) chloroquine for 4 h additional incubation before another medium exchange. LPEI polyplexes (at N/P 6, incubation with cells for 4 h longer period before medium exchange) were set as the reference. Metabolic activities (%) were presented as the percentage relative to the buffer treated control cells. The data are shown as mean + SD (n=5). A full set of data for all oligomer polyplexes is presented in **Figure 6.4**. The experiments were performed by Ana Krhac Levacic and Dr. Petra Kos (Pharmaceutical Biotechnology, LMU Munich).

Cellular uptake of pDNA polyplexes was investigated by flow cytometry using polyplexes formed with Cy5-labeled pDNA (**Figure 3.6**). Based on the transfection results, the majority of polyplexes were formed at N/P 12. For four-arm oligomers which displayed toxicity at higher N/P ratios, the optimum at lower N/P of 3 was chosen for the uptake study (**Figure 3.7**). In all cases folate-targeted oligomers mediated a higher cellular uptake than polyplexes of non-targeted control oligomer. This beneficial uptake of targeted polyplexes was consistent with the transfection data and confirmed the targeting effect.

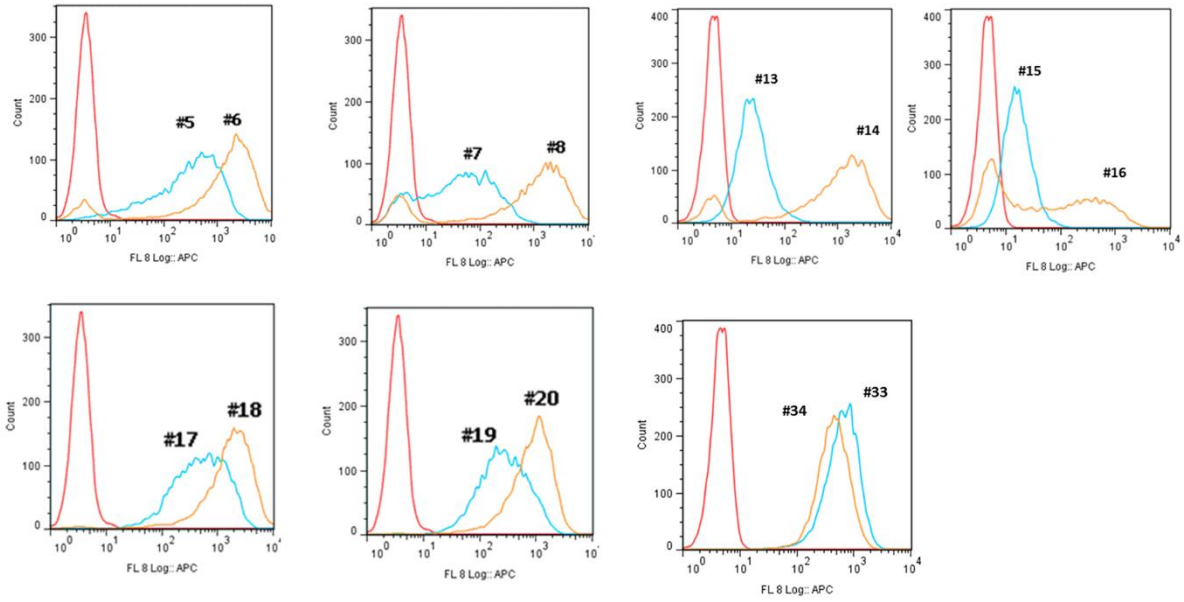

Figure 3.6 Cellular internalization of selected Cy5-labeled pDNA (N/P 12) polyplexes after 45 min determined by flow cytometry. The intensity of the Cy5 signal indicates the amount of polyplexes being internalized by KB cells. Red curve, HBG buffer only treated cells; orange curve, folate containing oligomers treated cells; and blue curve, ligand free control oligomers treated cells. All experiments were performed in triplicate. The experiment was performed by Ana Krhac Levacic (PhD student, Pharmaceutical Biotechnology, LMU Munich).

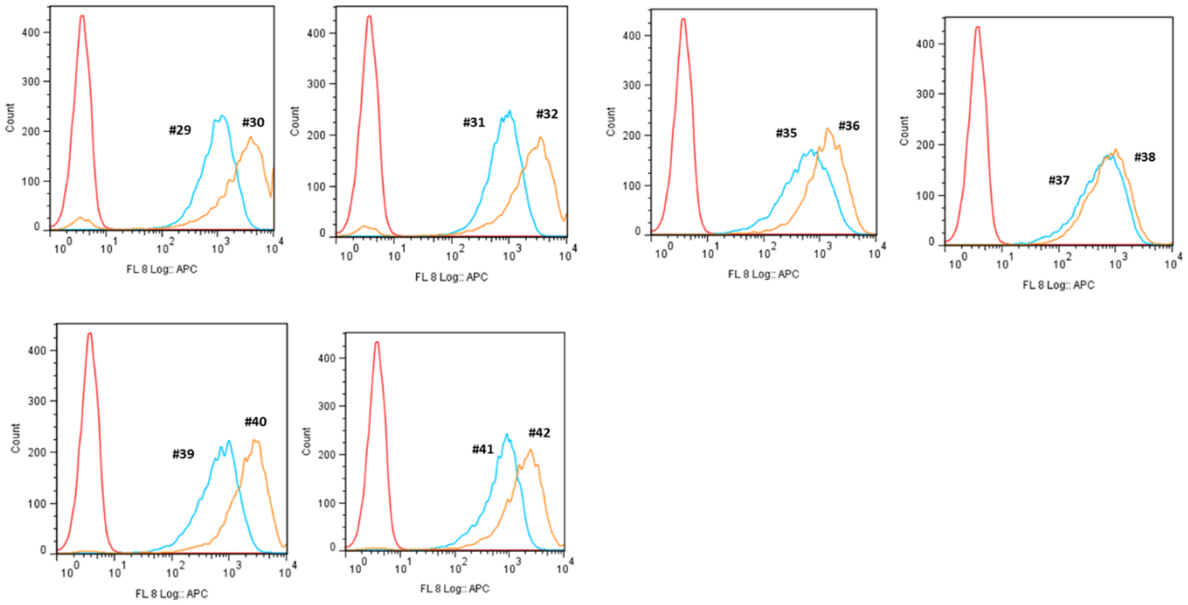

Figure 3.7 Cellular internalization of selected Cy5-labeled pDNA (N/P 3) polyplexes after 45 min determined by flow cytometry. The intensity of the Cy5 signal indicates the amount of polyplexes being internalized by KB cells. Red curve, HBG buffer only treated cells; orange curve, folate containing oligomers treated cells; and blue curve, ligand free control oligomers treated cells. All experiments were performed in triplicate. The experiment was performed by Ana Krhac Levacic (PhD student, Pharmaceutical Biotechnology, LMU Munich).

3.1.4 siRNA transfection

The oligomer library was also tested for its gene silencing ability with siRNA using KB-eGFPLuc cells. **Figure 3.8** and **3.9** present results with selected two-arm or four-arm oligomers, respectively, **Figure 6.5** presents the whole set of data. In this eGFP-luciferase gene silencing screen, FolA ligand containing oligomers were compared with ligand-free controls, and the specific siGFP was compared with control siRNA siCtrl. In addition, based on our previous studies with oligomer *356*,[113] siRNA modified with the endosomolytic Inf7 peptide was used to facilitate endosomal escape of polyplexes. As expected, oligomer *356* showed efficient gene silencing with siGFP-Inf7, and moderate knockdown with unmodified siGFP. When compared to the non-targeted oligomer *188*, a clear targeting effect was demonstrated. Sph substituted oligomers #1-2 (**Figure 3.8A**) could only mediate moderate gene silencing with siGFP-Inf7, while #3-4 (**Figure 6.5**) with one additional Sph on each arm displayed effective silencing comparable or even superior to *356*. However, no obvious receptor targeting effect was observed. This lack of receptor specificity was well consistent with the analogous pDNA transfection activity. The elongation of the oligocationic Sph arms seems to enable nonspecific cellular attachment and uptake. It may be noted that a change from three Sph units (a length equivalent of >18 aminoethane units) to four units (a length equivalent of >24 aminoethane units) results in an length of the oligocation arm beyond the 24 ethylene glycole units of the PEG shielding arm. Regarding histidine modified oligomers #5-8 (**Figure 3.8B**, **6.5**), despite the enhanced buffer capacity of these oligomers, only a moderate knockdown could be achieved. In case of tyrosine trimers containing two-arm oligomers #9-16 (**Figure 3.8C**, **6.5**), the folate-targeted compounds showed improved gene silencing of up to 60% compared to the non-targeted oligomers, however the transfection activity remained lower than that of *356*. The two-arm oligomers #17-20 (**Figure 3.8D**, **6.5**), modified with both histidine and tyrosine trimers, exhibited the most impressive gene silencing, comparable to *356* and even superior at low N/P ratios. Importantly, these oligomers could also mediate effective silencing to the same level for both siGFP with or without endosomolytic siGFP-Inf7. However, in sharp contrast to *356* and also to the pDNA transfection results, only small differences were observed between the targeted or non-targeted oligomers with regard to transfection (**Figure 3.8D**, **6.5**) and cellular uptake (see below). Apparently, the extension of the oligocation arms by histidines and tyrosines, together with the different characteristics of siRNA and pDNA polyplexes (**Figure 6.1, 6.2**, **3.3**), are responsible for this difference.

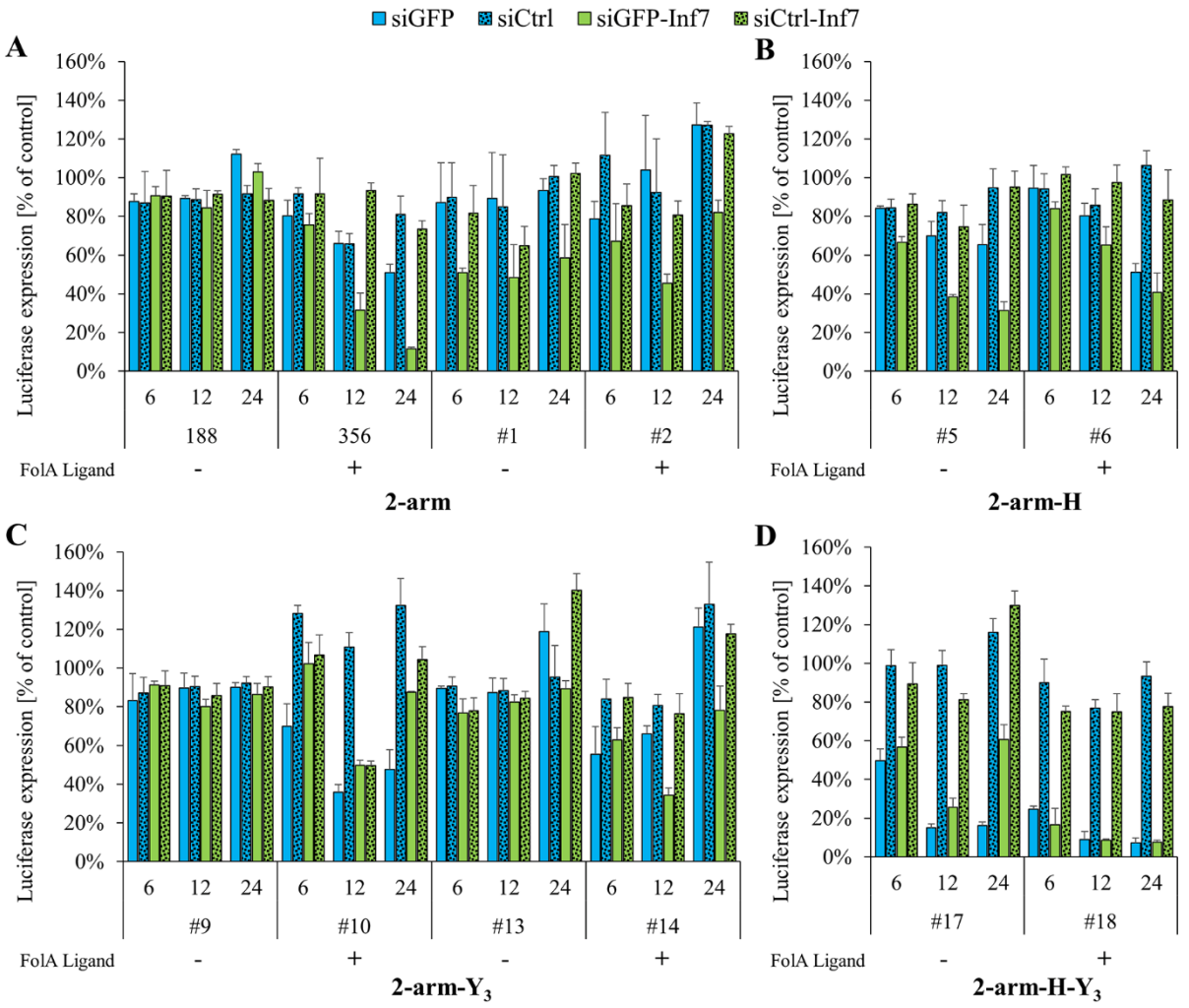

Figure 3.8 Gene silencing in folate receptor expressing KB-eGFPLuc cells with two-arm oligomers: (A) oligomers without core modification; (B) oligomers modified with histidines; (C) with tyrosine trimers; (D) with both histidines and tyrosine trimers. The lane FolA Ligand (- or +) refers to the absence or presence of folate ligand within the indicated oligomer. eGFP targeted siRNA (siGFP, blue bars), control siRNA (siCtrl, blue bars with pattern) polyplexes and corresponding Inf7 peptide modified siRNA polyplexes (siGFP-Inf7, green bars, and siCtrl-Inf7, green bars with pattern) formed at N/P 6, 12 and 24 were tested for eGFPLuc gene silencing in KB-eGFPLuc cells. Cells were incubated with polyplexes for a short period of only 45 min, followed by replacement of transfection medium with fresh medium. Luciferase activities at 48 h after transfection are presented in percentage of relative light units (RLU) obtained with buffer treated control cells. The data are shown as the mean + SD (n=3). A full set of data for all oligomers is presented in **Figure 6.5**. The experiment was performed by Katharina Müller (PhD student, Pharmaceutical Biotechnology, LMU Munich).

For four-arm oligomers (**Figure 3.9A**, **6.5**), regardless of the cationic building block, effective gene silencing equal to *356* or better was observed when using lytic siGFP-Inf7. However, also here no clear ligand dependency was detected. The oligomers #29-34 modified with histidines (**Figure 3.9B**, **6.5**) demonstrated a slightly reduced knockdown, but interestingly, oligomer #30 showed targeting efficiency compared to its negative control #29. The integration of tyrosine trimers into the four-arm structures led to loss of transfection activity (**Figure 3.9C**, **6.5**). Similar to two-arm oligomers, four-arm oligomers

#39 and #40 modified with both histidines and tyrosine trimers (**Figure 3.9D**, **6.5**) exhibited obvious knockdown even at the lowest N/P ratio of 6 and without using the lytic siGFP-Inf7. However, this type of oligomers again demonstrated no targeting effect, since the knockdown was independent of the presence of a targeting ligand.

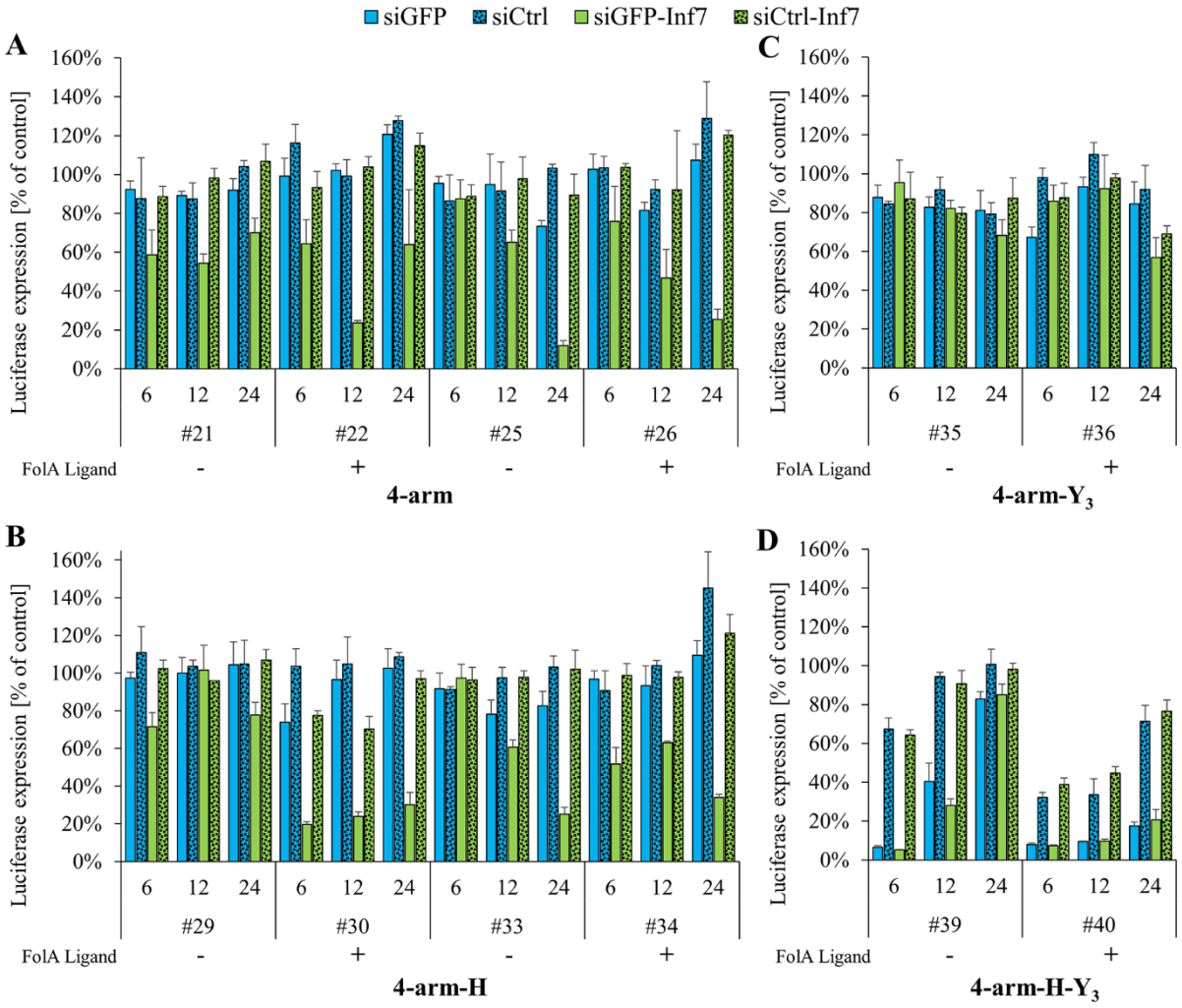

Figure 3.9 Gene silencing in folate receptor expressing KB-eGFPLuc cells with four-arm oligomers: (A) four-arm oligomers without core modification; (B) oligomers modified with histidines; (C) modified with tyrosine trimers; (D) modified with both histidines and tyrosine trimers. The lane FolA Ligand (- or +) refers to the absence or presence of folate ligand within the indicated oligomer. Polyplexes of eGFP targeted siRNA (siGFP, blue bars), control siRNA (siCtrl, blue bars with pattern) and corresponding Inf7 peptide modified siRNA (siGFP-Inf7, green bars, and siCtrl-Inf7, green bars with pattern) formed at N/P 6, 12 and 24 were tested for eGFPLuc gene silencing in KB-eGFPLuc cells. Cells were incubated with polyplexes for 45 min, followed by replacement of transfection medium by fresh medium. Luciferase activities at 48 h after transfection are presented as percentage of relative light units (RLU) obtained with buffer treated control cells. The data are shown as the mean + SD (n=3). A full set of data for all oligomers is presented in **Figure 6.5**. The experiments were performed by Katharina Müller (PhD student, Pharmaceutical Biotechnology, LMU Munich).

Four-arm oligomers (#39-42) with a combined modification of tyrosine trimers and histidines showed also a reduction of luciferase activity when transfected with siCtrl (**Figure 3.9**, **6.5**), consistent with an unspecific cytotoxicity which was also observed for

the corresponding pDNA polyplexes. All other oligomers transfected with siCtrl exhibited no obvious reduction of luciferase activity, suggesting good biocompatibility of these oligomers.

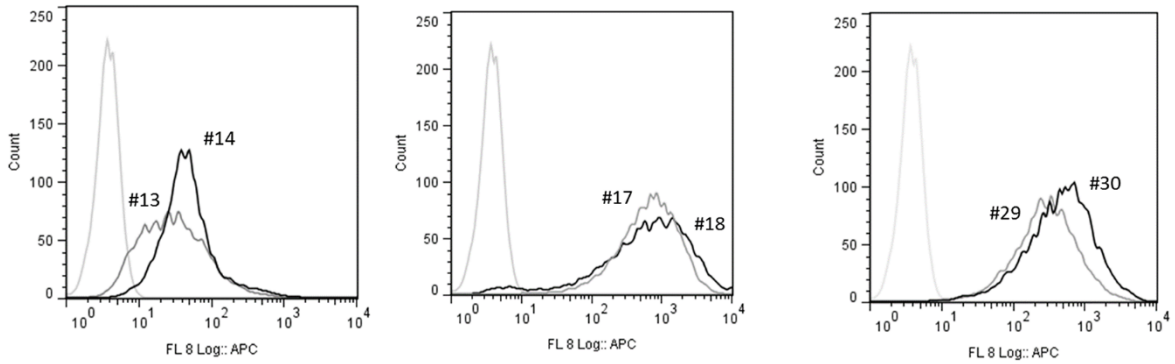

Figure 3.10 Cellular internalization of selected Cy5-labeled siRNA (N/P 12) polyplexes after 45 min determined by flow cytometry. The intensity of the Cy5 signal indicates the amount of polyplexes being internalized by KB-eGFPLuc cells. Light grey curve, HBG buffer only treated cells; dark grey curve, ligand free control oligomers treated cells; and black curve, folate containing oligomers treated cells. All experiments were performed in triplicate. The experiments were performed by Katharina Müller (PhD student, Pharmaceutical Biotechnology, LMU Munich).

Cellular uptake studies for siRNA polyplexes formed with Cy5-labeled siRNA in folate receptor overexpressing KB cells are presented in **Figure 3.10**. As many of the folate containing oligomers according to the transfection results showed no targeting effect, we chose the most promising members #14, #18, #30 and their corresponding negative controls #13, #17, #29 to evaluate the uptake properties. In all of these cases folate-targeted oligomers showed a slightly higher cellular uptake than non-targeted control oligomers. The high uptake of polyplexes formed with the oligomers #17 and #18 containing both histidine and tyrosine trimers was consistent with the efficient gene silencing of those oligomers.

3.2 Combinatorial polyplexes for folate receptor targeted siRNA delivery

Successful applications of RNAi-based cancer therapy require sufficient intracellular delivery of siRNA to the target site and effective knockdown of targeted transcripts. Thus, an ideal siRNA delivery system should possess multifunctionalities to conquer multiple barriers all the way to its site of action[151]. Despite recent development of various potential siRNA carriers, systemic delivery of siRNA with specificity to the tumor site remains a major limitation.

Derived from the classic gene carrier polyethylenimine (PEI) [127] a set of artificial amino acids was developed comprising repeats of the 1,2-diaminoethane motif [99]. Such artificial oligoamino acids, like succinoyl-tetraethylene pentamine (Stp) and succinoyl-pentaethylene hexamine (Sph) [100], in combination with natural α-amino acids, were applied in solid-phase assisted synthesis to generate sequence-defined cationic oligomers [101]. These oligomers provide excellent nucleic acid binding ability, endosomal buffering capacity, and site-specific positioning of multiple functionalities. Further studies have been undertaken to optimize such cationic carriers by systematic variation of the topology [103], inclusion of small chemical delivery motifs such as buffering histidines [23], fatty acids [102], tyrosine trimers [105], disulfide-forming units [106], targeting ligands [107, 109-113, 131] and combinations of such elements [152]. Accordingly, this strategy of a step-by-step optimization resulted in a library of >1000 oligomers which included precise multifunctional siRNA carriers.

Combination of two different oligomers from the library provides an alternative efficient option to obtain a multifunctional carrier, which may formulate therapeutic nucleic acids and overcome possible disadvantages of single oligomers. For example, a c-Met targeting PEGylated oligomer, which is deficient in DNA condensation, was combined in a 7/3 ratio with a 3-arm oligomer to facilitate nucleic acid compaction [110]. In our current work, we focused on the targeting of folate receptor (FR)-overexpressing tumors. We selected PEGylated folate-conjugated oligomers (for FR targeting and shielding of surface charges) and optimized the physicochemical properties of polyplexes by combination with a 3-arm oligomer (for optimizing particle size and stability) at various molar ratios. For uni-directional fast coupling between the two types of oligomer, we activated the cysteine thiol groups of one of the oligomers with 5,5'-dithio-bis(2-nitrobenzoic acid) (DTNB) to achieve a fast chemical linkage through disulfide formation with the free thiol groups of the other oligomer. These targeted combinatorial polyplexes (TCP) have been systemic investigated, regarding the particle size, zeta potential, siRNA compaction, receptor specific cellular uptake, and siRNA silencing *in vitro* and *in vivo*.

3.2.1 Oligomer synthesis and formation of targeted combinatorial polyplexes (TCPs)

Based on our previous studies, we selected four oligomers from the library to generate novel co-formulations for targeted siRNA delivery (**Scheme 3.1**). 3-arm Stp oligomers *386* and *689*, was chosen for their strong siRNA binding ability, which provide a highly stable

cationic core to compact siRNA [101, 102, 109, 153]. Moreover, PEG-folate-conjugated Sph oligomers (4-arm) *709* and (2-arm) *717*, were used for folate receptor (FR) targeting and surface shielding [152]. Here we combined these two types of oligomers, in order to optimize the siRNA polyplexes with a co-formulation strategy. All oligomers contain terminal cysteines with free thiol groups for subsequent disulfide formation within siRNA polyplexes. As standard disulfide formation by air oxidation was previously found to be a rather slow and incomplete process, we intended to make this step faster and more specific. Therefore, we activated the thiol groups of oligomer @1 with 5,5'-dithio-bis(2-nitrobenzoic acid) (DTNB) to produce TNB-modified oligomer (**Figure 3.11A**). The TNB-modified oligomer forms binary siRNA polyplex with siRNA, and the following incubation with the unmodified thio-oligomer @2 will undergo a fast uni-directional coupling of TNB-modified oligomer through disulfide formation with the free thiol groups of thio-oligomer @2. The combination of siRNA with both oligomers thus generates targeted combinatorial polyplexes (TCP), which are composed of compact cationic core for siRNA binding, well-shielded PEG layer and folates as targeting ligands (**Figure 3.11B**). TCPs were optimized by testing different TNB-modified oligomers @1/unmodified thiol oligomers @2 at various molar ratios, and evaluating different siRNA and the two oligomers mixing sequences. Preliminary gene silencing experiments (**Figure 6.6** and unpublished data) demonstrated similar efficiencies of the tested mixing sequences, with the first alternative (pre-incubated siRNA with the TNB-modified oligomer, followed by disulfide exchange reaction with thiol oligomer). For practical reasons, all further testing was performed with this mixing sequence. Four combinatorial formulations, TCP1, TCP2, TCP3 and TCP4 (**Scheme 3.1**), were developed. Both TCP1 and TCP3 contain *386* + *709* in disulfide-linked form, both TCP2 and TCP4 contain histidinylated 3-arm *689* + *717* PEG-folate 2-arm oligomer. Differences rise from the alterative TNB-activations of oligomers. After systematic screening and evaluating different molar ratios of oligomers (see **Tables 6.2-6.5** and next section), equal molar (1:1) oligomer ratios and an N/P ratio of 16 was determined as most useful for the subsequent TCP studies.

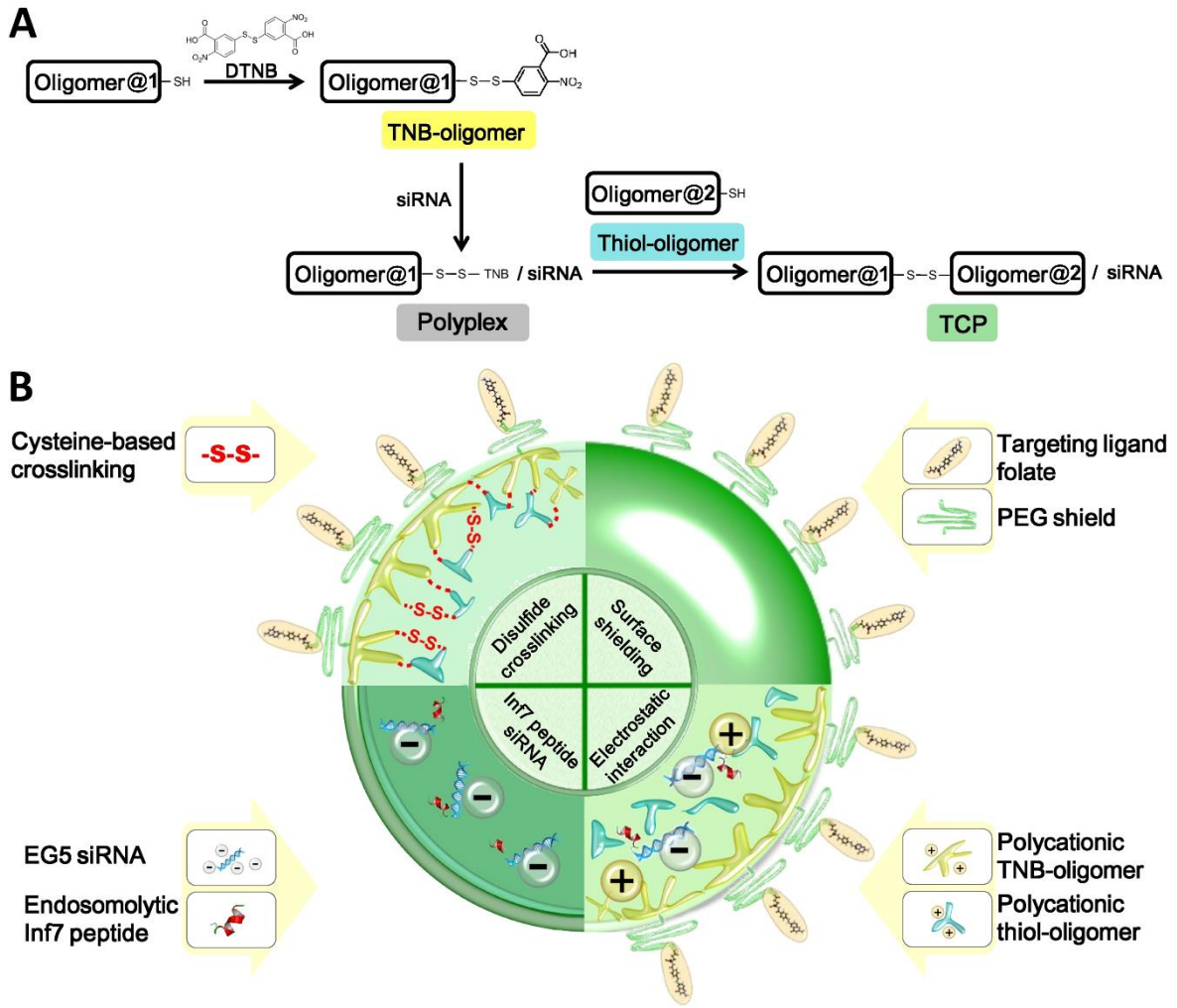

Figure 3.11 Targeted combinatorial polyplexes (TCP) with folate ligand for siRNA delivery. A) TNB-modified oligomer @1 was obtained by reacting the solid-phase derived oligomer with 10 eq DTNB for 2 h at room temperature. The incubation of TNB-modified oligomer @1 with siRNA formed polyplex. Addition of thio-oligomer resulted in fast uni-directional coupling of TNB-modified oligomer through disulfide formation with the free thiol groups of thio-oligomer @2. B) siRNA, TNB-modified oligomer @1 and unmodified thio-oligomer @2 were formulated to produce TCP. Endosomolytic Inf7 peptide was conjugated to siRNA for enhanced endosomal escape [113]. Figure design by Dian-Jang Lee (PhD student Pharmaceutical Biotechnology, LMU Munich).

	TCP1	TCP3
TNB Oligomer @1	(4-arm ***873***) K-(PEG$_{24}$-Folate)-K-[K-(Sph$_4$-C-TNB)$_2$]$_2$ (N/P 11.2)	(3-arm ***769***) TNB-C-Stp$_3$-K-(Stp$_3$-C-TNB)$_2$ (N/P 4.8)
Thiol Oligomer @2	(3-arm ***386***) C-Stp$_3$-K-(Stp$_3$-C)$_2$ (N/P 4.8)	(4-arm ***709***) K-(PEG$_{24}$-Folate)-K-[K-(Sph$_4$-C)$_2$]$_2$ (N/P 11.2)
Combined Structure	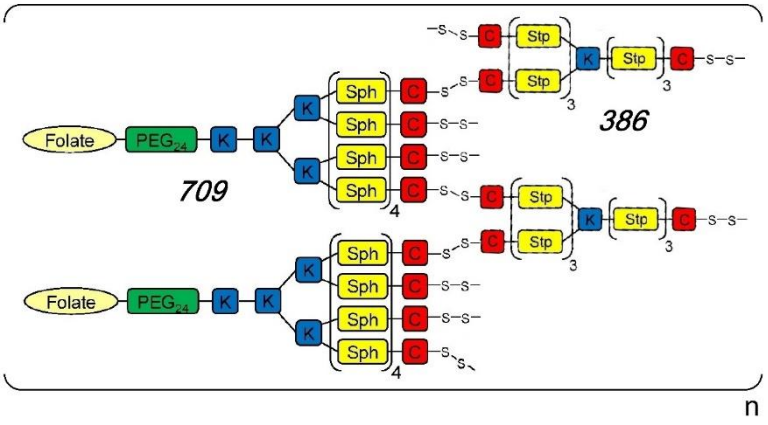	

(709-S-S-386-S-S)$_n$

	TCP2	TCP4
TNB Oligomer @1	(3-arm ***770***) TNB-C-H-(Stp-H)$_3$-K-[(H-Stp)$_3$-H-C-TNB]$_2$ (N/P 7.4)	(2-arm ***874***) K-(PEG$_{24}$-Folate)-K-(Sph$_4$-Y$_3$-C-TNB)$_2$ (N/P 8.6)
Thiol Oligomer @2	(2-arm ***717***) K-(PEG$_{24}$-Folate)-K-(Sph$_4$-Y$_3$-C)$_2$ (N/P 8.6)	(3-arm ***689***) C-H-(Stp-H)$_3$-K-[(H-Stp)$_3$-H-C]$_2$ (N/P 7.4)
Combined Structure	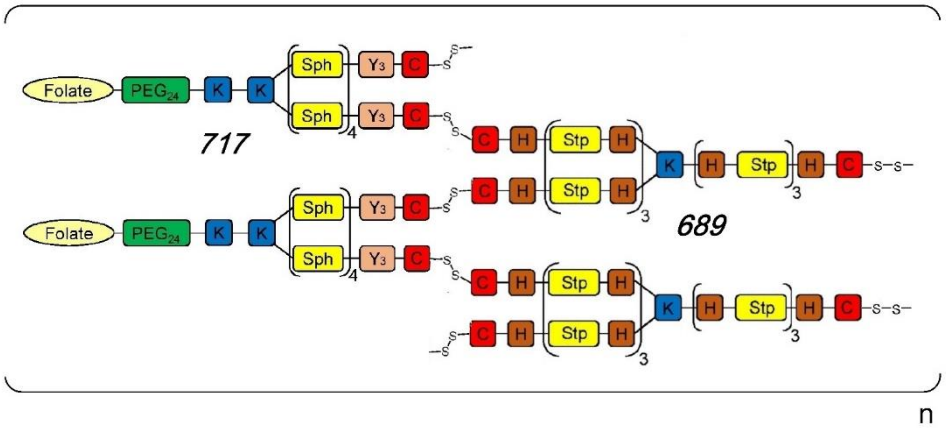	

(717-S-S-689-S-S)$_n$

Scheme 3.1 Targeted combinatorial polyplex (TCP) formulations. siRNA was co-formulated with TNB-modified oligomers @1 and unmodified thiol-oligomers @2 at various molar ratios to form the TCP carriers. In most experiments polyplexes were formed at N/P 16 using an equal molar oligomer ratio of 1:1; for these conditions the individual N/P ratio of each oligomer is presented. The oligomer sequences are indicated (left to right) from C- to N- terminus. C: cysteine; H: histidine; K: lysine; Y: tyrosine; S-S: disulfide crosslinking; PEG24: polyethylene glycol; TNB: 5-thio-2-nitrobenzoic acid; Stp: succinoyl-tetraethylene pentamine; Sph: succinoyl-pentaethylene hexamine. K-(and K-[refer to branchings by α- and ε-amino modification of lysines. Scheme design by Dian-Jang Lee (PhD student Pharmaceutical Biotechnology, LMU Munich).

3.2.2 Physico-chemical characteristics of TCPs

Formulating TCPs (**Scheme 3.1**) at N/P 16, we measured the particle sizes by dynamic laser-light scattering (DLS) based on different molar ratios of [TNB-modified oligomer @1 / unmodified thiol-oligomer @2] (**Table 6.2-6.5**). At the ratio of 1:1, the sizes of the two *386+709* formulations, TCP1 and TCP3, are 104 nm and 209 nm, respectively, whereas the two *689+717* formulations, TCP2 and TCP4, have a larger size of ~ 400 nm (**Table 3.3**). To examine the effect of PEG shielding on the surface charge of TCPs, zeta potentials of siRNA polyplexes at N/P 16 were measured (**Table 3.3**). For TCP1, TCP2 and TCP4, the zeta potential values were reduced from approximately ≥ +20 mV [101] to values around + 8-9 mV. It is interesting to see that TCP3, comprising the same oligomers by a different activation scheme, displays a highly positive zeta potential of +24 mV.

ID	Size (nm)	Zeta Potential (mV)
TCP1	103.5±0.8	9.1±0.2
TCP2	429.4±53	7.93±0.21
TCP3	208.8±3.4	24.3±0.3
TCP4	398.3±63.5	8.1±0.05

Table 3.3 Size and zeta potential of TCPs at N/P 16 measured by dynamic and electrophoretic light scattering. [TNB-modified oligomer / unmodified thio-oligomer] molar ratio = 1:1.

Moreover, to validate the siRNA binding activity of TCPs, we analyzed the siRNA polyplex formation by agarose gel shift assay (**Figure 6.7-6.10**). In general, when increasing the fraction of 3-arm Stp oligomers in TCP formulations, the siRNA binding was significantly increased. Apparently the 3-arm Stp oligomers were essential for the compaction and the stability of siRNA polyplexes.

3.2.3 Gene silencing efficiency of TCPs

We next evaluated their ability to induce target gene silencing. In order to validate this, we used siRNA targeting eGFP (siGFP) or control siRNA (siCtrl) to transfect the KB/eGFPLuc cells, which are stably expressing eGFP-Luciferase (eGFPLuc) fusion protein, and evaluated gene silencing of siRNA polyplexes via luciferase activity by luminometric analysis. Our previous studies indicated that PEGylated siRNA polyplexes, similar as several other PEG-shielded polyplexes [140], face the problem of endosomal entrapment into the cytosol [113]. For this reason, the synthetic peptide Inf7, previously designed as pH-specific analog of the influenza virus hemagglutinin subunit 2 (HA2) N-terminal fusion sequence [29, 144, 154], was covalently coupled to siRNA as

endosomolytic agent [42, 113, 131]. In this assay, we sought to compare the transfection efficiency of TCPs with the previously published *356* [113]. As shown in **Figure 3.12**, all the TCP formulations containing Inf7-modified siGFP (siGFP-Inf7) at N/P 16 mediated significant gene silencing efficiency in KB/eGFPLuc cells, as 75-94% of luciferase activity was suppressed. Among these TCP formulations, TCP1 exhibited the most potent gene silencing activity (94%), which is comparable to *356* nanoplexes (90%) and superior to the rest of TCPs. In contrast, in the cells treated with standard siGFP polyplexes, the silencing effect was significantly decreased (45-63% for TCPs and 35% for *356*). The luciferase activity in KB/eGFPLuc cells treated with controls, including siCtrl polyplexes and siCtrl-Inf7 polyplexes were similar to untreated cells, which suggested that there is no intrinsic cytotoxicity of TCPs.

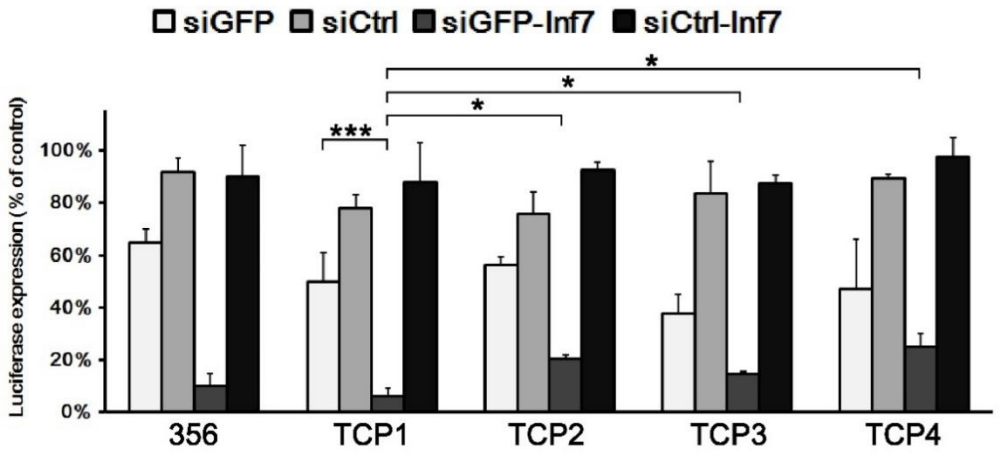

Figure 3.12 Gene silencing efficiency of TCPs in KB cells expressing eGFPLuc fusion protein (KB/eGFPLuc cells). The siRNA polyplexes were prepared at N/P 16 with different siRNA sequences: eGFP-targeted siRNA (siGFP), control siRNA (siCtrl), or siRNA chemically linked with the endosomolytic peptide Inf7 (siGFP-Inf7 or siCtrl-Inf7). Statistical analysis of the results (mean ± SEM) was evaluated by unpaired t test: *p<0.05; **p<0.01; ***p<0.001. The experiments were performed by Dian-Jang Lee (PhD student, Pharmaceutical Biotechnology, LMU Munich).

3.3 Sequence-defined branched oleoyl oligoaminoamides for nucleic acid delivery

3.3.1 Synthesis of sequence-defined branched oleoyl oligoaminoamides

Previous studies have demonstrated that solid-phase synthesis using artificial oligoamino acids (like Stp or Sph) as building blocks could be used to synthesis sequence defined cationic oligomers as carriers for nucleic acid delivery. Oligomers with different topology, such as linear, i-shape, T-shape, U-shape, 2-arm, 4-arm and comb structures, have been successfully assembled, and some of them have shown their suitability as nucleic acid

carriers. Previously, lipo-oligomers containing fatty acid have also been introduced as potential delivery vehicle for pDNA and siRNA. Here, we focused on the cationic counterpart of the lipo-oligomers, and investigate the influence of the different cationic branches on the nucleic acid compaction and gene transfer activity. For this purpose, we designed and synthesized a small library of lipo-oligomers with two oleic acid as the hydrophobic domain, while alternating the number of cationic arms with the introduction of lysine as the branching point. Oligomers with one, two, four and even eight cationic arms were assembled. To further identify the effects of the protonable amine on each arm, additionally, oligomers consisting of different numbers of Stp units (1 to 4) on each arm have been included for comparison (**Scheme 3.2**). Oligomers were synthesized via SPS start from Fmoc-Lys(ivDde)-OH loaded 2-Chlorotritylchloride resin, where lysine provides an asymmetrical branching point for the final attachment of oleic acid. For oligomers with one or two cationic arms (*905-908*), a resin with 0.1598 mmol/g loading was used, whereas for highly branched oligomers with four or eight cationic arms (*909-911*), a resin with rather low loading (=0,095 mmol/g) was used to avoid the aggregation during the synthesis. Terminal cysteines were integrated for polyplex stabilization via disulfide formation. The assembly of oligomers was finished after introducing the hydrophobic moiety by coupling oleic acid to an additional lysine, which was coupled to the ***ε-***amine of the preloaded lysine. The sequence of all oligomers used in this study are displayed in **Table 3.4**.

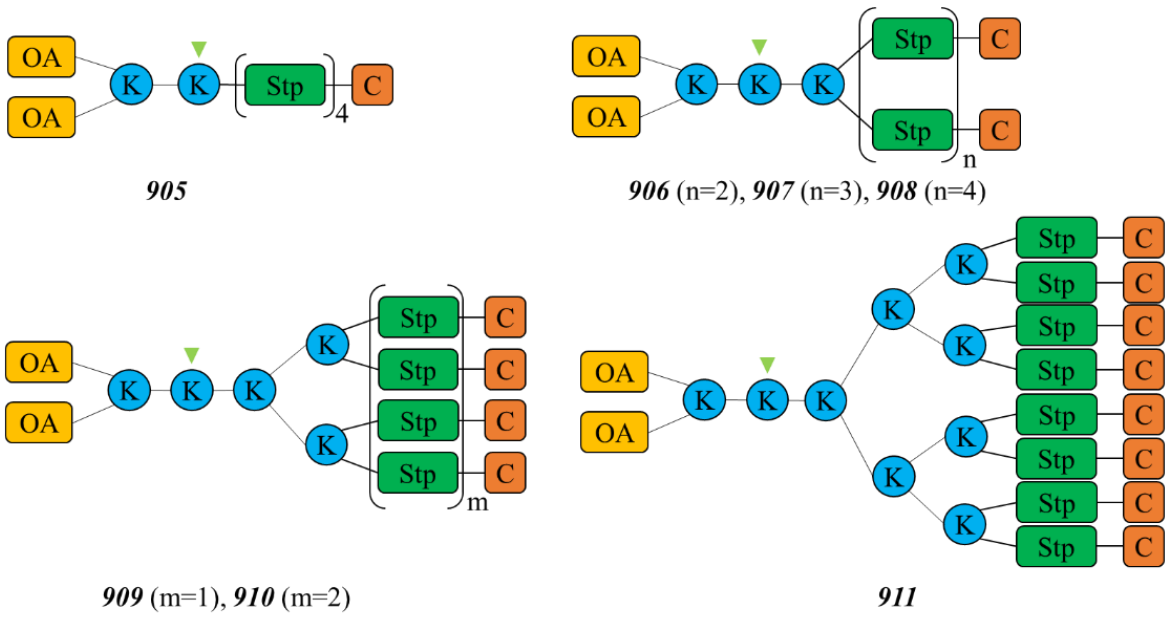

Scheme 3.2 Schematic structures of the synthesized lipo-oligomers. Stp, succinoyl-tetraethylene-pentamine; K, lysine; C, cysteine; OA, oleic aicd. The light green triangle stands for the starting point of SPS.

Table 3.4 Internal library identification number (ID), sequences (from C- to N- terminus) and topology of synthesized lipo-oliomers. Stp, succinoyl-tetraethylene-pentamine; K, lysine; C, cysteine; OA, oleic acid. K-(, K-[and K-{ refer to branchings by α- and ε-amino modification of lysines.

ID	Sequence (C- to N-terminus)	Topology
905	K-(K-OA_2)-Stp_4-C	Linear
906	K-(K-OA_2)-K-(Stp_2-C)$_2$	Two-arm
907	K-(K-OA_2)-K-(Stp_3-C)$_2$	Two-arm
908	K-(K-OA_2)-K-(Stp_4-C)$_2$	Two-arm
909	K-(K-OA_2)-K-[K-(Stp-C)$_2$]$_2$	Four-arm
910	K-(K-OA_2)-K-[K-(Stp2-C)$_2$]$_2$	Four-arm
911	K-(K-OA_2)-K-{K[K-(Stp-C)$_2$]$_2$}$_2$	Eight-arm

3.3.2 Biophysical poperties

To investigate the binding behavior of these oligomers with nucleic acids (pDNA or siRNA), agarose gel shift assays of the formed polyplexes were performed (**Figure 3.13**). For pDNA polyplexes, all oligomers with oleoyl modification showed effective pDNA binding already at a low N/P of 6, independent from the cationic backbone topology. Interestingly, oligomer *905* with linear cationic backbone and the least number of Stp units demonstrated the best binding which already retained the movement of the polyplexes at the lowest N/P ratio. (**Figure 3.13A**). As for siRNA polyplexes, due to the smaller size of siRNA as compared to pDNA, a general lower stability for all polyplexes in the agarose gel shift assay has been discovered (**Figure 3.13B**). Again, linear oligomer *905* showed the best binding ability with siRNA, 2-armed oligomer showed effective binding start from N/P6, while for 4-armed and 8-armed oligomers, an N/P ratio of 12 or higher was required for stable complexation. The stability of siRNA polyplexes were further investigated with an additional incubation of the polyplexes with 50% FBS (37°C) at N/P12 for all oligomers. The gel shift assay showed these polyplexes are relative stable.

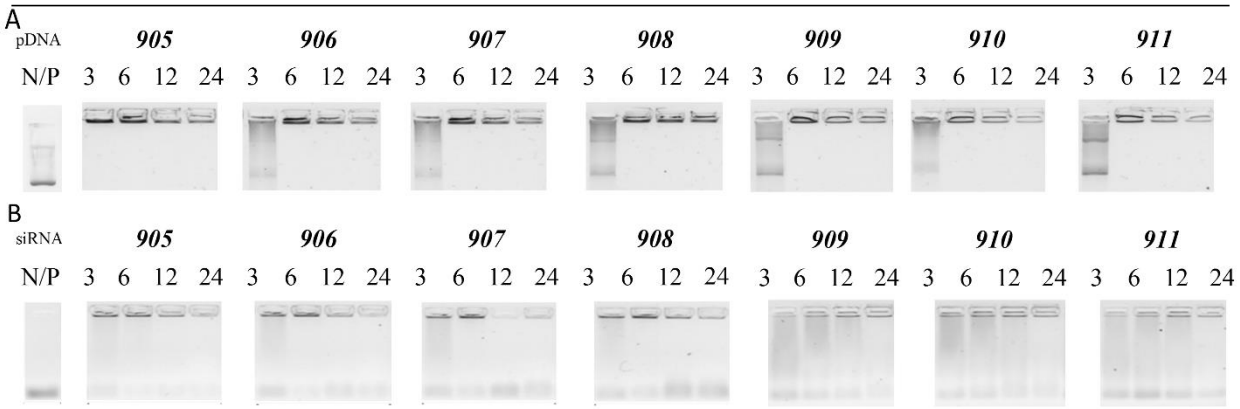

Figure 3.13 Gel retardation assays of pDNA (A) or siRNA (B) polyplexes formed in HBG at the indicated different N/P ratios. Left lanes: free pDNA or siRNA, respectively.

Other important biophysical parameters for the evaluation of suitable polyplexes are particle size and zeta potential (**Table 3.5**). For pDNA polyplexes, particle size determination by dynamic laser light scattering (DLS) showed that most of the oligomers formed nanoparticles with a Z-average diameter between 100-140 nm and zeta potentials between +26 mv and +30 mV. Oligomers with more cationic branches showed a more compacted particles. And for oligomers within the same topology, additional Stp units showed a slightly higher zeta potential compared to their analogs with less cationic building blocks. siRNA polyplexes formed particles with a size range between 127 nm to 170nm and zeta potentials between 26 mV to 31 mV; again a tendency towards smaller particle size with more branches could be discovered.

Table 3.5 Particle size (Z-average) and zeta potential of pDNA polyplexes (N/P 12) and siRNA polyplexes (N/P 16) in HBG buffer measured by DLS. Polyplexes were diluted 1:20 with HEPES buffer before measurement. Data were presented as mean ± SD (n=3).

Oligomer	pDNA polyplexes			siRNA polyplexes		
	Z-average (nm)	PDI	Zeta potential (mV)	Z-average (nm)	PDI	Zeta potential (mV)
905	142.8±0.8	0.155±0.012	29.9±0.8	166.4±3.4	0.297±0.009	27.9±1.4
906	130.8±1.2	0.141±0.016	27.6±3.2	149.9±2.7	0.197±0.002	30.0±1.9
907	117.4±0.6	0.139±0.015	27.6±0.2	166.7±0.7	0.179±0.011	28.9±1.0
908	127.7±0.6	0.153±0.009	28.4±1.6	168.1±2.3	0.268±0.011	26.8±2.3
909	118.3±1.3	0.146±0.008	26.9±1.5	141.3±3.5	0.165±0.006	29.0±0.8
910	115.7±0.2	0.154±0.012	28.8±0.4	135.4±2.8	0.157±0.017	30.0±1.5
911	104.7±0.4	0.150±0.020	28.4±2.0	127.4±1.5	0.176±0.011	30.5±1.9

3.3.3 Biological evaluation

The branched lipo-oligomers were used for pDNA transfection of N2A cells (**Figure 3.14**). These studies were performed by Ana Krhac Levacic (PhD student, Pharmaceutical Biotechnology, LMU Munich). LPEI was chosen as the positive control. Interestingly, the simplest structure *905* with a linear cationic backbone exhibit the highest gene transfer, almost to the same level as LPEI. 2-arm lipo-oligomers achieved the second place regard to the gene transfection efficiency, while 4-arm and 8-arm oligomers only mediate negligible to moderate gene transfer. In general, the gene expression level presented a tendency towards more branched oligomers with less gene transfer ability. For a more detailed comparison, oligomers with the same branched topology, those with more cationic Stp units, could mediate more efficient gene transfer. For example, 2-arm oligomers *906*-*908* could all mediate effective gene transfer to almost the same extinct at N/P 24 with an order of *908* > *907* >*906*.

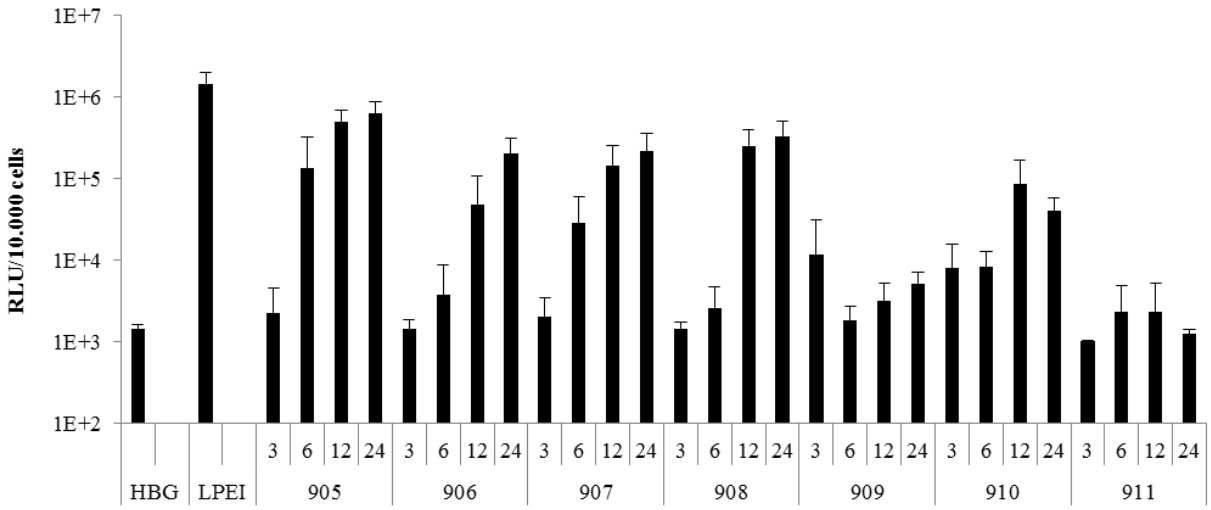

Figure 3.14 Gene transfection in Neuro2A cells with luciferase pDNA/lipo-oligomers polyplexes formed at N/P 3, 6, 12 or 24 (200 ng pDNA per well). LPEI polyplexes (at N/P 6) were set as the positive control. Luciferase activities at 24 h after transfection are presented in relative light units (RLU) as the mean + SD (n=5). The experiment was performed by Ana Krhac Levacic (PhD student, Pharmaceutical Biotechnology, LMU Munich).

In parallel to the gene transfer studies, cell viability of Neuro2a cells were evaluated by an MTT assay after transfection with the pDNA polyplexes.(**Figure 3.15**) Importantly, all tested pDNA polyplexes showed no obvious toxicity.

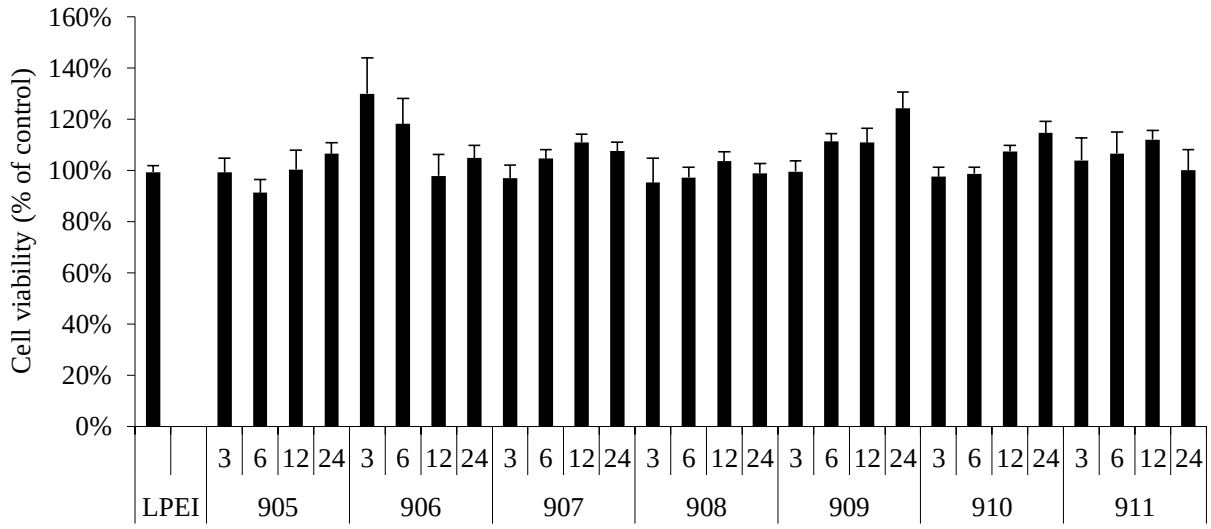

Figure 3.15 Cell viability of Neuro2a cells after transfection with the pDNA polyplexes as evaluated by an MTT assay. pDNA/oligomer polyplexes formed at N/P 3, 6, 12 or 24 and LPEI polyplexes (at N/P 6) were incubated with cells for 24 h. Cell viability (%) was presented as the percentage relative to the buffer treated control cells. The data are shown as mean + SD (n=5). The experiments were performed by Ana Krhac Levacic (PhD student, Pharmaceutical Biotechnology, LMU Munich).

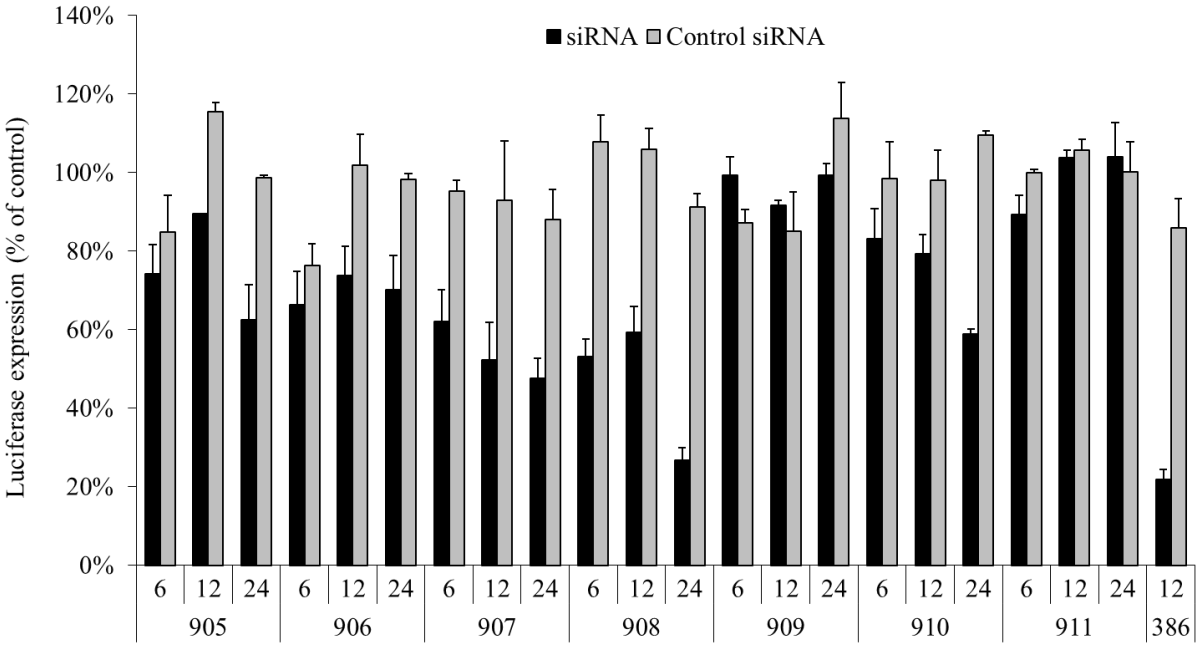

Figure 3.16 Gene silencing in Neuro2A/eGFPLuc cells with siRNA polyplexes formed at N/P 6, 12 and 24.. Black bars= eGFP targeted siRNA; grey bars= control siRNA; ***386*** (N/P 12) was used as positive control. Cells were incubated with polyplexes for 48 h after initial transfection, luciferase activities are presented in percentage of relative light units (RLU) obtained with buffer treated control cells. The data are shown as the mean + SD (n=3). The experiments were performed by Katharina Müller (PhD student, Pharmaceutical Biotechnology, LMU Munich).

The oligomer library was also tested for its gene silencing ability with siRNA using

N2a/eGFPLuc cells. **Figure 3.16** presents results with the tested oligomers, 3-arm oligomer *386* with 9 Stp units at N/P 12 was chosen as the positive control according to previous studies where it shows efficient knock down. In this eGFP-luciferase gene silencing studies, 4-arm oligomer *909* and and 8-arm *911* which only have 1 Stp units on each cationic arm, showed no transfection efficiency; Oligomers *905* and *910* only presented slight transfection efficiency at high N/P ratios, only 2-arm oligomers *906-908* represented moderate transfection with increasing amount of Stp per arm, and 2-arm *908* with 4 Stp units on each arm achieved the most effective silencing at N/P 24, almost to the same level of the positive control *386* at N/P 12.

3.3.4 Defined 2-arm oleoyl oligoaminoamides for folate targeted delivery

3.3.4.1 Synthesis of defined 2-arm oleoyl oligoaminoamides with folate

The 2-arm oligomer *908* with four Stp units on each cationic branch presented an effective pDNA and siRNA complexation, and also achieved the highest gene transfection among the branched lipo-oligomer library. Oligomer *908* contains 8 units of Stp for nucleic acid binding, terminal cysteine for crosslinking, and hydrophobic oleic acid for enhancement of polyplexes stability and uptake. In order to develop a potential carrier for targeted delivery, here we introduced folate as the targeting ligand and PEG_{24} as the shielding domain to the basic structure of *908*, giving out a multifunctional oligomer might be suitable for pDNA and siRNA delivery. To identify the specific receptor mediate uptake, a negative control with glutamate has been introduced for comparison. Additionally, we also alternate the coupling position and the amount of hydrophobic oleic acid. For synthesizing the targeted 2-arm lipo-oligomer, we started from a Dde-Lys(Fmoc)-OH loaded 2-Chlorotritylchloride resin where lysine provides an asymmetrical branching point, the PEG chain and folate was first coupled to the ***ε-***amine of the preloaded lysine. Regarding the different coupling position of oleic acid, oligomer *728* and *729* was assemble by stepwise coupling of Stp unis, followed with cysteine and terminal lysine with two oleic acid. Alternatively, for oligomer *730* and *731*, the synthesis was followed with the insertion of a Fmoc-Lys(Dde)−OH where oleic acid have been coupled to the ***ε-***amine, and finally, the assembly was completed with the repeated coupling of Stp units and the terminal cysteine. The exact structures of the targeted oligomers synthesized in this study are displayed in **Scheme 3.3**.

ID	Topology	Sequence (from C to N terminus)
728	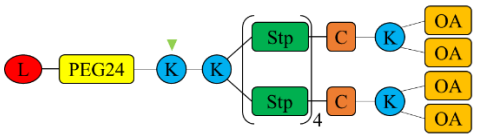	K-(PEG$_{24}$-E)-K(Stp$_4$-C-K-OA$_2$)$_2$
729		K-(PEG$_{24}$-FolA)-K(Stp$_4$-C-K-OA$_2$)$_2$
730	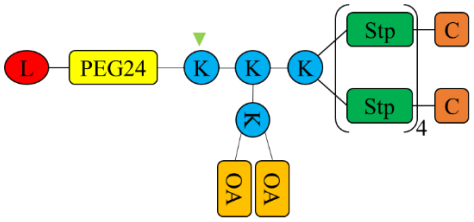	K-(PEG$_{24}$-E)-K-(K-OA$_2$)-K(Stp$_4$-C)$_2$
731		K-(PEG$_{24}$-FolA)-K-(K-OA$_2$)-K(Stp$_4$-C)$_2$

Scheme 3.3 Internal liberary identification number (ID), topology and sequences (from C to N terminus) of PEGylated lipo-oliomers. L stands for the targeting ligand or the corresponding negative control (FolA, folic acid; E, glutamate); PEG, polyethylene glycol; Stp, succinoyl-tetraethylene-pentamine; K, lysine; C, cysteine; OA, oleic aicd. K-(and K-[refer to branchings by α- and ε-amino modification of lysines.

3.3.4.2 Biophysical properties

Agarose gel shift assays were performed to investigate the compaction ability of these oligomers with nucleic acids (pDNA or siRNA) (**Figure 3.17**). For pDNA polyplexes, all oligomers showed almost complete compaction of pDNA binding already at the lowest N/P 3, independent from the position of oleic acid. For siRNA polyplexes, all oligomers again presented an effective compaction of siRNA started from N/P 3 and achieved almost complete siRNA compaction from N/P 6.

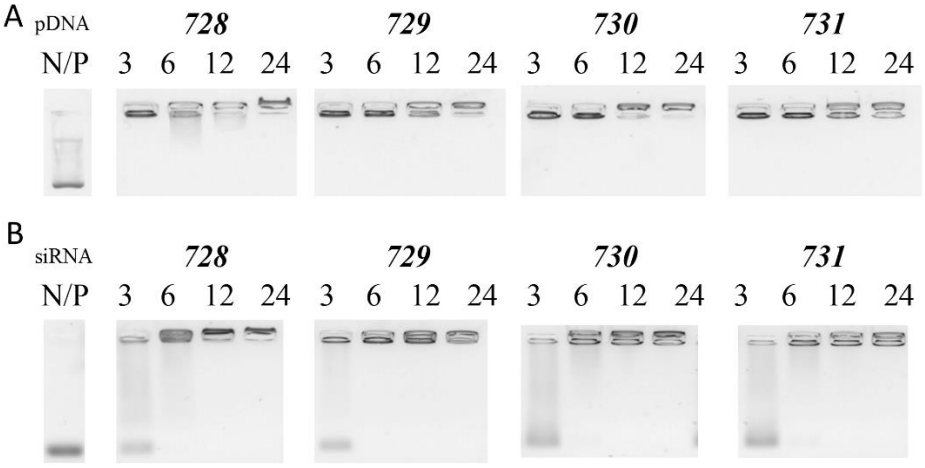

Figure 3.17 Gel retardation assays of pDNA (A) or siRNA (B) polyplexes formed in HBG at the indicated different N/P ratios. Left lanes: free pDNA or siRNA, respectively.

Next we investigated the particle sized and zeta potential of formed polyplexes by dynamic laser light scattering (DLS). (**Table 3.6**) Most of the pDNA polyplexes presented a Z-

average diameter between 175-265 nm and zeta potentials around +20 mV. The PEGylation partially shielded the polyplexes with a result of reduced zeta potential compared to the non-PEGylated *908* with a zeta potential of +28.4 mV. In contrast, the PEGylated siRNA nanoplexes are normally small and hardly measurable via DLS.

Table 3.6 Particle size (Z-average) and zeta potential of pDNA polyplexes (N/P 12) in HBG buffer measured by DLS. Polyplexes were diluted 1:20 with HEPES buffer before measurement. Data were presented as mean ± SD (n=3).

Oligomer	Z-average [nm]	PDI	Mean Zeta Potential [mV]
728	189.1±2.8	0.492±0.037	19.5±0.2
729	259.6±2.3	0.595±0.083	18.4±0.3
730	263.0±4.4	0.426±0.019	22.3±0.5
731	175.6±3.2	0.330±0.021	21.5±0.5

3.3.4.3 Biological evaluation

pDNA transfection of these oligomers have been performed in folate receptor-rich KB cells to evaluate their cellular specific gene transfer. (**Figure 3.18**). To identify the effective receptor-mediated uptake, the same strategy as in **section 3.1.3** was performed. Additionally every transfection was performed with or without endolysosomotropic agent chloroquine, which had been previously found to facilitate endosomal escape of entrapped polyplexes and also contribute to the polyplexes dissociation. All oligomers could hardly mediate any notable gene transfer in the absence of chloroquine, with the help of chloroquine, moderate gene transfer could be achieved for the Folate containing oligomers only at the lowest N/P 3. The results suggested that endosomal escape represented a serious bottleneck which still had to be overcome in this delivery system. Taking previous findings of the enhanced pDNA compaction with increased N/P ratio, another possible drawbacks might be the strong binding hindered the release of the cargo.

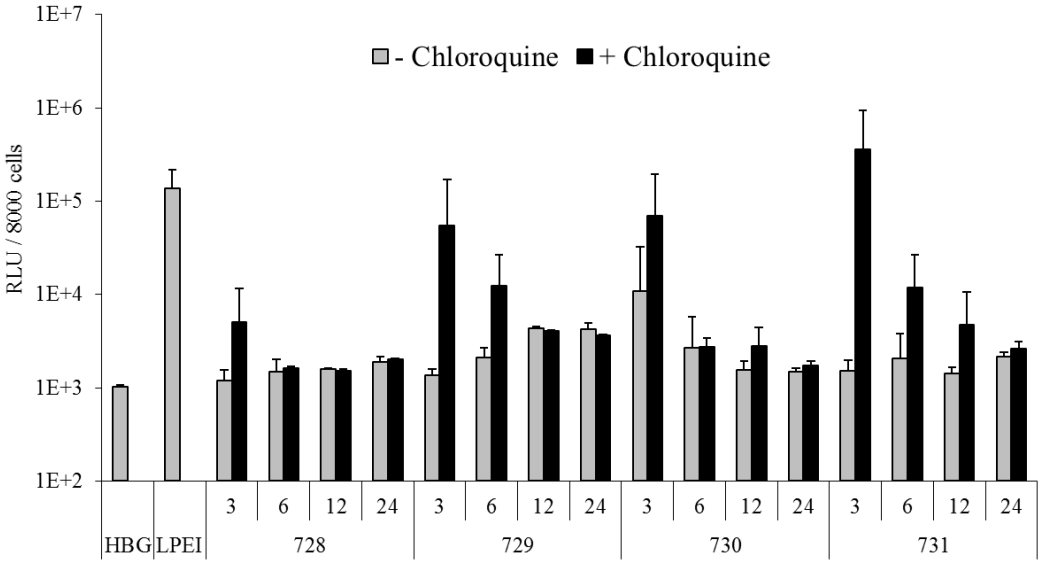

Figure 3.18 Gene transfer in folate receptor expressing KB cells with selected examples of A) two-arm and B) four-arm oligomers. Luciferase pDNA oligomer polyplexes formed at N/P 3, 6, 12 or 24 were incubated with KB cells for the short period of 45 min, followed by replacement of transfection medium by fresh medium with (black bars) or without (grey bars) chloroquine for 4 h additional incubation before another medium exchange. LPEI polyplexes (at N/P 6, incubation with cells for a 4 h longer period before medium exchange) were set as the positive control. Luciferase activities at 24 h after transfection are presented in relative light units (RLU) as the mean + SD (n=5). Transfection of KB cells with pDNA polyplexes at different N/P ratios. The experiments were performed by Dr. Petra Kos (Pharmaceutical Biotechnology, LMU Munich).

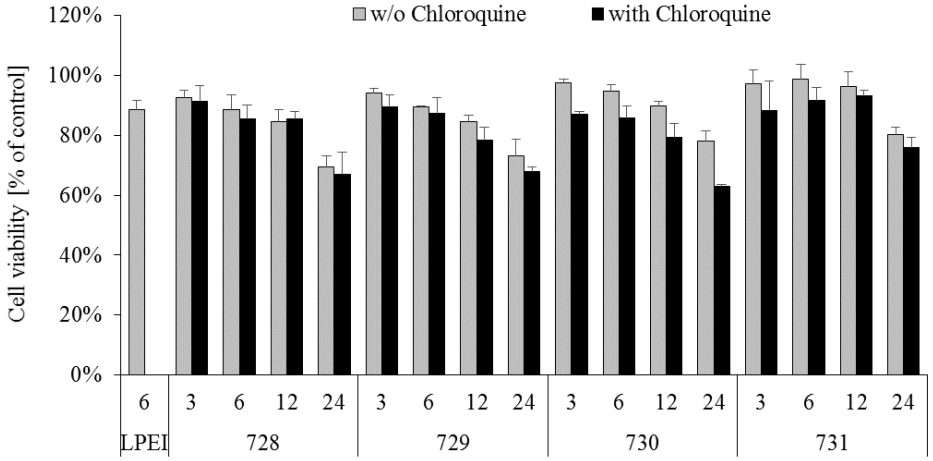

Figure 3.19 Cell viability of KB cells after transfection with the pDNA polyplexes as evaluated by an MTT assay. pDNA/oligomer polyplexes formed at N/P 3, 6, 12 or 24 were incubated with KB cells for 45 min, followed by replacement of fresh medium with (black bars) or without (grey bars) chloroquine for 4 h additional incubation before another medium exchange. LPEI polyplexes (at N/P 6, incubation with cells for 4 h longer period before medium exchange) were set as the reference. Cell viabilities (%) were presented as the percentage relative to the buffer treated control cells. The data are shown as mean + SD (n=5). The experiments were performed by Dr. Petra Kos (Pharmaceutical Biotechnology, LMU Munich).

These oligomers were also used for siRNA delivery in KB/eGFPLuc cells(**Figure 3.20**). The same transfection strategy described in **section 3.1.4** was used to identify the receptor-mediated uptake. The lytic Inf7 peptide modified siRNA was also used to

enhance the endosome escape. However, none of the oligomers could mediate effective gene silencing, while only Inf7 modified siGFP mediated slightly better silencing efficiency. Another transfection approach using endolysosomotropic agent chloroquine was applied, and presented efficient gene silencing, while oligomer *730* and *731* with two central located oleic acids achieved better silencing compared to *728* and *729* with four terminal oleic acids. None of the siRNA polyplexes showed any receptor specific silencing.

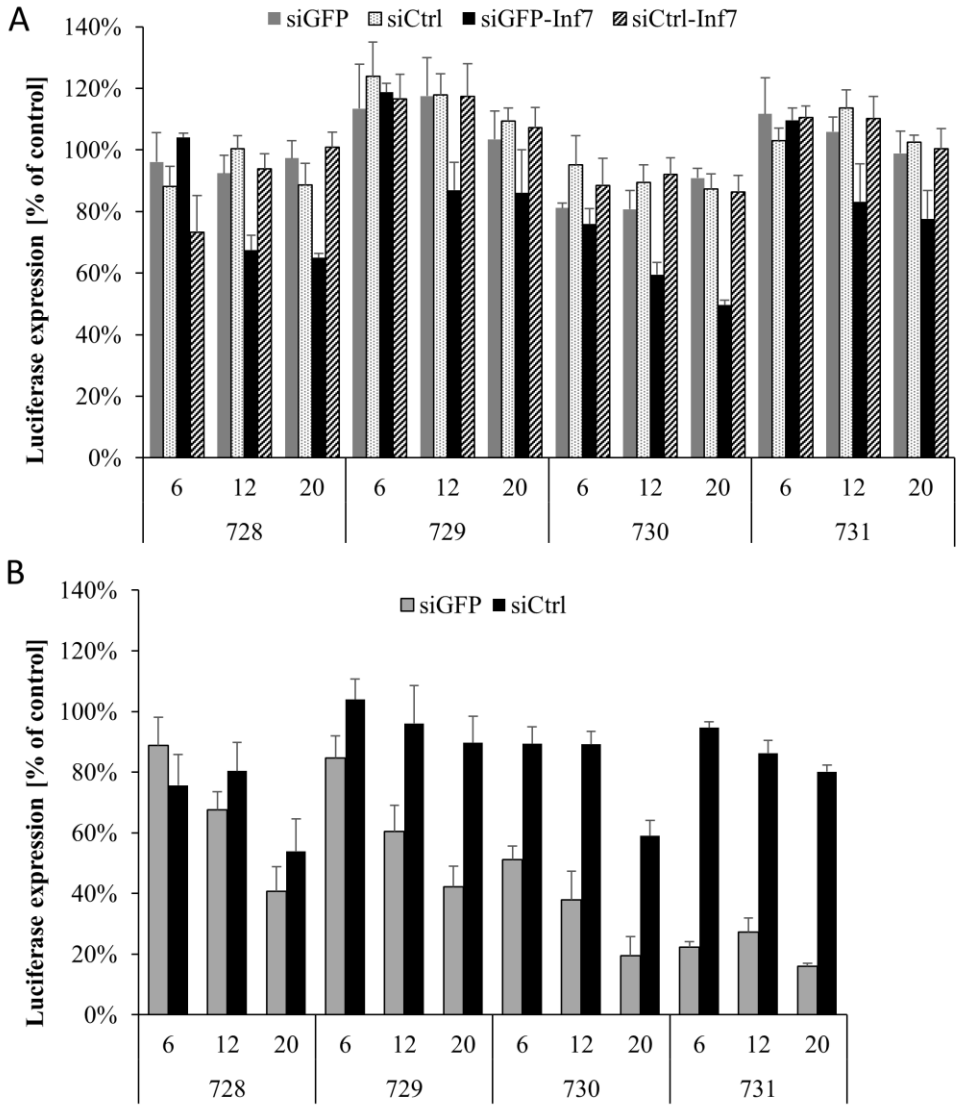

Figure 3.20 Gene silencing in folate receptor expressing KB-eGFPLuc cells. A) eGFP targeted siRNA (siGFP, grey bars), control siRNA (siCtrl, grey bars with dots) polyplexes and corresponding Inf7 peptide modified siRNA polyplexes (siGFP-Inf7, black bars, and siCtrl-Inf7, green bars with slash) formed at N/P 6, 12 and 20 were incubated with cells for a short period of only 45 min, followed by replacement of transfection medium with fresh medium; B) eGFP targeted siRNA (siGFP, grey bars), control siRNA (siCtrl, black bars) polyplexes formed at N/P 6, 12 and 20 with additional chloroquine were incubated with cells for 4 h before the replacement of transfection medium with fresh medium. Luciferase activities at 48 h after transfection are presented in percentage of relative light units (RLU) obtained with buffer treated control cells. The data are shown as the mean + SD (n=3). The experiments were performed by Katharina Müller (PhD student, Pharmaceutical Biotechnology, LMU Munich).

Cellular uptake study provide further information for siRNA polyplexes (**Figure 3.21**). Folate-targeted oligomers showed a slightly higher cellular uptake than non-targeted control oligomers. When compared with *356*, all oligomers showed an enhanced uptake. This might be contributed by the integration of the hydrophobic oleic acid which enhanced the interaction of the polyplexes by manipulating the amphiphilicity of the oligomers.

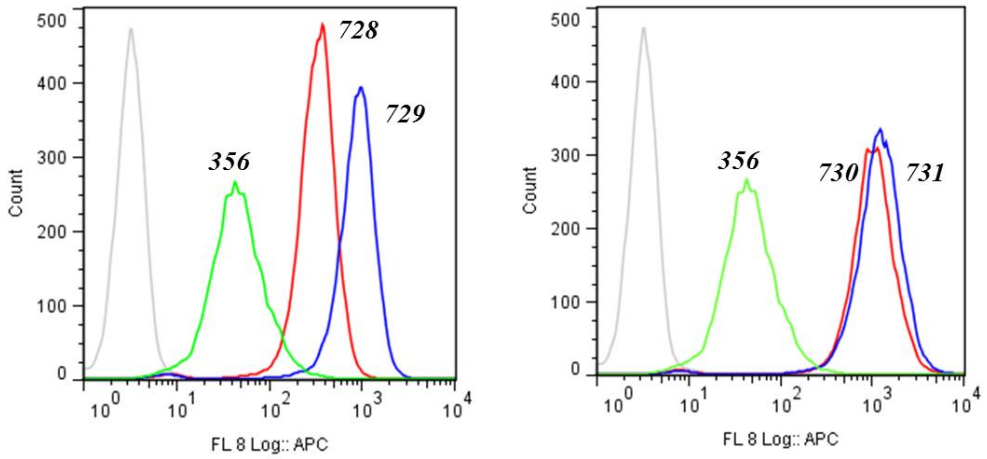

Figure 3.21 Cellular internalization of selected Cy5-labeled siRNA (N/P 12) polyplexes after 45 min determined by flow cytometry. The intensity of the Cy5 signal indicates the amount of polyplexes being internalized by KB-eGFPLuc cells. Light grey curve, HBG buffer only treated cells; green curve, folate containing ***356*** polyplexes treated cells as reference; red curve, ligand free control polyplexes treated cells; and blue curve, folate containing polyplexes treated cells. All experiments were performed in triplicate. The experiments were performed by Katharina Müller (PhD student, Pharmaceutical Biotechnology, LMU Munich).

4 Discussion

4.1 Combinatorial optimization of sequence-defined oligo(ethanamino)amides for folate receptor-targeted pDNA and siRNA delivery

For a successful nucleic acid therapy, an ideal carrier needs to overcome many different barriers. Thus, a multifunctional system is needed to achieve safe and efficient delivery. In this study, we present a combinatorial strategy to generate a library of precise oligomers for optimized intracellular transfer of nucleic acids. Solid-phase assisted synthesis enables sequence-defined incorporation of different functional domains into polymers with high precision.[52, 95, 96, 101] In the current work, we incorporated PEG chains for polyplex shielding, folate for receptor targeting, cationic two- or four-arm cores of Stp/Sph for nucleic acid packaging and endosomal buffering and terminal cysteines for polyplex stabilization by disulfide cross-linkage into oligoamino amide-based carriers. Optionally, as displayed in **Scheme 4.1** with the detailed chemical structures of two potent carriers (#18 and #40), we also incorporated endosomal buffering histidines,[23, 132, 133] and hydrophobically stabilizing tyrosines.[105, 135] The impact of these functional domains on nucleic acid binding and compaction ability as well as buffer capacity of these oligomers, particle sizes and zeta potential values, and transfection activities of formed polyplexes was determined in a series of biophysical and biological tests.

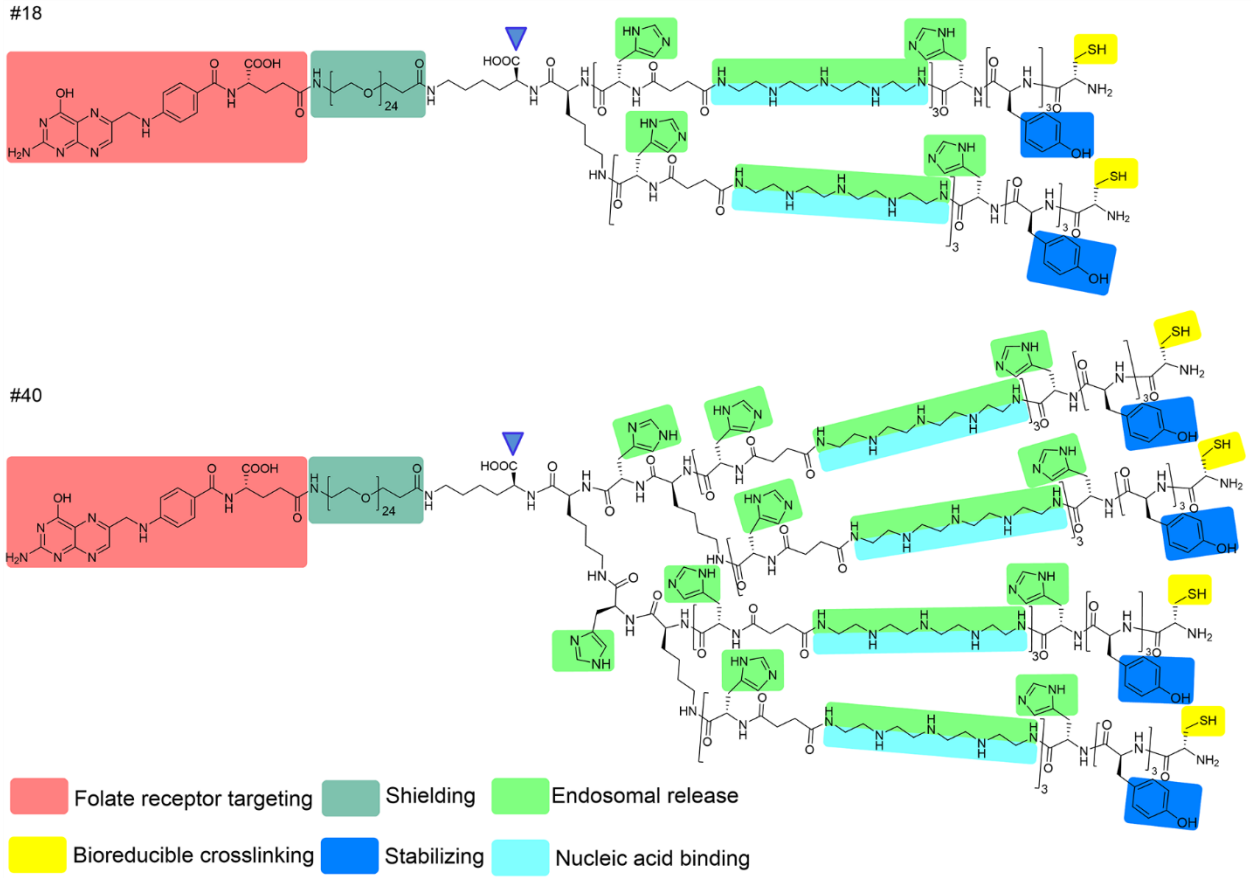

Scheme 4.1 Chemical structures and functional microdomains of oligomers #18 and #40. Two-arm (#18) and four-arm (#40) oligomers as synthesized by solid-phase assisted synthesis (small blue triangles: C-terminal linkage to solid support, start of synthesis) with folate for receptor targeting, PEG chains for polyplex shielding, repeated cationic Stp/Sph units for nucleic acid packaging and endosomal buffering, terminal cysteines for bioreducible crosslinking within polyplexes, histidines for additional endosomal buffering, and tyrosine trimers for hydrophobic stabilization. The functions of the individual domains are highlighted in color, two colors indicate a possible dual function.

Binding behavior studies of these oligomers with nucleic acids (pDNA or siRNA) by agarose gel shift assays presented effective pDNA binding regardless of the cationic backbone, histidine and tyrosine trimer modifications of these oligomers, and less effective siRNA binding due to the smaller size of siRNA as compared to pDNA[147]. Interestingly, integration of tyrosine trimers did not promote polyplex stability. This contradictory observation with our previous non-PEGylated siRNA lipopolyplexes studies,[105] can be explained by the presence of PEG increases solubility and thus counteracts the hydrophobic interactions of tyrosine trimer domains. Further evaluation of the complexation ability by an ethidium bromide exclusion assay revealed the cationic charge density of the backbone as most critical point for nucleic acid interaction, with more cationic domains provided a better compaction, and increased insertion of domains into the cationic backbone decreased complexation.

For pDNA polyplexes, their particle size and zeta potential can be easily analyzed by dynamic laser light scattering (DLS), in contrast, the rather small siRNA nanoplexes were not measurable under this condition[131]. Although most of the oligomers formed nanoparticles with a Z-average diameter between 100-300 nm, some FolA conjugates showed larger size compared to their corresponding control oligomers, and even aggregation. Apparently the combination of exposed hydrophobic FolA ligands with a reduced electrostatic repulsion between nanoparticles causes colloidal instability and flocculation of polyplexes, which is consistent with other related observations.[148]

Endosomal protonation is a key prerequisite for the transfection activity of the oligomers. The buffer capacity in the physiological pH range between extracellular and endolysosomal environment (between pH 7.4 and pH 5) for selected oligomers using alkalimetric back titration revealed that the incorporation of histidine domains significantly enhanced the buffer capacity of these oligomers, which might help in endosomal buffering, disruption of the endosomal membrane, and an enhanced endosomal escape through the hypothetical “proton sponge” effect.[21, 23, 55]

For pDNA transfection, our previously described Stp two-arm oligomer *356* mediated efficient gene transfer only with the help of chloroquine, suggesting that endosomal escape represented a serious bottleneck which still had to be overcome. In summary, gene transfer activity without chloroquine was enhanced compared to the lead-structure *356* by the incorporation of histidines and the assembly into four-arm structures with higher content of cationic units. The increased buffer capacity at endosomal pH and associated proton-sponge activity presumably is the main reason for this enhanced potency. For oligomers modified with tyrosine trimers, the transfection efficiency was mainly determined by the cationic backbone with a higher potency of the compounds containing the larger and better buffering Sph units.[23] Oligomers with high buffer capacity, such as two-arm oligomers based on Sph and four-arm oligomers, showed increased transfection efficiency with little or no further enhancement by chloroquine. The results indicate that the hydrophobic tyrosine trimers also contribute to the improved transfection, possibly by enhancing the interaction with lipid membranes. The highest transfection efficacy was achieved with the combination of histidines and tyrosine trimers in two-arm oligomers which by far outperformed the positive control LPEI. This class of best performing oligomers achieved highly efficient gene transfer in a ligand dependent manner, without the need for an additional external endosomal escape reagent. In

contrast, the transgene expression levels mediated by the analogous four-arm oligomers containing histidines and tyrosines dramatically decreased with increasing N/P ratio due to cytotoxicity.

Table 4.1 Summary of pDNA and siRNA transfection properties.

No.	Gene transfer	Gene silencing	Dependency		Receptor specificity		Toxicity	
			Chloro	Inf7	pDNA	siRNA	pDNA	siRNA
356	++	++	++	++	++	++	-	-
#2	++ (6)	+	++	++	++	-	-	-
#4	+ (6)	++	++	++	-	-	-	-
#6	++	+	+	++	++	-	-	-
#8	+++ (6)	+	+	++	++	-	-	-
#10	+ (24)	+	+	-	-	++	-	+
#12	+ (24)	+	+	-	-	++	-	-
#14	++	++	+	++	++	++	-	-
#16	++	+ (20)	-	+	++	+ (20)	-	-
#18	+++	++	+	-	++	+	-	-
#20	+++	++	+	-	++	+	-	+
#22	++	++	+	++	++	+	-	-
#24	++ (6)	++	+	++	++	+	-	-
#26	++	+	-	++	++	+	-	-
#28	++	++	+	++	+	-	-	-
#30	++ (3)	++	+	++	+	++	-	-
#32	++ (3)	+	+	++	+	-	+ (12)	-
#34	++	+	-	++	++	-	-	-
#36	+ (3)	-	-	-	+	-	+ (24)	-
#38	++ (3)	-	+	-	+	-	+ (12)	-
#40	+++ (3)	++	+	-	+	+	+ (12)	+
#42	+++ (3)	++	+	+	+	+	+ (12)	+

The polyplex N/P ratio is 12, unless defined differently (in brackets). Gene transfer (luciferase expression): +, 10^3-10^5 RLU; ++, 10^5-10^7 RLU; +++, >10^7 RLU. Gene silencing (siGFP-Inf7 sequence specific reduction of marker gene expression): -, 0%-20%; +, 20%-60%; ++, 60%-100%. Dependency on chloroquine (Chloro): ++, transfection only with chloroquine; +, more effective with chloroquine, -, as effective without as with chloroquine. Dependency on Inf7: ++, transfection only with siRNA-Inf7; +, more effective with siRNA-Inf7; -, as effective with siRNA as with siRNA-Inf7. Receptor specificity: -, no specificity; + moderate specificity (negative ligand control shows lower activity); ++, specific (only FolA ligand shows transfection activity). Toxicity (metabolic cell activity): +, metabolic activity $\leqslant$ 80%; -, metabolic cell activity > 80%.Summary prepared by Katharina Müller and Ana Krhac Levacic (PhD students, Pharmaceutical Biotechnology, LMU Munich).

For siRNA mediated gene silencing (**Table 4.1**), the use of endosomolytic Inf7-siRNA demonstrated a clear advantage for transfections. Oligomers with increased number of cationic building blocks or polycationic arms generally demonstrated enhanced silencing efficiency due to their enhanced compaction ability (compare **Figure 6.2** and **3.3**). Oligomers modified with only histidines or tyrosine trimers, exhibited slightly reduced knock down, despite the enhanced buffer capacity and membrane interaction. A possible explanation might be the decreased siRNA binding ability demonstrated by gel shift as well as ethidium bromide assay. For some of these oligomers, a modest targeting effect

could be observed in the transfection results. Similar to pDNA transfection, the combined integration of histidines and tyrosine trimers into two-arm structures turned out to be the most effective combination. Highly effective gene silencing could be achieved without coupling endosomolytic Inf7 peptide to the siRNA.

Cytotoxicity of the cationic oligomers is another major concerns for the use as nucleic acid carriers. MTT assay after transfection with the pDNA polyplexes revealed only the four-arm oligomers containing tyrosine trimers showed obvious toxicity at higher N/P ratios. Four-arm oligomers (#39-42) with a combined modification of tyrosine trimers and histidines also presented a reduction of luciferase activity when transfected with siCtrl polyplexes. Presumably, the increased hydrophobicity caused by the higher number of tyrosines in four-arm oligomers led to increased cytotoxicity. All other oligomers transfected with siCtrl exhibited no obvious reduction of luciferase activity, suggesting good biocompatibility of these oligomers.

Cellular uptake studies was performed to identify the receptor mediated uptake properties. For pDNA polyplexes, targeted polyplexes presented beneficial uptake which was consistent with the transfection data and confirmed the targeting effect. While for siRNA polyplexes, only a slightly higher cellular uptake than non-targeted control oligomers coulbe be observed.

The empirical finding that the same compound class turned out to be most effective pDNA and siRNA carriers was surprising, considering the different demands on pDNA and siRNA delivery, such as different biophysical polyplex stabilities and biological target site (i.e. cytosolic versus nuclear site of action). We conclude that critical early, shared steps of the delivery process, including polyplex stabilization, endocytosis and endosomal release were dominating the selection of favorable functional domains. Nevertheless, closer inspection revealed subtle differences; siRNA polyplexes displayed diminished receptor-specificity and ligand-dependency than pDNA polyplexes, consistent with their reduced polyplex stability and compaction (**Figure 6.1, 6.2, and 3.3**). In sum, the systematic screen of forty-two PEG-containing oligomers provided interesting structure-activity relations and identified oligomers with strongly improved nucleic acid transfection profile *in vitro*. It will be interesting to see their performance in future *in vivo* studies.

4.2 Combinatorial polyplexes for folate receptor targeted siRNA delivery

An ideal siRNA delivery system should possess multifunctionalities to conquer multiple barriers all the way to its site of action. Beside the step-by-step optimization strategy we discussed in the first part, here we developed an approach via combination of two different oligomers from the library to obtain a multifunctional carrier for siRNA delivery. In the current work, PEGylated folate-conjugated oligomers for folate receptor (FR) targeting and surface shielding, and 3-arm oligomers for siRNA binding and polyplexes stabilizing have been chosen to generate novel co-formulations for targeted siRNA delivery. By activation of the cysteine thiol groups of one of the oligomers with 5,5'-dithio-bis(2-nitrobenzoic acid) (DTNB), uni-directional fast coupling between the two types of oligomer could be achieved by a fast disulfide formation with the free thiol groups of the other oligomer. In combination with siRNA, TCPs have been generated with various mixing ratio of the two oligomers and the mixing sequence of siRNA with the two oligomers. The formation sequence of TCPs by first mixing of TNB modified oligomers with siRNA, followed with the adding of unmodified thiol-oligomers have been chosen for further studies. Generally, by alternating the TNB-modification of oligomers, four TCPs were developed and evaluated for their biophysico-chemical properties, and *in vitro* siRNA silencing properties.

DLS has been used to measure the particle sizes and zeta potential of TCPs based on different molar ratios of TNB-modified oligomer and unmodified thiol-oligomer. TCPs presented different particle sizes, despite their identical final consistent oligomers, such as TCP1 and TCP3, TCP2 and TCP4. Reduced surface charges, except TCP3, could be observed with the adding of PEGylated component. The results suggested the particle size and zeta potential could be influenced by the alternative TNB-activated oligomers. Agarose gel shift assay revealed that, non-PEGylated 3-arm oligomers were essential for the compaction of siRNA to form stable polyplexes, and the TCPs showed superior compaction of siRNA.

siRNA silencing studies showed all the TCP formulations containing Inf7-modified siGFP (siGFP-Inf7) at N/P 16 mediated significant gene silencing efficiency in KB/eGFPLuc cells, identified TCP1 as the most potent formulation, and further highlighted the benefice of using Inf7 modified siRNA for siRNA transfection. Furthermore, the adequate luciferase activity of siCtrl treated cells compare to the untreated cells suggested the high biocompatibility of TCPs.

These targeted combinatorial polyplexes (TCP) with favorable particle size and surface

charge showed significant tumor cell-specific eGFP-luciferase marker gene silencing without cytotoxicity *in vitro*. The *in vitro* EG5 gene knockdown ability, FR-mediated internalization by flow cytometry and immuno-TEM, and also *in vivo* studies, will be discussed in Dian-Jang Lee's thesis (PhD student, LMU Munich). Remarkably, after intravenous administration in tumor-bearing mice, the most promising TCP1 generated with a 3-arm Stp oligomer and a TNB-modified 4-arm PEGylated targeted Sph oligomer exhibited siRNA delivery into the tumor and resulted in *in vivo* EG5 gene silencing in the tumor as demonstrated at mRNA level.

4.3 Sequence-defined branched oleoyl oligoaminoamides for nucleic acid delivery

In the present work, solid-phase synthesis in combination with artificial oligoamino acids (like Stp or Sph), natural amino acids and oleic acid as building blocks were applied to assemble branched sequence defined oleoyl oligoaminoamides as carriers for nucleic acid delivery. To investigate whether the different cationic branches of the oligomer can influence the gene transfection, a small library of lipo-oligomers with two oleic acid as the hydrophobic domain and different cationic branches was synthesized and investigated. Oligomers consisting of different Stp units on each arm have been included to further address the effects of the protonable amines on each arm. Terminal cysteines were integrated for polyplex stabilization via disulfide formation.

Nucleic acids (pDNA or siRNA) complexation studies using agarose gel shift assays showed linear oligomer the best binding ability for both pDNA and siRNA, effective pDNA binding start from N/P 6 for all oligomers independent from the cationic backbone topology, and less siRNA binding with increased branches. This polyplex formation can be attributed to multivalent electrostatic interactions between the negatively charged nucleic acid with oligomers, therefore, oligomers with the same amount of Stp units which contribute to the positive charge of the oligomer showed a reduced charge density with increased branches. Similarly, oligomers of the same topology with additional Stp units present a higher charge density and leads to a better complexation.

Particle size determined by dynamic laser light scattering (DLS) showed a tendency towards smaller particle size with more branches oligomers for both pDNA and siRNA polyplexes. One possible reason is that the increasing amount of cysteine corresponding to increasing branches affects the particle size through additional disulfide crosslinking

resulting in a more compact structure. Compare to a previous study by Klein *et al*.[106] where more cysteines as CRC motifs integrated into the 3-arm structure resulted in smaller particle size of the formed polyplexes. And generally, pDNA polyplexes presented smaller particle size compared to the siRNA polyplexes. This might be resulted in the smaller size of siRNA which leads to a looser compaction.

pDNA transfection studies presented a tendency towards less gene transfer ability with more branched oligomers. While for siRNA silencing, almost the same phenomenon was discovered, only the liner oligomer showed no effective silencing. For a more detailed comparison of oligomers with the same branched topology, those with more cationic Stp units could mediate more efficient gene transfer. Generally, more protonatable amines per arm mean an overall increased charge density. This leads to not only the enhanced nucleic acid compaction, but also enhanced interaction with the negative charged cell surface, which is beneficial for non-specific uptake. And furthermore, more Stp units provide an increased buffer capacity with the remaining not protonated amines. This explains the low transfection of the linear oligomer. Since cytotoxicity remains one of the major issue for developing suitable gene carriers, both MTT assay and the high eGFP-Luc expression level of control siRNA transfected cell indicated the all the oligomers possess a favorable biocompatibility as nucleic acid carrier.

As the 2-arm oligomer *908* with four Stp units on each cationic branch presented an effective pDNA and siRNA complexation, and also achieved the highest gene transfection among the branched lipo-oligomer library, it was selected as the basic structure for further modification with the introduction of folate as the targeting ligand and PEG24 as the shielding domain, with the purpose to develop a multifunctional oligomer for targeted pDNA and siRNA delivery. Negative control ligand glutamate was introduced to address the specific receptor mediate uptake. Additionally, we also alternate the coupling position and the amount of hydrophobic oleic acid to identify the influence of the hydrophobic moiety.

Agarose gel shift assays identified all oligomers showed an effective compaction, and almost complete compaction of pDNA and siRNA start form N/P 3 and 6 respectively. A general slightly enhanced binding ability of oligomers was demonstrated compared to their basic structure *908* which does not have PEG modification. The zeta potential of polyplexes formed with the targeted PEGylated oligomers presented lower value compared to that of non-PEGylated *908*, demonstrating the partial shielding of polyplexes,

which would be beneficial for *in vivo* studies, to avoid unspecific interactions with serum proteins.

As for the pDNA transfection of these oligomers, a moderate gene transfer was observed only at the lowest N/P 3, and only with the presence of endolysosomotropic chloroquine, which had been previously found to facilitate endosomal escape of entrapped polyplexes and also contribute to the polyplex dissociation [23, 109]. For siRNA transfection studies, again chloroquine was shown to be crucial for efficient gene silencing. Including the cellular uptake study of an enhanced uptake compare to the oligomer 356 siRNA polyplexes without lipid, the delivery pathway might be caught in the endosomal escape and the following cargo release. The results suggested that endosomal escape represented a serious bottleneck which still had to be overcome in this delivery system. Taking previous findings of the enhanced pDNA compaction with increased N/P ratio, another possible drawback might be the strong binding hindered the release of the cargo. This would be consistent with siRNA polyplex transfections with lytic Inf7 modified siRNA, which have been proved to be beneficial for siRNA transfection with enhance endosomal escape, but only achieved slightly silencing effects. The interaction of the Inf7 peptide with the lipid moiety may strengthen the compaction and might also contribute for its loss of function. Another issue is the PEG chain, which has 24 ethylene glycol units compared to 24 protonable ethylenimine units of the oligomer, the endosomal escape process might be hindered.

5 Summary

Over the past twenty years, nucleic acid based therapy represents as a promising future treatment option for life threatening diseases caused by genetic defects, such as inherited single gene disorders, cancer and so on. However, the development of nucleic acid therapy has been caught in the development of efficient and safe delivery systems. Generally, the nucleic acid carrier needs to be multifunctional to conquer the multiple barriers all the way to its action site. In this thesis, based on the recent developed solid-phase synthesis platform with artificial polyamino acids, we focused on the development of sequence-defined multifunctional oligomers for nucleic acid delivery. With different aims, two strategies to optimize the targeted nucleic acid delivery system have been presented, and additional investigation on the influence of cationic branching units have been discussed.

In the first part, the stepwise optimization of oligomers for nucleic acid delivery was carried out by SPS. A library of forty-two sequence-defined oligomers comprising the artificial polyamino acids for nucleic acid complexation, monodisperse polyethylene glycol (PEG) for surface shielding, and folic acid for receptor-specific cellular uptake, with systemic variations of *(1)* the type of artificial oligoamino acid building block (Stp or Sph), *(2)* the topology (two-arm or four-arm), *(3)* additional histidines for enhanced endosomal pH-buffering and/or *(4)* terminal tyrosine trimers for enhanced stability of the formed polyplexes, have been synthesized and systematically evaluated for properties in pDNA and siRNA delivery. The resulting structure activity relationships identified different beneficial modules for the delivery of pDNA and siRNA, and oligomers with strongly improved nucleic acid transfection profile *in vitro*. Two-arm oligomers modified with a combination of histidines and tyrosine trimers achieved the most effective transfection of pDNA and siRNA. It will be interesting to see their performance in future *in vivo* studies.

In the second part, a combinatorial optimization strategy have been utilized to develop multifunctional folate-bearing targeted combined polyplexes (TCPs) for FR-directed siRNA delivery, this was achieved by reacting a TNB-modified oligomer with a thiol-containing oligomer and formulation with siRNA. The TCPs were spherical homogenous particles, with effective siRNA compaction ability and PEG-shielded nanoparticle surface. These TCPs showed significant tumor cell-specific eGFP-luciferase marker gene silencing without cytotoxicity *in vitro*, and identified TCP1 generated with a 3-arm Stp

oligomer and a TNB-modified 4-arm PEGylated targeted Sph oligomer as the most potent formulation. Further development of TCPs with siEG5 as therapeutic TCPs for tumor reveals TCPs as great potential for a safe and effective delivery system for RNAi-based cancer therapy.

In the third part, SPS has been applied to assemble branched sequence defined oleoyl oligoaminoamides as carriers for nucleic acid delivery. Special focus was put on the influence of different cationic branches of the oligomer on the nucleic acid compaction and gene transfer activity. A library of lipo-oligomers with two oleic acid as the hydrophobic domain and terminal cysteines for polyplex stabilization, while alternating the number of cationic arms (one, two, four, eight) and the number of Stp units (1 to 4) on each arm have been synthesized and investigated. The 2-arm oligomer *908* with four Stp units on each cationic branch presented an effective pDNA and siRNA complexation, and also achieved the highest gene transfection among the branched lipo-oligomer library. A further attempt to generate targeted lipo-oligomers by introducing folate as the targeting ligand and PEG24 as the shielding domain to the *908*, leads to inefficient transfection which might be caught in the endosome escape and/or cargo release pathway.

In summary, this doctoral study focused on the optimization of polyplexes for nucleic acid delivery based on the SPS platform. The structure activity relationship of sequence defined targeted oligomers, the achievement of targeted combinatorial polyplexes, and the up to now unsuccessful targeted lipo-oligomers, all provide interesting and useful information for future optimization of synthetic carriers for nucleic acid delivery.

6 Appendix

6.1 Abbreviations

ACN	Acetonitrile
Boc	*tert*-Butoxycarbonyl
c-Met	Hepatocyte growth factor receptor
CMV	Cytomegalovirus
Cy5	Cyanine 5
D_2O	Deuterium oxide
DAPI	4',6-Diamidino-2-phenylindole
DBU	1,8-Diazabicyclo[5.4.0]undec-7-ene
DCM	Dichloromethane
Dde	1-(4,4-Dimethyl-2,6-dioxocyclohex-1-ylidene)-3-ethyl
DIPEA	*N,N*-Diisopropylethylamine
DLS	Dynamic laser-light scattering
DMEM	Dulbecco's modified Eagle's medium
DMF	*N,N*-Dimethylformamide
DMSO	Dimethylsulfoxide
DNA	Desoxyribonucleic acid
DODT	3,6-Dioxa-1,8-octanedithiol
DPL	Poly(L-lysine) dendrimer
dsRNA	Double-stranded RNA
DTNB	5,5'-Dithio-bis(2-nitrobenzoic acid)
EDTA	Ethylendiaminetetraacetic acid

EtBr	Ethidium bromide
FBS	Fetal bovine serum
Fmoc	Fluorenylmethoxycarbonyl
FolA	Folic acid
FR	Folate receptor
Gtp	Glutaryl-tetraethylene pentamine
Gtt	Glutaryl-triethylene tetramine
HBG	HEPES buffered glucose
HCl	Hydrochloric acid
HEPES	*N*-(2-hydroxethyl) piperazine-N‘-(2-ethansulfonic acid)
HOBt	1-Hydroxybenzotriazole
ivDde	1-(4,4-Dimethyl-2,6-dioxocyclohex-1-ylidene)-3-methylbutyl
KCN	Potassium cyanide
LPEI	Linear polyethylenimine
miRNA	MicroRNA
mRNA	Messenger RNA
MTBE	Methyl *tert*-butyl ether
MTT	3-(4,5-Dimethylthiazol-2-yl)-2,5-diphenyltetrazolium bromide
N/P ratio	Nitrogen/phosphate ratio
NaOH	Sodium hydroxide
NMR	Nuclear magnetic resonance
PAA	Polyamino acid
PAMAM	Poly(amidoamine) dendrimer
PBS	Phosphate buffered saline
pCMVLuc	Plasmid encoding firefly luciferase under the control of the CMV promoter

PDI	Polydispersity index
pDNA	Plasmid DNA
PEG	Polyethylene glycol
PEHA	Pentaethylene hexamine
PPI	Polypropylenimine
Poly(I:C)	Polyinosinic polycytidylic acid
PyBOP	Benzotriazol-1-yloxy-tripyrrolidinophosphonium hexafluorophosphate
RLU	Relative light units
RP-HPLC	Reversed-phase high performance liquid chromatography
RPMI	Roswell Park Memorial Institute medium
RT	Room temperature
SEC	Size-exclusion chromatography
siRNA	Small interfering RNA
Sph	Succinoyl-pentaethylene hexamine
SPS	Solid-phase synthesis
Stp	Succinoyl-tetraethylene pentamine
TBE	Tris-boric acid-EDTA buffer
TCEP	Tris(2-carboxyethyl)phosphine
TEPA	Tetraethylene pentamine
TEM	Transmission electron microscopy
TFA	Trifluoroacetic acid
TIS	Triisopropylsilane

6.2 Supporting figures and tables

Table 6.1 Overview of the synthesized PEGylated oligomers, their numbers in the manuscript, internal library compound IDs, and sequences (left to right: from C- to N-terminus).

No.	ID	Sequence (C to N terminus)
356	***356***	C-Stp$_4$-K-(PEG$_{24}$-FolA)-Stp$_4$-C
#1	***690***	K-(PEG$_{24}$-Acetate)-K-(Sph$_3$-C)$_2$
#2	***691***	K-(PEG$_{24}$-FolA)-K-(Sph$_3$-C)$_2$
#3	***692***	K-(PEG$_{24}$-Acetate)-K-(Sph$_4$-C)$_2$
#4	***693***	K-(PEG$_{24}$-FolA)-K-(Sph$_4$-C)$_2$
#5	***788***	K-(PEG$_{24}$-E)-K-[(H-Stp)$_3$-H-C]$_2$
#6	***789***	K-(PEG$_{24}$-FolA)-K-[(H-Stp)$_3$-H-C]$_2$
#7	***790***	K-(PEG$_{24}$-E)-K-[(H-Stp)$_4$-H-C]$_2$
#8	***791***	K-(PEG$_{24}$-FolA)-K-[(H-Stp)$_4$-H-C]$_2$
#9	***879***	K-(PEG$_{24}$-E)-K-(Stp$_3$-Y$_3$-C)$_2$
#10	***880***	K-(PEG$_{24}$-FolA)-K-(Stp$_3$-Y$_3$-C)$_2$
#11	***881***	K-(PEG$_{24}$-E)-K-(Stp$_4$-Y$_3$-C)$_2$
#12	***882***	K-(PEG$_{24}$-FolA)-K-(Stp$_4$-Y$_3$-C)$_2$
#13	***714***	K-(PEG$_{24}$-E)-K-(Sph$_3$-Y$_3$-C)$_2$
#14	***715***	K-(PEG$_{24}$-FolA)-K-(Sph$_3$-Y$_3$-C)$_2$
#15	***716***	K-(PEG$_{24}$-E)-K-(Sph$_4$-Y$_3$-C)$_2$
#16	***717***	K-(PEG$_{24}$-FolA)-K-(Sph$_4$-Y$_3$-C)$_2$
#17	***792***	K-(PEG$_{24}$-E)-K-[(H-Stp)$_3$-H-Y$_3$-C]$_2$
#18	***793***	K-(PEG$_{24}$-FolA)-K-[(H-Stp)$_3$-H-Y$_3$-C]$_2$
#19	***794***	K-(PEG$_{24}$-E)-K-[(H-Stp)$_4$-H-Y$_3$-C]$_2$
#20	***795***	K-(PEG$_{24}$-FolA)-K-[(H-Stp)$_4$-H-Y$_3$-C]$_2$
#21	***732***	K-(PEG$_{24}$-E)-K-[K-(Stp$_3$-C)$_2$]$_2$
#22	***733***	K-(PEG$_{24}$-FolA)-K-[K-(Stp$_3$-C)$_2$]$_2$
#23	***734***	K-(PEG$_{24}$-E)-K-[K-(Stp$_4$-C)$_2$]$_2$
#24	***735***	K-(PEG$_{24}$-FolA)-K-[K-(Stp$_4$-C)$_2$]$_2$
#25	***706***	K-(PEG$_{24}$-A)-K-[K-(Sph$_3$-C)$_2$]$_2$
#26	***707***	K-(PEG$_{24}$-FolA)-K-[K-(Sph$_3$-C)$_2$]$_2$
#27	***708***	K-(PEG$_{24}$-A)-K-[K-(Sph$_4$-C)$_2$]$_2$
#28	***709***	K-(PEG$_{24}$-FolA)-K-[K-(Sph$_4$-C)$_2$]$_2$
#29	***761***	K-(PEG$_{24}$-E)-K-[H-K-((H-Stp)$_3$-H-C)$_2$]$_2$
#30	***762***	K-(PEG$_{24}$-FolA)-K-[H-K-((H-Stp)$_3$-H-C)$_2$]$_2$
#31	***763***	K-(PEG$_{24}$-E)-K-[H-K-((H-Stp)$_4$-H-C)$_2$]$_2$
#32	***764***	K-(PEG$_{24}$-FolA)-K-[H-K-((H-Stp)$_4$-H-C)$_2$]$_2$
#33	***712***	K-(PEG$_{24}$-E)-K-[H-K-((H-Sph)$_3$-H-C)$_2$]$_2$
#34	***713***	K-(PEG$_{24}$-FolA)-K-[H-K-((H-Sph)$_3$-H-C)$_2$]$_2$
#35	***875***	K-(PEG$_{24}$-E)-K-[K-(Stp$_3$-Y$_3$-C)$_2$]$_2$
#36	***876***	K-(PEG$_{24}$-FolA)-K-[K-(Stp$_3$-Y$_3$-C)$_2$]$_2$
#37	***877***	K-(PEG$_{24}$-E)-K-[K-(Stp$_4$-Y$_3$-C)$_2$]$_2$
#38	***878***	K-(PEG$_{24}$-FolA)-K-[K-(Stp$_4$-Y$_3$-C)$_2$]$_2$
#39	***765***	K-(PEG$_{24}$-E)-K-[H-K-((H-Stp)$_3$-H-Y$_3$-C)$_2$]$_2$
#40	***766***	K-(PEG$_{24}$-FolA)-K-[H-K-((H-Stp)$_3$-H-Y$_3$-C)$_2$]$_2$
#41	***767***	K-(PEG$_{24}$-E)-K-[H-K-((H-Stp)$_4$-H-Y$_3$-C)$_2$]$_2$
#42	***768***	K-(PEG$_{24}$-FolA)-K-[H-K-((H-Stp)$_4$-H-Y$_3$-C)$_2$]$_2$

FolA, folic acid as targeting ligand; A, alanine; E, glutamate; or acetate as corresponding ligand controls; Stp, succinoyl-tetraethylene-pentamine; Sph, succinoyl-pentaethylene-hexamine; PEG, polyethylene glycol; K, lysine; H, histidine; Y, tyrosine; and C, cysteine. K-[and K-(refer to branching by α- and ε-amino modification.

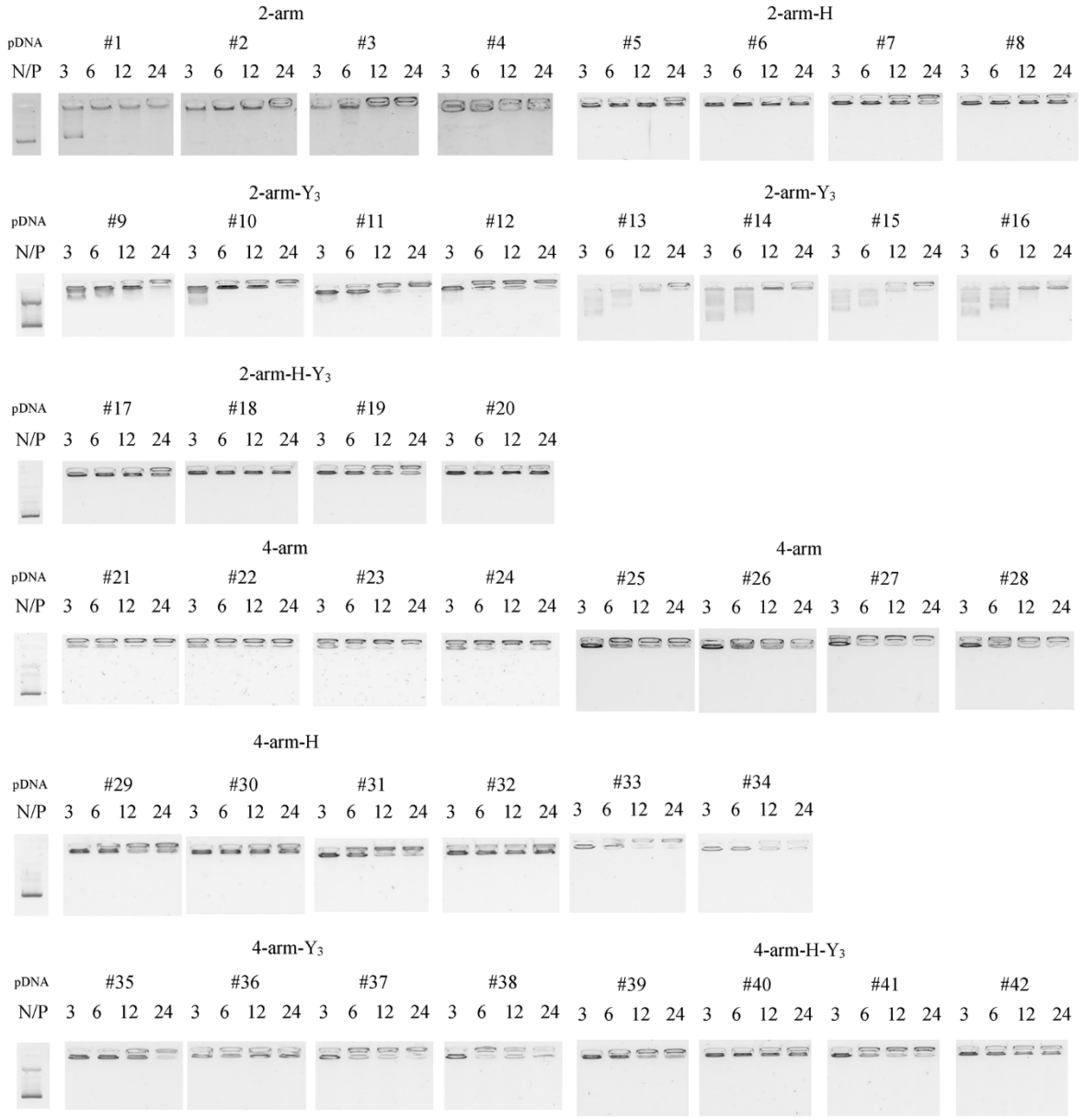

Figure 6.1. Gel retardation assays of pDNA polyplexes formed with oligomers at different indicated N/P ratios in HBG. Left lane: free pDNA.

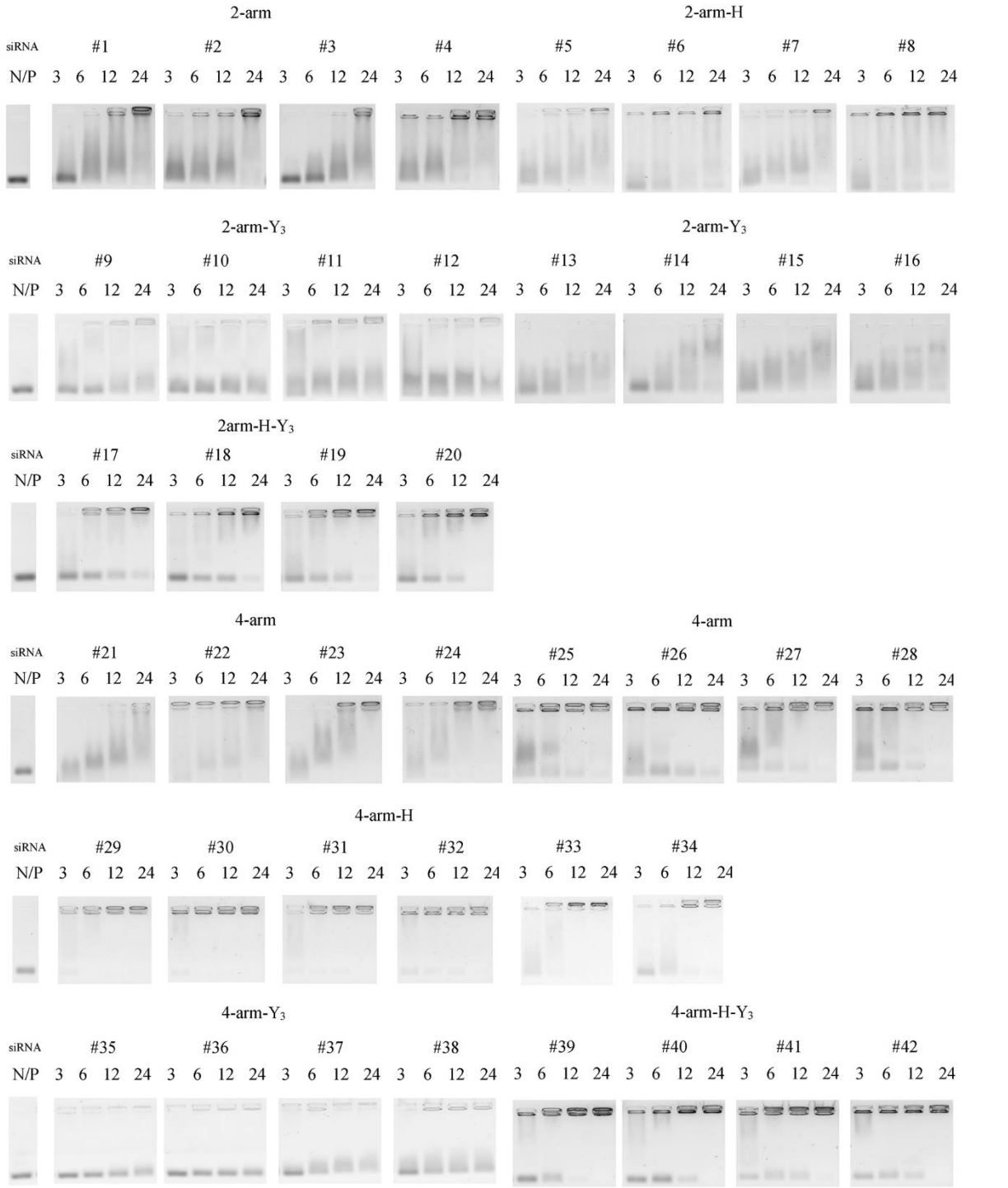

Figure 6.2 Gel retardation assays of siRNA polyplexes formed with oligomers at different indicated N/P ratios in HBG. Left lane: free siRNA.

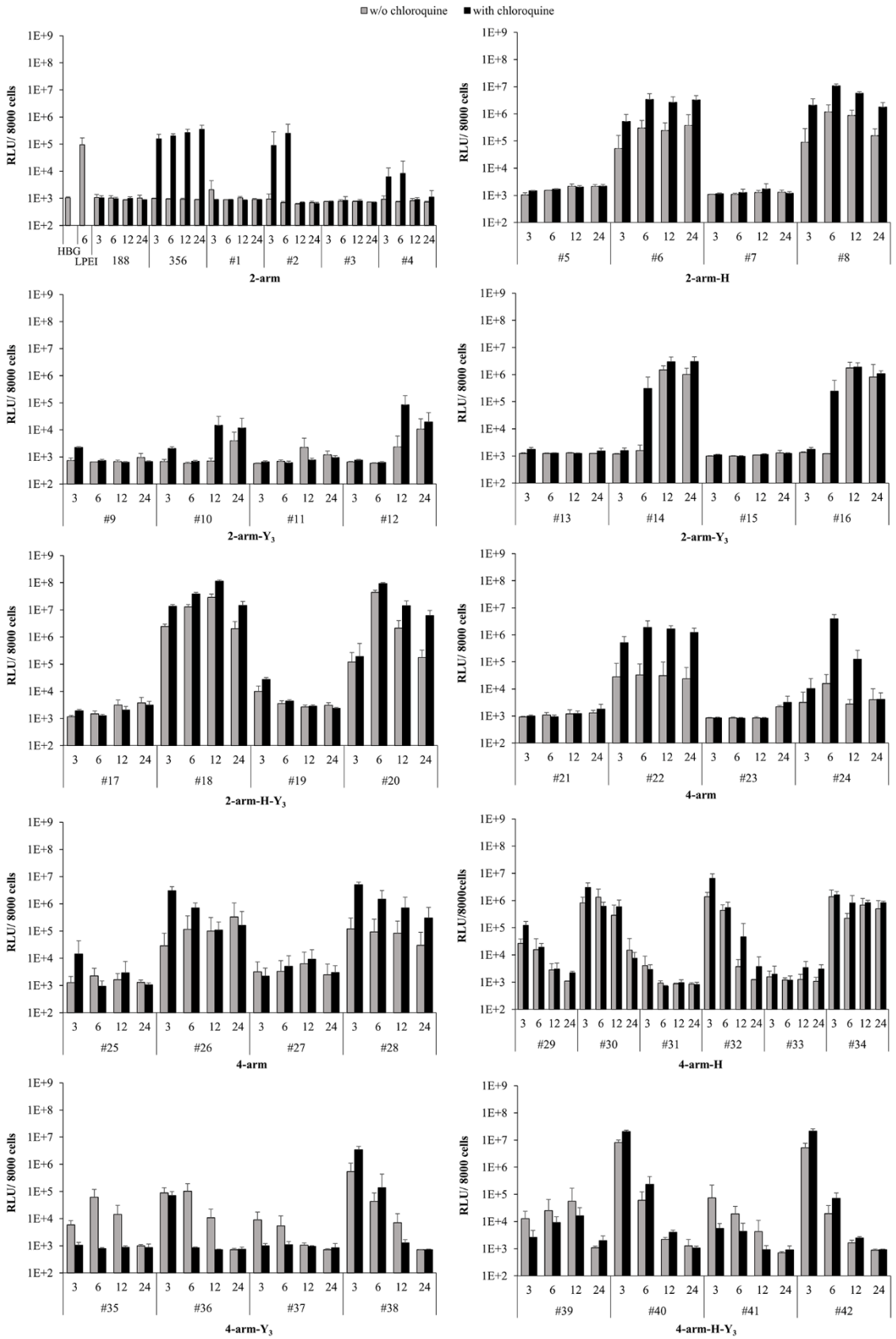

Figure 6.3. Luciferase pDNA transfection in folate receptor expressing KB cells with synthesized oligomers. Luciferase polyplexes were formed at the indicated N/P ratios of 3, 6, 12 or 24 and incubated with KB cells (200ng pCMVLuc per well) for the short period of 45 min in folate-free serum-supplemented medium, followed by replacement of transfection medium by fresh medium with (black bars) or without (grey bars) chloroquine. LPEI polyplexes (at N/P 6, incubation with cells for a longer 4 h period before medium exchange) were set as the positive control, HBG buffer served as negative control. Luciferase activities at

24 h after transfection are presented in relative light units (RLU) as the mean + SD (n= 5). The experiments were performed by Ana Krhac Levacic and Dr. Petra Kos (Pharmaceutical Biotechnology, LMU Munich).

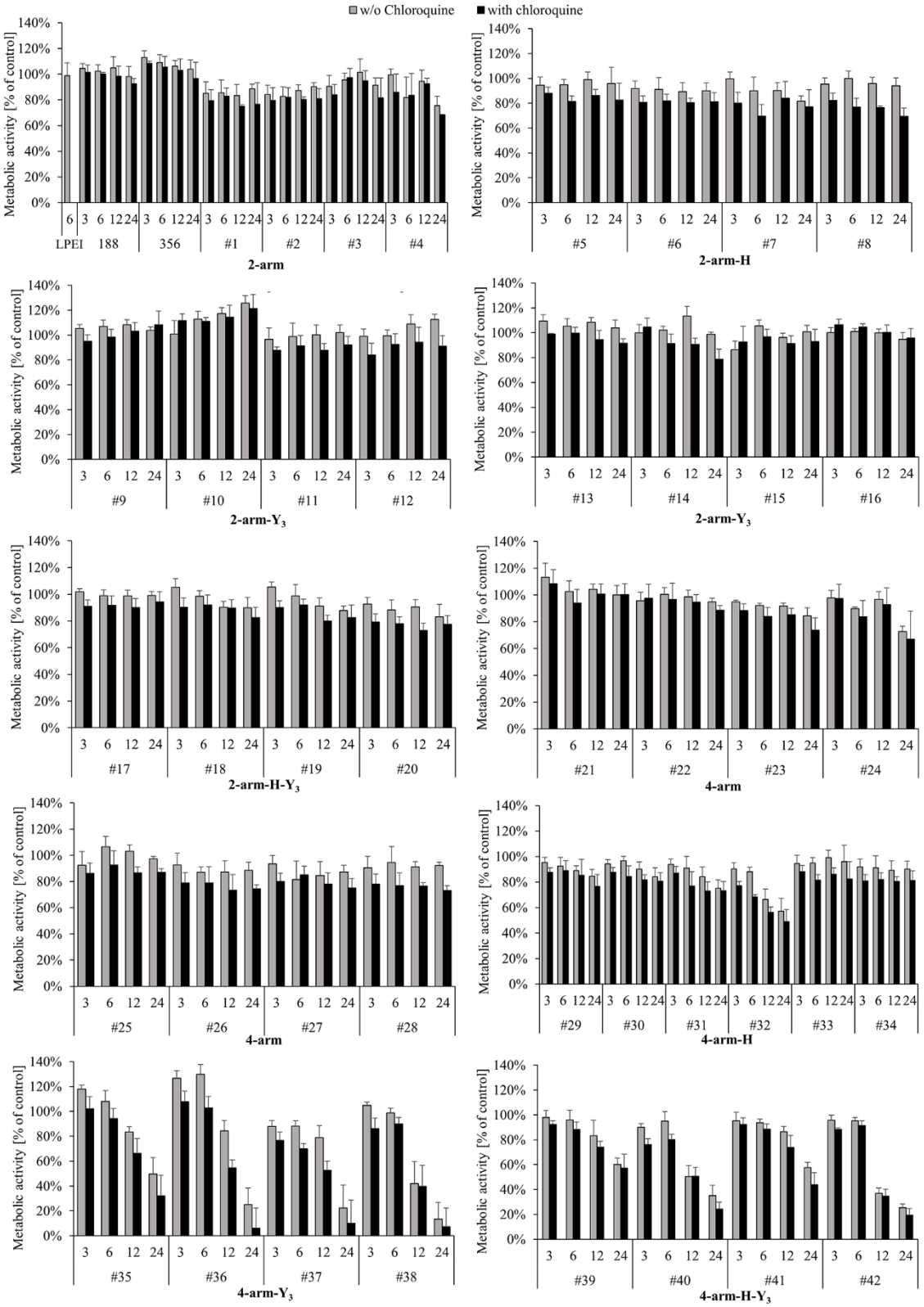

Figure 6.4 Metabolic activities of KB cells after transfection with the pDNA polyplexes as evaluated by an MTT assay. pDNA/oligomer polyplexes formed at N/P 3, 6, 12 or 24 were incubated with KB cells for 45 min, followed by replacement of fresh medium with (black bars) or without (grey bars) chloroquine for 4h additional incubation before medium exchange. LPEI polyplexes (at N/P 6, incubation with cells for 4 h period before medium exchange) were set as the reference. Metabolic activities (%) were presented as the percentage relative to the buffer treated control wells. The data are shown as mean + SD (n=5). The

experiments were performed by Ana Krhac Levacic and Dr. Petra Kos (Pharmaceutical Biotechnology, LMU Munich).

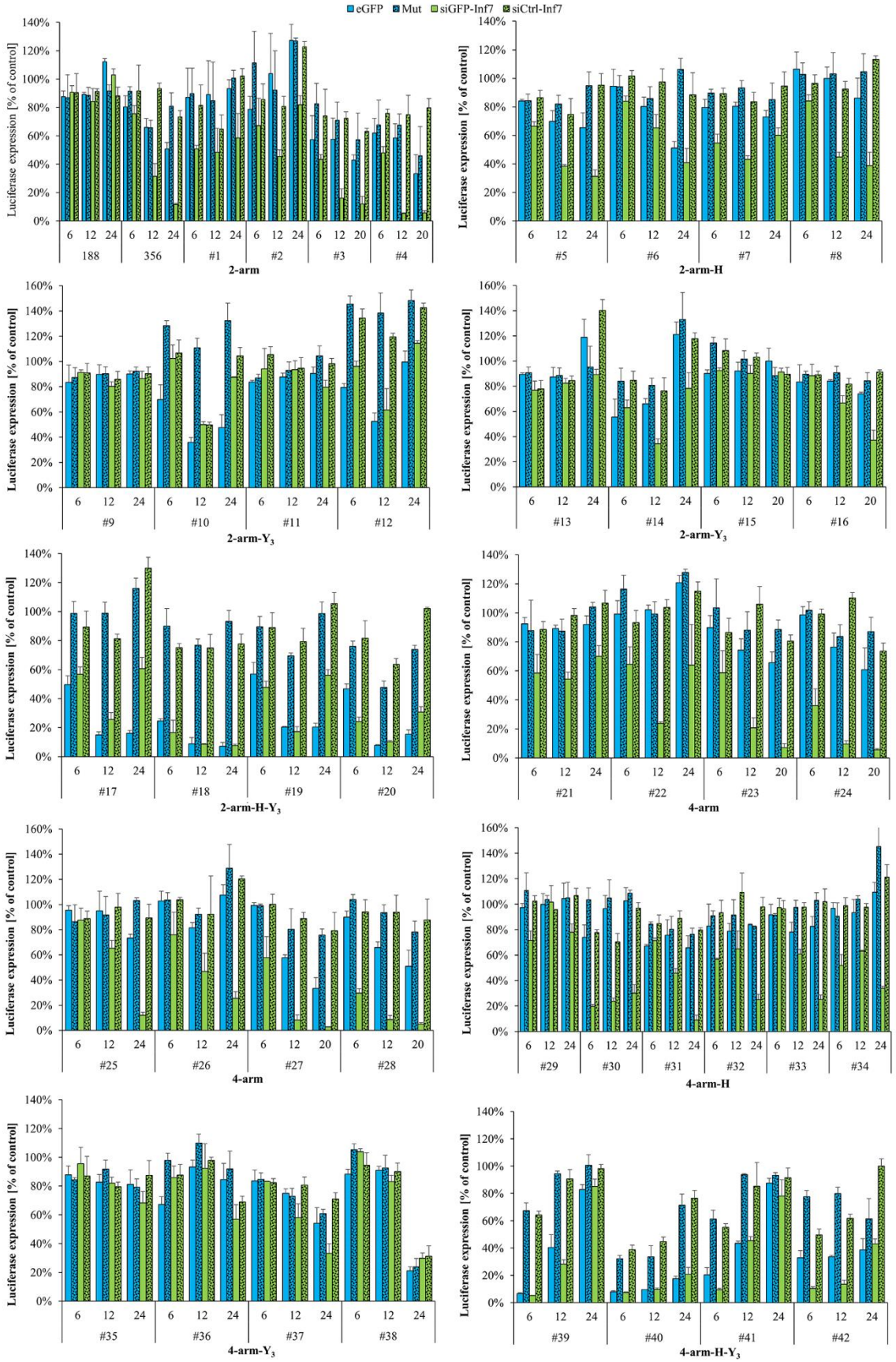

Figure 6.5 Gene silencing in folate receptor expressing KB-eGFPLuc cells with two-arm oligomers: (A) two-arm oligomers without core modification; (B) oligomers modified with histidines; (C) with tyrosine trimers; (D) with both histidines and tyrosine trimers. The lane FolA Ligand (- or +) refers to the absence

or presence of folate ligand within the indicated oligomer. eGFP targeted siRNA (siGFP, blue bars), control siRNA (siCtrl, blue bars with dots) polyplexes and corresponding Inf7 peptide modified eGFP targeted (siGFP-Inf7, green bars) and control (siCtrl-Inf7, green bars with dots) siRNA polyplexes formed at N/P 6, 12 and 20 or 24 for eGFPLuc gene silencing were incubated with KB-eGFPLuc cells for 45 min, followed by replacement of transfection medium by fresh medium. Luciferase activities at 48 h after transfection are presented in percentage of relative light units (RLU) obtained with buffer treated control cells. The data are shown as the mean + SD (n=3). The experiment was performed by Katharina Müller (PhD student, Pharmaceutical Biotechnology, LMU Munich).

Table 6.2 Size (by dynamic light scattering) and zeta potential of TCP1 at N/P 16. K-(PEG_{24}-Folate)-K-[K-(Sph_4-C-TNB)$_2$]$_2$ (*873*) as TNB-modified oligomer and C-Stp_3-K-(Stp_3-C)$_2$ (*386*) as unmodified oligomer were co-formulated according to different molar ratios to form siRNA polyplexes for size assessments. n.d. = not detectable.

[TNB-Modified Oligomer / Unmodified Oligomer] Molar Ratio		Individual N/P Ratios		Size (nm)	Zeta Potential (mV)
TNB-Modified Oligomer	Unmodified Oligomer	TNB-Modified Oligomer	Unmodified Oligomer		
100%	-	16	0	n.d.	n.d.
80%	20%	14.5	1.5	n.d.	n.d.
60%	40%	12.5	3.5	98.2±9.4	14.7±1.5
50%	50%	11.2	4.8	103.5±0.8	9.1±0.2
40%	60%	9.8	6.2	71.3±20	11.9±0.4
20%	80%	5.9	10.1	129.8±31	11.5±0.9
-	100%	0	16	883.7±80.2	24.1±0.9

Table 6.3 Size (by dynamic light scattering) and zeta potential of TCP2 at N/P 16. TNB-C-H-(Stp-H)$_3$-K-[(H-Stp)$_3$-H-C-TNB]$_2$ (*770*) as TNB-modified oligomer and K-(PEG_{24}-Folate)-K-(Sph_4-Y_3-C)$_2$ (*717*) as unmodified oligomer were co-formulated according to different molar ratios to form siRNA polyplexes for size assessments. n.d. = not detectable.

[TNB-Modified Oligomer / Unmodified Oligomer] Molar Ratio		Individual N/P Ratios		Size (nm)	Zeta Potential (mV)
TNB-Modified Oligomer	Unmodified Oligomer	TNB-Modified Oligomer	Unmodified Oligomer		
100%	-	16	0	289.3±43.62	14.3±0.1
80%	20%	12.4	3.6	512.8±39.39	7.90±0.146
60%	40%	9.0	7.0	473.5±45.8	7.79±0.1
50%	50%	7.4	8.6	429.4±52.54	7.93±0.2
40%	60%	5.8	10.2	448.8±15.27	11.4±0.52
20%	80%	2.8	13.2	569.9±27.36	12.3±0.115
-	100%	0	16	n.d.	n.d.

Table 6.4 Size (by dynamic light scattering) and zeta potential of TCP3 at N/P 16. TNB-C-Stp_3-K-(Stp_3-C-TNB)$_2$ (*769*) as TNB-modified oligomer and K-(PEG_{24}-Folate)-K-[K-(Sph_4-C)$_2$]$_2$ (*709*) as unmodified oligomer were co-formulated according to different molar ratios to form siRNA polyplexes for size assessments.n.d. = not detectable.

[TNB-Modified Oligomer / Unmodified Oligomer] Molar Ratio		Individual N/P Ratios		Size (nm)	Zeta Potential (mV)
TNB-Modified Oligomer	Unmodified Oligomer	TNB-Modified Oligomer	Unmodified Oligomer		
100%	-	16	0	266.3±7.4	17.9±0.1
80%	20%	10.1	5.9	159.8±5.4	23.2±0.4
60%	40%	6.2	9.8	195.5±3.2.	27.5±1.3
50%	50%	4.8	11.2	208.8±3.4	24.3±0.3
40%	60%	3.5	12.5	n.d.	n.d.
20%	80%	1.5	14.5	n.d.	n.d.
-	100%	0	16	n.d.	n.d.

Table 6.5 Size (by dynamic light scattering) and zeta potential of TCP4 at N/P 16. K-(PEG_{24}-Folate)-K-(Sph_4-Y_3-C-TNB)$_2$ (*874*) as TNB-modified oligomer and C-H-(Stp-H)$_3$-K-[(H-Stp)$_3$-H-C]$_2$ (*689*) as unmodified oligomer were co-formulated according to different molar ratios to form siRNA polyplexes for size assessments. n.d. = not detectable.

[TNB-Modified Oligomer / Unmodified Oligomer] Molar Ratio		Individual N/P Ratios		Size (nm)	Zeta Potential (mV)
TNB-Modified Oligomer	Unmodified Oligomer	TNB-Modified Oligomer	Unmodified Oligomer		
100%	-	16	0	454.4±72.3	5.3±0.4
80%	20%	13.2	2.8	332.3±67.2	8.2±0.3
60%	40%	10.2	5.8	442.7±105.7	7.8±0.2
50%	50%	8.6	7.4	398.3±63.5	8.1±0.5
40%	60%	7.0	9.0	445.2±62.7	8.6±0.2
20%	80%	3.6	12.4	393.3±48.7	10.1±0.2
-	100%	0	16	139.3±4.9	14.9±1.2

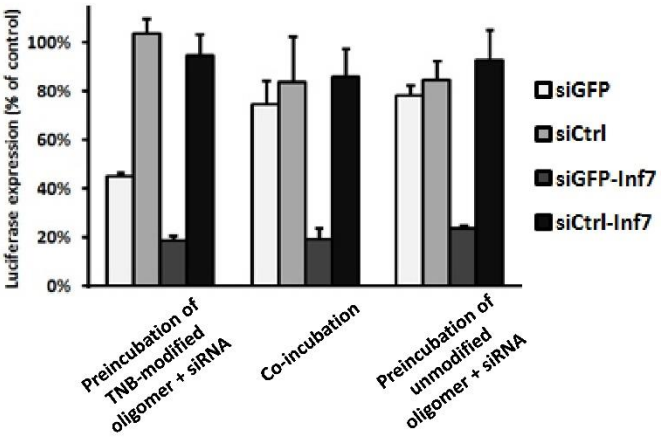

Figure 6.6 Gene silencing efficiency of TCP1 in KB/eGFPLuc cells using different alternative mixing sequences. The siRNA polyplexes were prepared at N/P 16 with 370 nM different siRNA sequences: eGFP-targeted siRNA (siGFP), control siRNA (siCtrl), or siRNA chemically linked with the endosomolytic peptide Inf7 (siGFP-Inf7 or siCtrl-Inf7). The different mixing sequences were compared: Alternative 1), also used for the majority of experiments; the TNB-modified oligomer solution was pre-incubated with siRNA solution for 30 min, then was incubated with unmodified oligomer solution for 40 min. Alternative 2) The TNB-modified oligomer solution and unmodified oligomer solution were incubated all together with siRNA solution for 40 min. Alternative 3) Unmodified oligomer solution was pre-incubated with siRNA solution for 30 min, then further incubated with TNB-modified oligomer solution for 40 min. The experiments were performed by Dian-Jang Lee (PhD student, Pharmaceutical Biotechnology, LMU Munich).

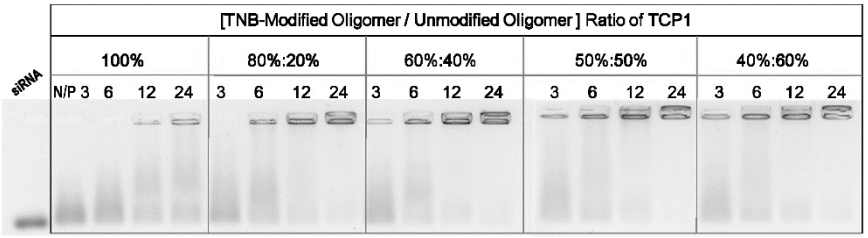

Figure 6.7 siRNA binding of TCP1 determined by agarose gel shift assay. K-(PEG_{24}-Folate)-K-[K-(Sph_4-C-TNB)$_2$]$_2$ (*873*) as TNB-modified oligomer and C-Stp_3-K-(Stp_3-C)$_2$ (*386*) as unmodified oligomer were co-formulated according to different molar ratios to form siRNA polyplexes at N/P 3, 6, 12 and 24. Free siRNA was used as control.

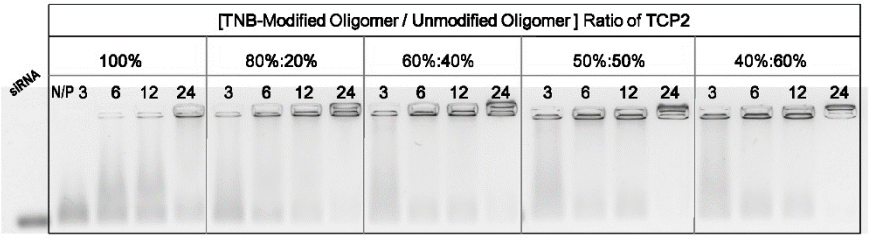

Figure 6.8 siRNA binding of TCP2 determined by agarose gel shift assay. TNB-C-H-(Stp-H)$_3$-K-[(H-Stp)$_3$-H-C-TNB]$_2$ (*770*) as DTNB-modified oligomer and K-(PEG_{24}-Folate)-K-(Sph_4-Y_3-C)$_2$ (*717*) as unmodified oligomer were co-formulated according to different molar ratios to form siRNA polyplexes at N/P 3, 6, 12 and 24. Free siRNA was used as control.

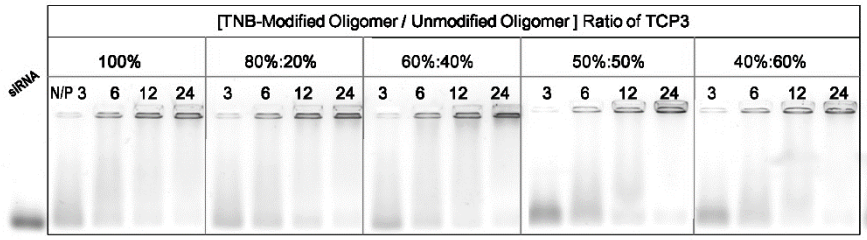

Figure 6.9 siRNA binding of TCP3 determined by agarose gel shift assay. TNB-C-Stp_3-K-(Stp_3-C-TNB)$_2$ (*769*) as DTNB-modified oligomer and K-(PEG_{24}-Folate)-K-[K-(Sph_4-C)$_2$]$_2$ (*709*) as unmodified oligomer were co-formulated according to different molar ratios to form siRNA polyplexes at N/P 3, 6, 12 and 24. Free siRNA was used as control.

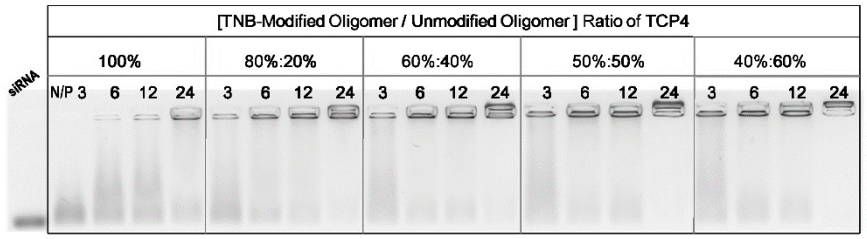

Figure 6.10 siRNA binding of TCP4 determined by agarose gel shift assay. K-(PEG_{24}-Folate)-K-(Sph_4-Y_3-C-TNB)$_2$ (*874*) as DTNB-modified oligomer and C-H-(Stp-H)$_3$-K-[(H-Stp)$_3$-H-C]$_2$ (*689*) as unmodified oligomer were co-formulated according to different molar ratios to form siRNA polyplexes at N/P 3, 6, 12 and 24. Free siRNA was used as control.

6.3 Analytical data

^{1}H-NMR Data of Oligomers

#1(690): K-(PEG_{24}-Acetate)-K-(Sph_3-C)$_2$

^{1}H-NMR spectrum in D_2O. δ (ppm) = 1.2-1.6 (m, 12 H, βγδH lysine), 1.97 (s, 3H, acetate CH_3), 2.4-2.7 (m, 26 H, -CO-CH_2-CH_2-CO-, -CO-CH_2- $dPEG_{24}$), 3.0-3.6 (m, 128 H, -CH_2-Tp, εH lysine and βH cysteine), 3.6-3.8 (m, 98 H, -CH_2-O- $dPEG_{24}$, -CH_2-N- $dPEG_{24}$), 4.1-4.4 (m, 4 H, αH lysine and αH cysteine).

#2(*691*): K-(PEG_{24}-FolA)-K-(Sph_3-C)$_2$

^{1}H-NMR spectrum in D_2O. δ (ppm) = 1.2-1.6 (m, 12 H, βγδH lysine), 2.1-2.4 (m, 4 H, βγH glutamic acid), 2.4-2.6 (m, 26 H, -CO-CH_2-CH_2-CO-, -CO-CH_2- $dPEG_{24}$), 3.0-3.6 (m, 128 H, -CH_2- Tp, εH lysine and βH cysteine), 3.6-3.8 (m, 98 H, -CH_2-O- $dPEG_{24}$, -CH_2-N- $dPEG_{24}$), 4.1-4.6 (m, 7H, αH lysine, αH cysteine, αH glutamic acid and -CH_2-N- pteroic acid), 6.7-6.9 (d, 2H, aromatic ring H pteroic acid), 7.6-7.7 (d, 2H, aromatic ring H pteroic acid), 8.8 (s, 1H, aromatic ring H pteroic acid).

#3(*692*): K-(PEG_{24}-Acetate)-K-(Sph_4-C)$_2$

^{1}H-NMR spectrum in D_2O. δ (ppm) = 1.2-1.6 (m, 12 H, βγδH lysine), 1.98 (s, 3H, acetate CH_3), 2.4-2.7 (m, 34 H, -CO-CH_2-CH_2-CO-, -CO-CH_2- $dPEG_{24}$), 3.0-3.6 (m, 168 H, -CH_2- Tp, εH lysine and βH cysteine), 3.6-3.7 (m, 98 H, -CH_2-O- $dPEG_{24}$, -CH_2-N- $dPEG_{24}$), 4.1-4.4 (m, 4 H, αH lysine and αH cysteine).

#4(*693*): K-(PEG_{24}-FolA)-K-(Sph_4-C)$_2$

^{1}H-NMR spectrum in D_2O. δ (ppm) = 1.2-1.6 (m, 12 H, βγδH lysine), 2.0-2.4 (m, 4 H, βγH glutamic acid), 2.4-2.7 (m, 34 H, -CO-CH_2-CH_2-CO-, -CO-CH_2- $dPEG_{24}$), 2.6-3.1 (m, 8 H, εH lysine and cysteine), 3.0-3.6 (m, 160 H, -CH_2- Tp), 3.6-3.7 (m, 98 H, -CH_2-O- $dPEG_{24}$, -CH_2-N- $dPEG_{24}$), 4.1-4.6 (m, 7H, αH lysine, αH cysteine, αH glutamic acid and -CH_2-N- pteroic acid), 6.7-6.9 (d, 2H, aromatic ring H pteroic acid), 7.6-7.7 (d, 2H, aromatic ring H pteroic acid), 8.8 (s, 1H, aromatic ring H pteroic acid).

#5(*788*): K-(PEG_{24}-E)-K-[(H-Stp)$_3$-H-C]$_2$

^{1}H-NMR spectrum in D_2O. δ (ppm) =1.1-1.8 (m, 12 H, βγδH lysine), 1.8-2.2 (m, 4 H, βγH glutamic acid), 2.3-2.6 (m, 26 H, -CO-CH_2-CH_2-CO-, -CO-CH_2- $dPEG_{24}$), 2.9-3.5 (m, 120 H, -CH_2- Tp, εH lysine, βH cysteine and βH histidine), 3.5-3.7 (m, 98 H, -CH_2-O- $dPEG_{24}$, -CH_2-N- $dPEG_{24}$), 4.1-4.7 (m, 13 H, αH lysine, αH cysteine, αH histidine, αH glutamic acid), 7.1-7.4 (m, 8 H, aromatic H histidine), 8.5 (m, 8 H, aromatic H histidine).

#6(*789*): K-(PEG_{24}-FolA)-K-[(H-Stp)$_3$-H-C]$_2$

^{1}H-NMR spectrum in D_2O. δ (ppm) =1.1-1.7 (m, 12 H, βγδH lysine), 1.8-2.2 (m, 4 H, βγH glutamic acid), 2.3-2.5 (m, 26 H, -CO-CH_2-CH_2-CO-, -CO-CH_2- $dPEG_{24}$), 2.9-3.5 (m, 120 H, -CH_2- Tp, εH lysine, βH cysteine and βH histidine), 3.5-3.7 (m, 98 H, -CH_2-O- $dPEG_{24}$, -CH_2-N- $dPEG_{24}$), 4.0-4.7 (m, 15 H, αH lysine, αH cysteine, αH histidine, αH glutamic acid and -CH_2-N- pteroic acid), 6.6-6.8 (d, 2H, aromatic ring H pteroic acid), 7.1-7.3 (m, 8 H, aromatic H histidine), 7.5-7.6 (d, 2H, aromatic ring H pteroic acid), 8.5-8.6 (m, 8 H, aromatic H histidine), 8.68 (s, 1H, aromatic ring H pteroic acid).

#7(*790*): K-(PEG_{24}-E)-K-[(H-Stp)$_4$-H-C]$_2$

^{1}H-NMR spectrum in D_2O. δ (ppm) =1.1-1.7 (m, 12 H, βγδH lysine), 1.8-2.2 (m, 4 H, βγH glutamic acid), 2.3-2.6 (m, 26 H, -CO-CH_2-CH_2-CO-, -CO-CH_2- $dPEG_{24}$), 2.9-3.5 (m, 156

H, -CH_2- Tp, εH lysine, βH cysteine and βH histidine), 3.5-3.6 (m, 98 H, -CH_2-O- $dPEG_{24}$, -CH_2-N- $dPEG_{24}$), 4.0-4.7 (m, 15 H, αH lysine, αH cysteine, αH histidine, αH glutamic acid), 7.1-7.3 (m, 8 H, aromatic H histidine), 8.5-8.7 (m, 8 H, aromatic H histidine).

#8(*791*): K-(PEG_{24}-FolA)-K-[(H-$Stp)_4$-H-C]$_2$

^{1}H-NMR spectrum in D_2O. δ (ppm) = 1.1-1.7 (m, 12 H, βγδH lysine), 1.8-2.2 (m, 4 H, βγH glutamic acid), 2.3-2.6 (m, 34 H, -CO-CH_2-CH_2-CO-, -CO-CH_2- $dPEG_{24}$), 2.9-3.5 (m, 128 H, -CH_2- Tp, εH lysine, βH cysteine and βH histidine), 3.5-3.7 (m, 98 H, -CH_2-O- $dPEG_{24}$, -CH_2-N- $dPEG_{24}$), 4.0-4.7 (m, 17 H, αH lysine, αH cysteine, αH histidine, αH glutamic acid and -CH_2-N- pteroic acid), 6.6-6.8 (d, 2H, aromatic ring H pteroic acid), 7.1-7.4 (m, 10 H, aromatic H histidine), 7.5-7.7 (d, 2H, aromatic ring H pteroic acid), 8.4-8.6 (m, 10 H, aromatic H histidine), 8.7 (s, 1H, aromatic ring H pteroic acid).

#9(*879*): K-(PEG_{24}-E)-K-(Stp_3-Y_3-C)$_2$

^{1}H-NMR spectrum in D_2O. δ (ppm) = 1.2-1.6 (m, 12 H, βγδH lysine), 2.1-2.4 (m, 4 H, βγH glutamic acid), 2.4-2.6 (m, 26 H, -CO-CH_2-CH_2-CO-, -CO-CH_2- $dPEG_{24}$), 2.7-3.5 (m, 96 H, -CH_2- Tp, εH lysine, βH cysteine and βH tyrosine), 3.5-3.7 (m, 98 H, -CH_2-O- $dPEG_{24}$, -CH_2-N- $dPEG_{24}$), 4.0-4.7 (m, 11 H, αH lysine, αH cysteine, αH glutamic acid, αH tyrosine), 6.7-7.2 (m, 24 H, aromatic ring tyrosine).

#10(*880*): K-(PEG_{24}-FolA)-K-(Stp_3-Y_3-C)$_2$

^{1}H-NMR spectrum in D_2O. δ (ppm) = 1.2-1.6 (m, 12 H, βγδH lysine), 2.1-2.4 (m, 4 H, βγH glutamic acid), 2.4-2.6 (m, 26 H, -CO-CH_2-CH_2-CO-, -CO-CH_2- $dPEG_{24}$), 2.7-3.5 (m, 116 H, -CH_2- Tp, εH lysine, βH cysteine and βH tyrosine), 3.5-3.7 (m, 98 H, -CH_2-O- $dPEG_{24}$, -CH_2-N- $dPEG_{24}$), 4.0-4.7 (m, 13 H, αH lysine, αH cysteine, αH tyrosine, αH glutamic acid and -CH_2-N- pteroic acid), 6.6-7.2 (m, 26 H, aromatic ring H tyrosine, aromatic ring H pteroic acid), 7.6-7.7 (d, 2H, aromatic ring H pteroic acid), 8.79 (s, 1H, aromatic ring H pteroic acid).

#11(*881*): K-(PEG_{24}-E)-K-(Stp_4-Y_3-C)$_2$

^{1}H-NMR spectrum in D_2O. δ (ppm) = 1.2-1.6 (m, 12 H, βγδH lysine), 2.1-2.4 (m, 4 H, βγH glutamic acid), 2.4-2.6 (m, 34 H, -CO-CH_2-CH_2-CO-, -CO-CH_2- $dPEG_{24}$), 2.7-3.5 (m, 148 H, -CH_2- Tp), 3.5-3.7 (m, 98 H, -CH_2-O- $dPEG_{24}$, -CH_2-N- $dPEG_{24}$), 4.0-4.7 (m, 11 H, αH lysine, αH cysteine, αH glutamic acid, αH tyrosine), 6.6-7.1 (m, 24 H, aromatic ring

tyrosine).

#12(*882*): K-(PEG$_{24}$-FolA)-K-(Stp$_4$-Y$_3$-C)$_2$

^{1}H-NMR spectrum in D_2O. δ (ppm) = 1.2-1.6 (m, 12 H, βγδH lysine), 2.1-2.4 (m, 4 H, βγH glutamic acid), 2.4-2.6 (m, 34 H, -CO-CH_2-CH_2-CO-, -CO-CH_2- dPEG$_{24}$), 2.7-3.5 (m, 148 H, -CH_2- Tp, εH lysine, βH cysteine and βH tyrosine), 3.5-3.7 (m, 98 H, -CH_2-O- dPEG$_{24}$, -CH_2-N- dPEG$_{24}$), 4.0-4.7 (m, 13 H, αH lysine, αH cysteine, αH tyrosine, αH glutamic acid and -CH_2-N- pteroic acid), 6.7-7.2 (m, 26 H, aromatic ring H tyrosine, aromatic ring H pteroic acid), 7.6-7.7 (d, 2H, aromatic ring H pteroic acid), 8.7 (s, 1H, aromatic ring H pteroic acid).

#13(*714*): K-(PEG$_{24}$-E)-K-(Sph$_3$-Y$_3$-C)$_2$

^{1}H-NMR spectrum in D_2O. δ (ppm) = 1.2-1.6 (m, 12 H, βγδH lysine), 1.9-2.3 (m, 4 H, βγH glutamic acid), 2.5-2.6 (m, 26 H, -CO-CH_2-CH_2-CO-, -CO-CH_2- dPEG$_{24}$), 2.7-3.6 (m, 140 H, -CH_2- Tp, εH lysine, βH cysteine and βH tyrosine), 3.6-3.7 (m, 98 H, -CH_2-O- dPEG$_{24}$, -CH_2-N- dPEG$_{24}$), 4.0-4.6 (m, 11 H, αH lysine, αH cysteine, αH glutamic acid, αH tyrosine), 6.7-7.2 (m, 24 H, aromatic ring tyrosine).

#14(*715*): K-(PEG$_{24}$-FolA)-K-(Sph$_3$-Y$_3$-C)$_2$

^{1}H-NMR spectrum in D_2O. δ (ppm) = 1.2-1.6 (m, 12 H, βγδH lysine), 1.9-2.2 (m, 4 H, βγH glutamic acid), 2.4-2.6 (m, 26 H, -CO-CH_2-CH_2-CO-, -CO-CH_2- dPEG$_{24}$), 2.7-3.6 (m, 140 H, -CH_2- Tp, εH lysine, βH cysteine and βH tyrosine), 3.6-3.7 (m, 98 H, -CH_2-O- dPEG$_{24}$, -CH_2-N- dPEG$_{24}$), 4.0-4.7 (m, 13 H, αH lysine, αH cysteine, αH tyrosine, αH glutamic acid and -CH_2-N- pteroic acid), 6.7-7.2 (m, 26 H, aromatic ring H tyrosine, aromatic ring H pteroic acid), 7.6-7.8 (d, 2H, aromatic ring H pteroic acid), 8.8 (s, 1H, aromatic ring H pteroic acid).

#15(*716*): K-(PEG$_{24}$-E)-K-(Sph$_4$-Y$_3$-C)$_2$

^{1}H-NMR spectrum in D_2O. δ (ppm) = 1.2-1.6 (m, 12 H, βγδH lysine), 1.9-2.2 (m, 4 H, βγH glutamic acid), 2.5-2.7 (m, 34 H, -CO-CH_2-CH_2-CO-, -CO-CH_2- dPEG$_{24}$), 2.7-3.6 (m, 160 H, -CH_2- Tp, εH lysine, βH cysteine and βH tyrosine), 3.6-3.7 (m, 98 H, -CH_2-O- dPEG$_{24}$, -CH_2-N- dPEG$_{24}$), 4.0-4.5 (m, 11 H, αH lysine, αH cysteine, αH glutamic acid, αH tyrosine), 6.7-7.2 (m, 24 H, aromatic ring tyrosine).

#16(*717*): K-(PEG_{24}-FolA)-K-(Sph_4-Y_3-C)$_2$

^{1}H-NMR spectrum in D_2O. δ (ppm) = 1.2-1.6 (m, 12 H, βγδH lysine), 2.1-2.4 (m, 4 H, βγH glutamic acid), 2.4-2.6 (m, 34 H, -CO-CH_2-CH_2-CO-, -CO-CH_2- $dPEG_{24}$), 2.7-3.6 (m, 160 H, -CH_2- Tp, εH lysine, βH cysteine and βH tyrosine), 3.6-3.7 (m, 98 H, -CH_2-O- $dPEG_{24}$, -CH_2-N- $dPEG_{24}$), 4.0-4.7 (m, 13 H, αH lysine, αH cysteine, αH tyrosine, αH glutamic acid and -CH_2-N- pteroic acid), 6.6-7.2 (m, 26 H, aromatic ring H tyrosine, aromatic ring H pteroic acid), 7.6-7.7 (d, 2H, aromatic ring H pteroic acid), 8.79 (s, 1H, aromatic ring H pteroic acid).

#17(*792*): K-(PEG_{24}-E)-K-[(H-Stp)$_3$-H-Y_3-C]$_2$

^{1}H-NMR spectrum in D_2O. δ (ppm) = 1.1-1.7 (m, 12 H, βγδH lysine), 1.9-2.2 (m, 4 H, βγH glutamic acid), 2.3-2.5 (m, 26 H, -CO-CH_2-CH_2-CO-, -CO-CH_2- $dPEG_{24}$), 2.6-3.5 (m, 132 H, -CH_2- Tp, εH lysine, βH cysteine, βH tyrosine and βH histidine), 3.5-3.7 (m, 98 H, -CH_2-O- $dPEG_{24}$, -CH_2-N- $dPEG_{24}$), 4.0-4.7 (m, 19 H, αH lysine, αH cysteine, αH tyrosine, αH glutamic acid, αH histidine), 6.5-7.3 (m, 32 H, aromatic H tyrosine, aromatic H histidine), 8.4-8.6 (m, 8 H, aromatic H histidine).

#18(*793*): K-(PEG_{24}-FolA)-K-[(H-Stp)$_3$-H-Y_3-C]$_2$

^{1}H-NMR spectrum in D_2O. δ (ppm) = 1.1-1.5 (m, 12 H, βγδH lysine), 1.9-2.1 (m, 4 H, βγH glutamic acid), 2.3-2.5 (m, 26 H, -CO-CH_2-CH_2-CO-, -CO-CH_2- $dPEG_{24}$), 2.6-3.5 (m, 132 H, -CH_2- Tp, εH lysine, βH cysteine, βH tyrosine and βH histidine), 3.5-3.6 (m, 98 H, -CH_2-O- $dPEG_{24}$, -CH_2-N- $dPEG_{24}$), 4.0-4.7 (m, 21 H, αH lysine, αH cysteine, αH tyrosine, αH glutamic acid, αH histidine and -CH_2-N- pteroic acid), 6.5-7.3 (m, 34 H, aromatic H tyrosine, aromatic ring H pteroic acid, aromatic H histidine), 7.2-7.4 (m, 8 H,), 7.5-7.6 (d, 2H, aromatic ring H pteroic acid), 8.4-8.6 (m, 8 H, aromatic H histidine), 8.69 (s, 1H, aromatic ring H pteroic acid).

#19(*794*): K-(PEG_{24}-E)-K-[(H-Stp)$_4$-H-Y_3-C]$_2$

^{1}H-NMR spectrum in D_2O. δ (ppm) = 1.1-1.5 (m, 12 H, βγδH lysine), 1.8-2.1 (m, 4 H, βγH glutamic acid), 2.3-2.5 (m, 26 H, -CO-CH_2-CH_2-CO-, -CO-CH_2- $dPEG_{24}$), 2.6-3.5 (m, 168 H, -CH_2- Tp, εH lysine, βH cysteine, βH tyrosine and βH histidine), 3.5-3.7 (m, 98 H, -CH_2-O- $dPEG_{24}$, -CH_2-N- $dPEG_{24}$), 4.0-4.7 (m, 21 H, αH lysine, αH cysteine, αH tyrosine, αH glutamic acid, αH histidine), 6.5-7.3 (m, 34 H, aromatic H tyrosine, aromatic H histidine),

8.4-8.6 (m, 10 H, aromatic H histidine).

#20(*795*): K-(PEG$_{24}$-FolA)-K-[(H-Stp)$_4$-H-Y$_3$-C]$_2$

^{1}H-NMR spectrum in D_2O. δ (ppm) = 1.0-1.5 (m, 12 H, βγδH lysine), 1.8-2.1 (m, 4 H, βγH glutamic acid), 2.3-2.5 (m, 34 H, -CO-CH_2-CH_2-CO-, -CO-CH_2- dPEG$_{24}$), 2.6-3.5 (m, 168 H, -CH_2- Tp, εH lysine, βH cysteine, βH tyrosine and βH histidine), 3.5-3.7 (m, 98 H, -CH_2-O- dPEG$_{24}$, -CH_2-N- dPEG$_{24}$), 4.0-4.7 (m, 23 H, αH lysine, αH cysteine, αH tyrosine, αH glutamic acid, αH histidine and -CH_2-N- pteroic acid), 6.5-7.3 (m, 34 H, aromatic ring H tyrosine, aromatic ring H pteroic acid and aromatic H histidine), 7.5-7.6 (d, 2H, aromatic ring H pteroic acid), 8.4-8.6 (m, 10 H, aromatic H histidine), 8.69 (s, 1H, aromatic ring H pteroic acid).

#21(*732*): K-(PEG$_{24}$-E)-K-[K-(Stp$_3$-C)$_2$]$_2$

^{1}H-NMR spectrum in D_2O. δ (ppm) = 1.0-1.5 (m, 24 H, βγδH lysine), 1.9-2.2 (m, 4 H, βγH glutamic acid), 2.3-2.5 (m, 50 H, -CO-CH_2-CH_2-CO-, -CO-CH_2- dPEG$_{24}$), 2.9-3.5 (m, 208 H, -CH_2- Tp, εH lysine and βH cysteine), 3.5-3.7 (m, 98 H, -CH_2-O- dPEG$_{24}$, -CH_2-N-dPEG$_{24}$), 4.0-4.6 (m, 9 H, αH lysine, αH cysteine, αH glutamic acid).

#22(*733*): K-(PEG$_{24}$-FolA)-K-[K-(Stp$_3$-C)$_2$]$_2$

^{1}H-NMR spectrum in D_2O. δ (ppm) = 1.0-1.5 (m, 24 H, βγδH lysine), 1.9-2.2 (m, 4 H, βγH glutamic acid), 2.4-2.6 (m, 50 H, -CO-CH_2-CH_2-CO-, -CO-CH_2- dPEG$_{24}$), 2.9-3.5 (m, 208 H, -CH_2- Tp, εH lysine and βH cysteine), 3.5-3.7 (m, 98 H, -CH_2-O- dPEG$_{24}$, -CH_2-N-dPEG$_{24}$), 4.0-4.6 (m, 11H, αH lysine, αH cysteine, αH glutamic acid and -CH_2-N- pteroic acid), 6.7-6.8 (d, 2H, aromatic ring H pteroic acid), 7.5-7.7 (d, 2H, aromatic ring H pteroic acid), 8.75 (s, 1H, aromatic ring H pteroic acid).

#23(*734*): K-(PEG$_{24}$-E)-K-[K-(Stp$_4$-C)$_2$]$_2$

^{1}H-NMR spectrum in D_2O. δ (ppm) = 1.0-1.5 (m, 24 H, βγδH lysine), 1.9-2.2 (m, 4 H, βγH glutamic acid), 2.3-2.5 (m, 66 H, -CO-CH_2-CH_2-CO-, -CO-CH_2- dPEG$_{24}$), 2.9-3.5 (m, 272 H, -CH_2- Tp, εH lysine and βH cysteine), 3.5-3.7 (m, 98 H, -CH_2-O- dPEG$_{24}$, -CH_2-N-dPEG$_{24}$), 4.0-4.6 (m, 9 H, αH lysine, αH cysteine, αH glutamic acid).

#24(*735*): K-(PEG$_{24}$-FolA)-K-[K-(Stp$_4$-C)$_2$]$_2$

^{1}H-NMR spectrum in D_2O. δ (ppm) = 1.0-1.5 (m, 24 H, βγδH lysine), 1.9-2.2 (m, 4 H, βγH

glutamic acid), 2.4-2.6 (m, 66 H, -CO-CH_2-CH_2-CO-, -CO-CH_2- $dPEG_{24}$), 2.9-3.5 (m, 272 H, -CH_2- Tp, εH lysine and βH cysteine), 3.5-3.7 (m, 98 H, -CH_2-O- $dPEG_{24}$, -CH_2-N- $dPEG_{24}$), 4.0-4.7 (m, 11H, αH lysine, αH cysteine, αH glutamic acid and -CH_2-N- pteroic acid), 6.7-6.8 (d, 2H, aromatic ring H pteroic acid), 7.5-7.7 (d, 2H, aromatic ring H pteroic acid), 8.75 (s, 1H, aromatic ring H pteroic acid).

#25(*706*): K-(PEG_{24}-A)-K-[K-(Sph_3-C)$_2$]$_2$

^{1}H-NMR spectrum in D_2O. δ (ppm) = 1.2-1.6 (m, 27 H, βH alanine, βγδH lysine), 2.4-2.6 (m, 50 H, -CO-CH_2-CH_2-CO-, -CO-CH_2- $dPEG_{24}$), 3.0-3.6 (m, 256 H, -CH_2- Tp, εH lysine and βH cysteine), 3.6-3.7 (m, 98 H, -CH_2-O- $dPEG_{24}$, -CH_2-N- $dPEG_{24}$), 4.0-4.4 (m, 9 H, αH lysine, αH cysteine, αH alanine).

#26(*707*): K-(PEG_{24}-FolA)-K-[K-(Sph_3-C)$_2$]$_2$

^{1}H-NMR spectrum in D_2O. δ (ppm) = 1.2-1.6 (m, 24 H, βγδH lysine), 1.9-2.2 (m, 4 H, βγH glutamic acid), 2.4-2.6 (m, 50 H, -CO-CH_2-CH_2-CO-, -CO-CH_2- $dPEG_{24}$), 3.0-3.5 (m, 256 H, -CH_2- Tp, εH lysine and βH cysteine), 3.6-3.7 (m, 98 H, -CH_2-O- $dPEG_{24}$, -CH_2-N- $dPEG_{24}$), 4.0-4.6 (m, 11H, αH lysine, αH cysteine, αH glutamic acid and -CH_2-N- pteroic acid), 6.8-6.9 (d, 2H, aromatic ring H pteroic acid), 7.6-7.7 (d, 2H, aromatic ring H pteroic acid), 8.82 (s, 1H, aromatic ring H pteroic acid).

#27(*708*): K-(PEG_{24}-A)-K-[K-(Sph_4-C)$_2$]$_2$

^{1}H-NMR spectrum in D_2O. δ (ppm) = 1.2-1.6 (m, 27 H, βH alanine, βγδH lysine), 2.4-2.7 (m, 66 H, -CO-CH_2-CH_2-CO-, -CO-CH_2- $dPEG_{24}$), 3.0-3.6 (m, 336 H, -CH_2- Tp, εH lysine and βH cysteine), 3.5-3.7 (m, 98 H, -CH_2-O- $dPEG_{24}$, -CH_2-N- $dPEG_{24}$), 4.0-4.7 (m, 9 H, αH lysine, αH cysteine, αH alanine).

#28(*709*): K-(PEG_{24}-FolA)-K-[K-(Sph_4-C)$_2$]$_2$

^{1}H-NMR spectrum in D_2O. δ (ppm) = 1.2-1.6 (m, 24 H, βγδH lysine), 1.9-2.2 (m, 4 H, βγH glutamic acid), 2.4-2.7 (m, 66 H, -CO-CH_2-CH_2-CO-, -CO-CH_2- $dPEG_{24}$), 3.0-3.5 (m, 336 H, -CH_2- Tp, εH lysine and βH cysteine), 3.6-3.7 (m, 98 H, -CH_2-O- $dPEG_{24}$, -CH_2-N- $dPEG_{24}$), 4.0-4.6 (m, 11H, αH lysine, αH cysteine, αH glutamic acid and -CH_2-N- pteroic acid), 6.7-6.9 (d, 2H, aromatic ring H pteroic acid), 7.6-7.7 (d, 2H, aromatic ring H pteroic acid), 8.81 (s, 1H, aromatic ring H pteroic acid).

#29(*761*): K-(PEG_{24}-E)-K-[H-K-((H-Stp)$_3$-H-C)$_2$]$_2$

^{1}H-NMR spectrum in D_2O. δ (ppm) = 1.0-1.7 (m, 24 H, βγδH lysine), 1.8-2.2 (m, 4 H, βγH glutamic acid), 2.3-2.5 (m, 50 H, -CO-CH_2-CH_2-CO-, -CO-CH_2- $dPEG_{24}$), 2.9-3.5 (m, 244 H, -CH_2- Tp, εH lysine, βH cysteine and βH histidine), 3.5-3.7 (m, 98 H, -CH_2-O- $dPEG_{24}$, -CH_2-N- $dPEG_{24}$), 4.0-4.7 (m, 27 H, αH lysine, αH cysteine, αH histidine, αH glutamic acid), 7.1-7.3 (m, 18 H, aromatic H histidine), 8.5-8.6 (m, 18 H, aromatic H histidine).

#30(*762*): K-(PEG_{24}-FolA)-K-[H-K-((H-Stp)$_3$-H-C)$_2$]$_2$

^{1}H-NMR spectrum in D_2O. δ (ppm) = 1.0-1.7 (m, 24 H, βγδH lysine), 1.8-2.2 (m, 4 H, βγH glutamic acid), 2.3-2.5 (m, 50 H, -CO-CH_2-CH_2-CO-, -CO-CH_2- $dPEG_{24}$), 2.9-3.5 (m, 244 H, -CH_2- Tp, εH lysine, βH cysteine and βH histidine), 3.5-3.7 (m, 98 H, -CH_2-O- $dPEG_{24}$, -CH_2-N- $dPEG_{24}$), 4.0-4.7 (m, 29 H, αH lysine, αH cysteine, αH histidine, αH glutamic acid and -CH_2-N- pteroic acid), 6.6-6.8 (d, 2H, aromatic ring H pteroic acid), 7.1-7.3 (m, 18 H, aromatic H histidine), 7.5-7.6 (d, 2H, aromatic ring H pteroic acid), 8.4-8.6 (m, 18 H, aromatic H histidine), 8.69 (s, 1H, aromatic ring H pteroic acid).

#31(*763*): K-(PEG_{24}-E)-K-[H-K-((H-Stp)$_4$-H-C)$_2$]$_2$

^{1}H-NMR spectrum in D_2O. δ (ppm) = 1.0-1.7 (m, 24 H, βγδH lysine), 1.8-2.2 (m, 4 H, βγH glutamic acid), 2.3-2.6 (m, 66 H, -CO-CH_2-CH_2-CO-, -CO-CH_2- $dPEG_{24}$), 2.9-3.5 (m, 256 H, -CH_2- Tp, εH lysine, βH cysteine and βH histidine), 3.5-3.7 (m, 98 H, -CH_2-O- $dPEG_{24}$, -CH_2-N- $dPEG_{24}$), 4.0-4.7 (m, 31 H, αH lysine, αH cysteine, αH histidine, αH glutamic acid), 7.1-7.3 (m, 22 H, aromatic H histidine), 8.4-8.6 (m, 22 H, aromatic H histidine).

#32(*764*): K-(PEG_{24}-FolA)-K-[H-K-((H-Stp)$_4$-H-C)$_2$]$_2$

^{1}H-NMR spectrum in D_2O. δ (ppm) = 1.0-1.7 (m, 24 H, βγδH lysine), 1.8-2.2 (m, 4 H, βγH glutamic acid), 2.3-2.6 (m, 66 H, -CO-CH_2-CH_2-CO-, -CO-CH_2- $dPEG_{24}$), 2.8-3.5 (m, 316 H, -CH_2- Tp, εH lysine, βH cysteine and βH histidine), 3.5-3.7 (m, 98 H, -CH_2-O- $dPEG_{24}$, -CH_2-N- $dPEG_{24}$), 4.0-4.7 (m, 33 H, αH lysine, αH cysteine, αH histidine, αH glutamic acid and -CH_2-N- pteroic acid), 6.6-6.8 (d, 2H, aromatic ring H pteroic acid), 7.1-7.3 (m, 22 H, aromatic H histidine), 7.5-7.6 (d, 2H, aromatic ring H pteroic acid), 8.4-8.6 (m, 22 H, aromatic H histidine), 8.69 (s, 1H, aromatic ring H pteroic acid).

#33(*712*): K-(PEG_{24}-E)-K-[H-K-((H-Sph)$_3$-H-C)$_2$]$_2$

^{1}H-NMR spectrum in D_2O. δ (ppm) = 1.1-1.5 (m, 24 H, βγδH lysine), 1.9-2.2 (m, 4 H, βγH glutamic acid), 2.4-2.6 (m, 50 H, -CO-CH_2-CH_2-CO-, -CO-CH_2- dPEG$_{24}$), 2.8-3.6 (m, 292 H, -CH_2- Tp, εH lysine, βH cysteine and βH histidine), 3.6-3.7 (m, 98 H, -CH_2-O- dPEG$_{24}$, -CH_2-N- dPEG$_{24}$), 3.9-4.7 (m, 27 H, αH lysine, αH cysteine, αH histidine, αH glutamic acid), 7.2-7.4 (m, 18 H, aromatic H histidine), 8.5-8.7 (m, 18 H, aromatic H histidine).

#34(*713*): K-(PEG$_{24}$-FolA)-K-[H-K-((H-Sph)$_3$-H-C)$_2$]$_2$

^{1}H-NMR spectrum in D_2O. δ (ppm) = 1.1-1.5 (m, 24 H, βγδH lysine), 1.9-2.2 (m, 4 H, βγH glutamic acid), 2.4-2.6 (m, 50 H, -CO-CH_2-CH_2-CO-, -CO-CH_2- dPEG$_{24}$), 2.9-3.6 (m, 292 H, -CH_2- Tp, εH lysine, βH cysteine and βH histidine), 3.6-3.7 (m, 98 H, -CH_2-O- dPEG$_{24}$, -CH_2-N- dPEG$_{24}$), 4.1-4.7 (m, 29 H, αH lysine, αH cysteine, αH histidine, αH glutamic acid and -CH_2-N- pteroic acid), 6.7-6.9 (d, 2H, aromatic ring H pteroic acid), 7.2-7.4 (m, 18 H, aromatic H histidine), 7.6-7.7 (d, 2H, aromatic ring H pteroic acid), 8.5-8.7 (m, 18 H, aromatic H histidine), 8.78 (s, 1H, aromatic ring H pteroic acid).

#35(*875*): K-(PEG$_{24}$-E)-K-[K-(Stp$_3$-Y$_3$-C)$_2$]$_2$

^{1}H-NMR spectrum in D_2O. δ (ppm) = 1.0-1.5 (m, 24 H, βγδH lysine), 1.9-2.2 (m, 4 H, βγH glutamic acid), 2.4-2.6 (m, 50 H, -CO-CH_2-CH_2-CO-, -CO-CH_2- dPEG$_{24}$), 2.6-3.5 (m, 232 H, -CH_2- Tp, εH lysine, βH cysteine and βH tyrosine), 3.5-3.7 (m, 98 H, -CH_2-O- dPEG$_{24}$, -CH_2-N- dPEG$_{24}$), 4.0-4.5 (m, 21 H, αH lysine, αH cysteine, αH glutamic acid, αH tyrosine), 6.6-7.1 (m, 48 H, aromatic ring tyrosine).

#36(*876*): K-(PEG$_{24}$-FolA)-K-[K-(Stp$_3$-Y$_3$-C)$_2$]$_2$

^{1}H-NMR spectrum in D_2O. δ (ppm) = 1.0-1.5 (m, 24 H, βγδH lysine), 1.9-2.2 (m, 4 H, βγH glutamic acid), 2.4-2.6 (m, 50 H, -CO-CH_2-CH_2-CO-, -CO-CH_2- dPEG$_{24}$), 2.6-3.5 (m, 232 H, -CH_2- Tp, εH lysine, βH cysteine and βH tyrosine), 3.5-3.7 (m, 98 H, -CH_2-O- dPEG$_{24}$, -CH_2-N- dPEG$_{24}$), 4.0-4.6 (m, 23 H, αH lysine, αH cysteine, αH tyrosine, αH glutamic acid and -CH_2-N- pteroic acid), 6.6-7.2 (m, 50 H, aromatic ring H tyrosine, aromatic ring H pteroic acid), 7.5-7.7 (d, 2H, aromatic ring H pteroic acid), 8.71 (s, 1H, aromatic ring H pteroic acid).

#37(*877*): K-(PEG$_{24}$-E)-K-[K-(Stp$_4$-Y$_3$-C)$_2$]$_2$

^{1}H-NMR spectrum in D_2O. δ (ppm) = 1.0-1.5 (m, 24 H, βγδH lysine), 1.9-2.2 (m, 4 H, βγH glutamic acid), 2.4-2.6 (m, 66 H, -CO-CH_2-CH_2-CO-, -CO-CH_2- dPEG$_{24}$), 2.6-3.5 (m, 296

H, -CH_2- Tp, εH lysine, βH cysteine and βH tyrosine), 3.5-3.7 (m, 98 H, -CH_2-O- $dPEG_{24}$, -CH_2-N- $dPEG_{24}$), 4.0-4.6 (m, 21 H, αH lysine, αH cysteine, αH glutamic acid, αH tyrosine), 6.6-7.1 (m, 48 H, aromatic ring tyrosine).

#38(*878*): K-(PEG_{24}-FolA)-K-[K-(Stp_4-Y_3-C)$_2$]$_2$

^{1}H-NMR spectrum in D_2O. δ (ppm) = 1.0-1.5 (m, 24 H, βγδH lysine), 1.9-2.2 (m, 4 H, βγH glutamic acid), 2.4-2.6 (m, 66 H, -CO-CH_2-CH_2-CO-, -CO-CH_2- $dPEG_{24}$), 2.6-3.5 (m, 296 H, -CH_2- Tp, εH lysine, βH cysteine and βH tyrosine), 3.5-3.7 (m, 98 H, -CH_2-O- $dPEG_{24}$, -CH_2-N- $dPEG_{24}$), 4.0-4.6 (m, 23 H, αH lysine, αH cysteine, αH tyrosine, αH glutamic acid and -CH_2-N- pteroic acid), 6.6-7.2 (m, 50 H, aromatic ring H tyrosine, aromatic ring H pteroic acid), 7.5-7.7 (d, 2H, aromatic ring H pteroic acid), 8.71 (s, 1H, aromatic ring H pteroic acid).

#39(*765*): K-(PEG_{24}-E)-K-[H-K-((H-Stp)$_3$-H-Y_3-C)$_2$]$_2$

^{1}H-NMR spectrum in D_2O. δ (ppm) = 1.0-1.5 (m, 24 H, βγδH lysine), 1.8-2.1 (m, 4 H, βγH glutamic acid), 2.3-2.5 (m, 50 H, -CO-CH_2-CH_2-CO-, -CO-CH_2- $dPEG_{24}$), 2.6-3.5 (m, 268 H, -CH_2- Tp, εH lysine, βH cysteine, βH tyrosine, βH histidine), 3.5-3.7 (m, 98 H, -CH_2-O- $dPEG_{24}$, -CH_2-N- $dPEG_{24}$), 3.9-4.7 (m, 39 H, αH lysine, αH cysteine, αH tyrosine, αH glutamic acid, αH histidine), 6.5-7.1 (m, 48 H, aromatic ring tyrosine), 7.1-7.3 (m, 18 H, aromatic H histidine), 8.4-8.6 (m, 18 H, aromatic H histidine).

#40(*766*): K-(PEG_{24}-FolA)-K-[H-K-((H-Stp)$_3$-H-Y_3-C)$_2$]$_2$

^{1}H-NMR spectrum in D_2O. δ (ppm) = 1.0-1.5 (m, 24 H, βγδH lysine), 1.8-2.1 (m, 4 H, βγH glutamic acid), 2.3-2.5 (m, 50 H, -CO-CH_2-CH_2-CO-, -CO-CH_2- $dPEG_{24}$), 2.6-3.5 (m, 268 H, -CH_2- Tp, εH lysine, βH cysteine, βH tyrosine, βH histidine), 3.5-3.7 (m, 98 H, -CH_2-O- $dPEG_{24}$, -CH_2-N- $dPEG_{24}$), 3.9-4.7 (m, 41 H, αH lysine, αH cysteine, αH tyrosine, αH glutamic acid, αH histidine and -CH_2-N- pteroic acid), 6.5-7.1 (m, 50 H, aromatic ring H tyrosine, aromatic ring H pteroic acid), 7.1-7.3 (m, 18 H, aromatic H histidine), 7.5-7.6 (d, 2H, aromatic ring H pteroic acid), 8.4-8.6 (m, 18 H, aromatic H histidine), 8.64 (s, 1H, aromatic ring H pteroic acid).

#41(*767*): K-(PEG_{24}-E)-K-[H-K-((H-Stp)$_4$-H-Y_3-C)$_2$]$_2$

^{1}H-NMR spectrum in D_2O. δ (ppm) = 1.0-1.5 (m, 24 H, βγδH lysine), 1.8-2.1 (m, 4 H, βγH glutamic acid), 2.3-2.5 (m, 66 H, -CO-CH_2-CH_2-CO-, -CO-CH_2- $dPEG_{24}$), 2.6-3.5 (m, 340

H, -CH_2- Tp, εH lysine, βH cysteine, βH tyrosine, βH histidine), 3.5-3.7 (m, 98 H, -CH_2-O-$dPEG_{24}$, -CH_2-N- $dPEG_{24}$), 3.9-4.7 (m, 43 H, αH lysine, αH cysteine, αH tyrosine, αH glutamic acid, αH histidine), 6.5-7.1 (m, 48 H, aromatic ring tyrosine), 7.1-7.3 (m, 22 H, aromatic H histidine), 8.4-8.6 (m, 22 H, aromatic H histidine).

#42(*768*): K-(PEG_{24}-FolA)-K-[H-K-((H-Stp)$_3$-H-Y_3-C)$_2$]$_2$

^{1}H-NMR spectrum in D_2O. δ (ppm) = 1.0-1.5 (m, 24 H, βγδH lysine), 1.8-2.1 (m, 4 H, βγH glutamic acid), 2.3-2.5 (m, 66 H, -CO-CH_2-CH_2-CO-, -CO-CH_2- $dPEG_{24}$), 2.6-3.5 (m, 340 H, -CH_2- Tp, εH lysine, βH cysteine, βH tyrosine, βH histidine), 3.5-3.7 (m, 98 H, -CH_2-O-$dPEG_{24}$, -CH_2-N- $dPEG_{24}$), 3.9-4.7 (m, 45 H, αH lysine, αH cysteine, αH tyrosine, αH glutamic acid, αH histidine and -CH_2-N- pteroic acid), 6.5-7.1 (m, 50 H, aromatic ring H tyrosine, aromatic ring H pteroic acid), 7.1-7.3 (m, 22 H, aromatic H histidine), 7.5-7.6 (d, 2H, aromatic ring H pteroic acid), 8.4-8.6 (m, 22 H, aromatic H histidine), 8.69 (s, 1H, aromatic ring H pteroic acid).

***769*:** TNB-C-Stp_3-K-(Stp_3-C-TNB)$_2$

^{1}H-NMR spectrum in D_2O.δ (ppm) = 1.1-1.4 (m, 6H, βγδH lysine), 2.3-2.7 (m, 36 H, -CO-CH_2-CH_2-CO- succinic acid), 2.9-3.8 (m, 152 H, -CH_2- tepa, βH cysteine, εH lysine), 4.1-4.7 (m, 4 H, αH cysteine, lysine), 7.5-7.8 (m, 6 H, aromatic H TNB), 7.9-8.1(m, 3 H, aromatic H TNB)

***770*:** TNB-C-H-(Stp-H)$_3$-K-(H-Stp)$_3$-H-C-TNB)$_2$

^{1}H-NMR spectrum in D_2O.δ (ppm) = 1.1-1.4 (m, 6H, βγδH lysine), 2.3-2.7 (m, 36 H, -CO-CH_2-CH_2-CO- succinic acid), 2.9-3.8 (m, 176 H, -CH_2- tepa, βH cysteine, βH histidine, εH lysine), 4.1-4.7 (m, 16 H, αH cysteine, lysine, histidine), 7.2-7.4 (m, 12 H, aromatic H histidine), 7.5-7.8 (m, 6 H, aromatic H TNB), 7.9-8.1(m, 3 H, aromatic H TNB), 8.5-8.7 (m, 12 H, aromatic H histidine).

***873*:** K-(PEG_{24}-FolA)-K-[K-(Sph_4-C-TNB)$_2$]$_2$

^{1}H-NMR spectrum in D_2O. δ (ppm) = 1.2-1.6 (m, 24 H, βγδH lysine), 1.9-2.2 (m, 4 H, βγH glutamic acid), 2.4-2.7 (m, 66 H, -CO-CH_2-CH_2-CO-, -CO-CH_2- $dPEG_{24}$), 3.0-3.5 (m, 336 H, -CH_2- Tp, εH lysine and βH cysteine), 3.6-3.7 (m, 98 H, -CH_2-O- $dPEG_{24}$, -CH_2-N-$dPEG_{24}$), 4.0-4.6 (m, 11H, αH lysine, αH cysteine, αH glutamic acid and -CH_2-N- pteroic acid), 6.7-6.9 (d, 2H, aromatic ring H pteroic acid), 7.5-8.1 (m, 14H, aromatic ring H pteroic

acid, aromatic H TNB), 8.81 (s, 1H, aromatic ring H pteroic acid).

***874*:** K-(PEG$_{24}$-FolA)-K-(Sph$_4$-Y$_3$-C-TNB)$_2$

^{1}H-NMR spectrum in D$_2$O. δ (ppm) = 1.2-1.6 (m, 12 H, βγδH lysine), 2.1-2.4 (m, 4 H, βγH glutamic acid), 2.4-2.6 (m, 34 H, -CO-CH$_2$-CH$_2$-CO-, -CO-CH$_2$- dPEG$_{24}$), 2.7-3.6 (m, 160 H, -CH2- Tp, εH lysine, βH cysteine and βH tyrosine), 3.6-3.7 (m, 98 H, -CH$_2$-O- dPEG$_{24}$, -CH$_2$-N- dPEG$_{24}$), 4.0-4.7 (m, 13 H, αH lysine, αH cysteine, αH tyrosine, αH glutamic acid and -CH$_2$-N- pteroic acid), 6.6-7.2 (m, 26 H, aromatic ring H tyrosine, aromatic ring H pteroic acid), 7.5-8.1 (m, 8H, aromatic ring H pteroic acid, aromatic H TNB), 8.79 (s, 1H, aromatic ring H pteroic acid).

905: K-(K-OA$_2$)-Stp$_4$-C

^{1}H-NMR spectrum in D$_2$O. δ(ppm)= 0.7-0.8 (m, 6 H, -CH$_3$ oleic acid), 1.2-2.2 (m, 68 H, -CH$_2$ oleic acid, βγδH lysine, αH oleic acid), 2.4-2.6 (m, 16 H, -CO-CH$_2$-CH$_2$-CO- succinic acid), 2.9-3.1 (m, 6 H, εH lysine, βH cysteine), 3.2-3.5 (m, 64 H, -CH$_2$- TEPA), 4.1-4.2 (m, 3 H, αH lysine, αH cysteine), 5.0-5.3 (m, 4 H, =CH- oleic acid).

906: K-(K-OA$_2$)-K-(Stp$_2$-C)$_2$

^{1}H-NMR spectrum in D$_2$O. δ(ppm)= 0.7-0.8 (m, 6 H, -CH$_3$ oleic acid), 1.2-2.2 (m, 74 H, -CH$_2$ oleic acid, βγδH lysine, αH oleic acid), 2.4-2.6 (m, 16 H, -CO-CH$_2$-CH$_2$-CO- succinic acid), 2.9-3.1 (m, 10 H, εH lysine, βH cysteine), 3.2-3.5 (m, 64 H, -CH$_2$- TEPA), 4.1-4.2 (m, 5 H, αH lysine, αH cysteine), 5.0-5.3 (m, 4 H, =CH- oleic acid).

907: K-(K-OA$_2$)-K-(Stp$_3$-C)$_2$

^{1}H-NMR spectrum in D$_2$O. δ(ppm)= 0.7-0.8 (m, 6 H, -CH$_3$ oleic acid), 1.2-2.2 (m, 74 H, -CH$_2$ oleic acid, βγδH lysine, αH oleic acid), 2.4-2.6 (m, 24 H, -CO-CH$_2$-CH$_2$-CO- succinic acid), 2.9-3.1 (m, 10 H, εH lysine, βH cysteine), 3.2-3.5 (m, 96 H, -CH$_2$- TEPA), 4.1-4.2 (m, 5 H, αH lysine, αH cysteine), 5.0-5.3 (m, 4 H, =CH- oleic acid).

908: K-(K-OA$_2$)-K-(Stp$_4$-C)$_2$

^{1}H-NMR spectrum in D$_2$O. δ(ppm)= 0.7-0.8 (m, 6 H, -CH$_3$ oleic acid), 1.2-2.2 (m, 74 H, -CH$_2$ oleic acid, βγδH lysine, αH oleic acid), 2.4-2.6 (m, 32 H, -CO-CH$_2$-CH$_2$-CO- succinic acid), 2.9-3.1 (m, 10 H, εH lysine, βH cysteine), 3.2-3.5 (m, 128 H, -CH$_2$- TEPA), 4.1-4.2 (m, 5 H, αH lysine, αH cysteine), 5.0-5.3 (m, 4 H, =CH- oleic acid).

909: K-(K-OA_2)-K-[K-(Stp-C)$_2$]$_2$

^{1}H-NMR spectrum in D_2O. δ(ppm)= 0.7-0.8 (m, 6 H, -CH_3 oleic acid), 1.2-2.2 (m, 86 H, -CH_2 oleic acid, βγδH lysine, αH oleic acid), 2.4-2.6 (m, 16 H, -CO-CH_2-CH_2-CO- succinic acid), 2.9-3.1 (m, 18 H, εH lysine, βH cysteine), 3.2-3.5 (m, 64 H, -CH_2- TEPA), 4.1-4.2 (m, 9 H, αH lysine, αH cysteine), 5.0-5.3 (m, 4 H, =CH- oleic acid).

910: K-(K-OA_2)-K-[K-(Stp_2-C)$_2$]$_2$

^{1}H-NMR spectrum in D_2O. δ(ppm)= 0.7-0.8 (m, 6 H, -CH_3 oleic acid), 1.2-2.2 (m, 86 H, -CH_2 oleic acid, βγδH lysine, αH oleic acid), 2.4-2.6 (m, 32 H, -CO-CH_2-CH_2-CO- succinic acid), 2.9-3.1 (m, 18 H, εH lysine, βH cysteine), 3.2-3.5 (m, 128 H, -CH_2- TEPA), 4.1-4.2 (m, 9 H, αH lysine, αH cysteine), 5.0-5.3 (m, 4 H, =CH- oleic acid).

911: K-(K-OA_2)-K-{K[K-(Stp-C)$_2$]$_2$}$_2$

^{1}H-NMR spectrum in D_2O. δ(ppm)= 0.7-0.8 (m, 6 H, -CH_3 oleic acid), 1.2-2.2 (m, 110 H, -CH_2 oleic acid, βγδH lysine, αH oleic acid), 2.4-2.6 (m, 32 H, -CO-CH_2-CH_2-CO- succinic acid), 2.9-3.1 (m, 34 H, εH lysine, βH cysteine), 3.2-3.5 (m, 128 H, -CH_2- TEPA), 4.1-4.2 (m, 17 H, αH lysine, αH cysteine), 5.0-5.3 (m, 4 H, =CH- oleic acid).

728: K-(PEG_{24}-E)-K-(Stp_4-C-K-OA_2)$_2$

^{1}H-NMR spectrum in D_2O. δ (ppm) = 0.76 (m, 12 H, -CH_3 oleic acid), 1.0-2.25 (m, 136 H, βγδH lysine, βH glutamic acid, -CH_2- oleic acid), 2.4-2.6 (m, 34 H, -CO-CH_2-CH_2-CO- Tepa, -CO-CH_2- $dPEG_{24}$), 2.8-3.1 (m, 14 H, εH lysine, βH cysteine, γH glutamic acid), 3.1-3.5 (m, 128 H, -CH_2- Tepa), 3.5-3.6 (m, 98 H, -CH_2-O- $dPEG_{24}$, -CH_2-N- $dPEG_{24}$), 4.0-4.5 (m, 7 H, αH lysine, αH cysteine, αH glutamic acid), 4.9-5.3 (m, 8 H, =CH- oleic acid).

729: K-(PEG_{24}-FolA)-K-(Stp_4-C-K-OA_2)$_2$

^{1}H-NMR spectrum in D_2O. δ (ppm) = 0.71 (m, 12 H, -CH_3 oleic acid), 0.8-2.3 (m, 136 H, βγδH lysine, βH glutamic acid, -CH_2- oleic acid), 2.4-2.6 (m, 34 H, -CO-CH_2-CH_2-CO- Tepa, -CO-CH_2- $dPEG_{24}$), 2.6-3.1 (m, 14 H, εH lysine, βH cysteine, γH glutamic acid), 3.1-3.5 (m, 128 H, -CH_2- Tepa), 3.5-3.6 (m, 98 H, -CH_2-O- $dPEG_{24}$, -CH_2-N- $dPEG_{24}$), 4.0-4.7 (m, 9 H, αH lysine, αH cysteine, αH glutamic acid, -CH_2-N- pteroic acid), 4.8-5.3 (m, 8 H, =CH- oleic acid), 6.7 (d,2H, aromatic ring H pteroic acid), 7.6 (d, 2H, aromatic ring H pteroic acid), 8.7 (s, 1H, aromatic ring H pteroic acid).

730:K-(PEG$_{24}$-E)-K-(K-OA$_2$)-K-(Stp$_4$-C)$_2$

^{1}H-NMR spectrum in D_2O. δ(ppm)= 0.7-0.8 (m, 6 H, -CH_3 oleic acid), 1.2-2.2 (m, 82 H, -CH_2 oleic acid, βγδH lysine, βH glutamic acid, αH oleic acid), 2.4-2.6 (m, 34 H, -CO-CH_2-CH_2-CO- Tepa, -CO-CH_2- dPEG$_{24}$), 2.8-3.1 (m, 14 H, εH lysine, βH cysteine, γH glutamic acid), 3.1-3.5 (m, 128 H, -CH_2- Tepa), 3.5-3.6 (m, 98 H, -CH_2-O- dPEG$_{24}$, -CH_2-N- dPEG$_{24}$), 4,1-4,2 (m, 7 H, αH lysine, αH cysteine, αH glutamic acid), 5.0-5.4 (m, 4 H, =CH- oleic acid).

731: K-(PEG$_{24}$-FolA)-K-(K-OA$_2$)-K-(Stp$_4$-C)$_2$

^{1}H-NMR spectrum in D_2O. δ(ppm)= 0.7-0.8 (m, 6 H, -CH_3 oleic acid), 1.2-2.2 (m, 82 H, -CH_2 oleic acid, βγδH lysine, βH glutamic acid, αH oleic acid), 2.4-2.6 (m, 34 H, -CO-CH_2-CH_2-CO- Tepa, -CO-CH_2- dPEG$_{24}$), 2.7-3.1 (m, 14 H, εH lysine, βH cysteine, γH glutamic acid), 3.1-3.5 (m, 128 H, -CH_2- Tepa), 3.5-3.6 (m, 98 H, -CH_2-O- dPEG$_{24}$, -CH_2-N- dPEG$_{24}$), 4.0-4.7 (m, 9 H, αH lysine, αH cysteine, αH glutamic acid, -CH_2-N- pteroic acid), 5.0-5.4 (m, 4 H, =CH- oleic acid), 6.7 (d, 2H, aromatic ring H pteroic acid), 7.6 (d, 2H, aromatic ring H pteroic acid), 8.7 (s, 1H, aromatic ring H pteroic acid).

7 Reference

[1] Avery OT, MacLeod CM, McCarty M. Studies on the chemical nature of the substance inducing transformation of pneumococcal types: induction of transformation by a desoxyribonucleic acid fraction isolated from pneumococcus type III. The Journal of Experimental Medicine 1944, 79, 137-158.

[2] Watson JD, Crick FHC. Molecular structure of nucleic acids: a structure for deoxyribose nucleic acid. Nature 1953, 171, 737-738.

[3] Crick F. Central dogma of molecular biology. Nature 1970, 227, 561-563.

[4] Venter JC, Adams MD, Myers EW, Li PW, Mural RJ, Sutton GG, *et al*. The sequence of the human genome. Science 2001, 291, 1304-1351.

[5] Labbadia J, Morimoto RI. Huntington's disease: underlying molecular mechanisms and emerging concepts. Trends in biochemical sciences 2013, 38, 378-385.

[6] Rosenecker J, Huth S, Rudolph C. Gene therapy for cystic fibrosis lung disease: current status and future perspectives. Current Opinion in Molecular Therapeutics 2006, 8, 439-445.

[7] Mulligan RC. The basic science of gene therapy. Science 1993, 260, 926-932.

[8] Szybalska EH, Szybalski W. Genetics of human cell lines, IV. DNA-mediated heritable transformation of a biochemical trait. Proceedings of the National Academy of Sciences USA 1962, 48, 2026-2034.

[9] Rosenberg SA, Aebersold P, Cornetta K, Kasid A, Morgan RA, Moen R, *et al*. Gene transfer into humans--immunotherapy of patients with advanced melanoma, using tumor-infiltrating lymphocytes modified by retroviral gene transduction. The New England Journal of Medicine 1990, 323, 570-578.

[10] Gene therapy clinical trials worldwide database provided by the journal of gene medicine, http://www.wiley.com/legacy/wileychi/genmed/clinical/July 2015

[11] Pearson S, Jia H, Kandachi K. China approves first gene therapy. Nature Biotechnology 2004, 22, 3-4.

[12] Wirth T, Parker N, Yla-Herttuala S. History of gene therapy. Gene 2013, 525, 162-169.

[13] Blaese RM, Culver KW, Miller AD, Carter CS, Fleisher T, Clerici M, *et al*. T lymphocyte-directed gene therapy for ADA- SCID: initial trial results after 4 years. Science 1995, 270, 475-480.

[14] Fire A, Xu S, Montgomery MK, Kostas SA, Driver SE, Mello CC. Potent and specific genetic interference by double-stranded RNA in Caenorhabditis elegans. Nature 1998, 391, 806-811.

[15] Elbashir SM, Harborth J, Lendeckel W, Yalcin A, Weber K, Tuschl T. Duplexes of 21-

nucleotide RNAs mediate RNA interference in cultured mammalian cells. Nature 2001, 411, 494-498.

[16] Fella C, Walker GF, Ogris M, Wagner E. Amine-reactive pyridylhydrazone-based PEG reagents for pH-reversible PEI polyplex shielding. European Journal of Pharmaceutical Sciences 2008, 34, 309-320.

[17] Laga R, Carlisle R, Tangney M, Ulbrich K, Seymour LW. Polymer coatings for delivery of nucleic acid therapeutics. Journal of Controlled Release 2012, 161, 537-553.

[18] Tseng WC, Jong CM. Improved stability of polycationic vector by dextran-grafted branched polyethylenimine. Biomacromolecules 2003, 4, 1277-1284.

[19] Maeda H. The enhanced permeability and retention (EPR) effect in tumor vasculature: the key role of tumor-selective macromolecular drug targeting. Advances in Enzyme Regulation 2001, 41, 189-207.

[20] Ogris M, Wagner E. To be targeted: is the magic bullet concept a viable option for synthetic nucleic Acid therapeutics? Human Gene Therapy 2011, 22, 799-807.

[21] Behr JP. The proton sponge: A trick to enter cells the viruses did not exploit. Chimia 1997, 51, 34-36.

[22] Midoux P, Monsigny M. Efficient gene transfer by histidylated polylysine/pDNA complexes. Bioconjugate Chemistry 1999, 10, 406-411.

[23] Lächelt U, Kos P, Mickler FM, Herrmann A, Salcher EE, Rödl W, *et al*. Fine-tuning of proton sponges by precise diaminoethanes and histidines in pDNA polyplexes. Nanomedicine: Nanotechnology, Biology and Medicine 2014, 10, 35-44.

[24] Pack DW, Putnam D, Langer R. Design of imidazole-containing endosomolytic biopolymers for gene delivery. Biotechnology and Bioengineering 2000, 67, 217-223.

[25] Zorko M, Langel Ü. Cell-penetrating peptides: mechanism and kinetics of cargo delivery. Advanced Drug Delivery Reviews 2005, 57, 529-545.

[26] Fawell S, Seery J, Daikh Y, Moore C, Chen LL, Pepinsky B, *et al*. Tat-mediated delivery of heterologous proteins into cells. Proceedings of the National Academy of Sciences USA 1994, 91, 664-668.

[27] Boeckle S, Fahrmeir J, Roedl W, Ogris M, Wagner E. Melittin analogs with high lytic activity at endosomal pH enhance transfection with purified targeted PEI polyplexes. Journal of Controlled Release 2006, 112, 240-248.

[28] Chen CP, Kim JS, Steenblock E, Liu D, Rice KG. Gene transfer with poly-melittin peptides. Bioconjugate Chemistry 2006, 17, 1057-1062.

[29] Plank C, Oberhauser B, Mechtler K, Koch C, Wagner E. The influence of endosome-disruptive peptides on gene transfer using synthetic virus-like gene transfer systems. The Journal of Biological Chemistry 1994, 269, 12918-12924.

[30] Wagner E, Plank C, Zatloukal K, Cotten M, Birnstiel ML. Influenza virus hemagglutinin HA-2 N-terminal fusogenic peptides augment gene transfer by transferrin-polylysine-DNA complexes: toward a synthetic virus-like gene-transfer vehicle. Proceedings of the

National Academy of Sciences USA 1992, 89, 7934-7938.

[31] Wyman TB, Nicol F, Zelphati O, Scaria PV, Plank C, Szoka FC, Jr. Design, synthesis, and characterization of a cationic peptide that binds to nucleic acids and permeabilizes bilayers. Biochemistry 1997, 36, 3008-3017.

[32] Ezzat K, Andaloussi SE, Zaghloul EM, Lehto T, Lindberg S, Moreno PM, *et al*. PepFect 14, a novel cell-penetrating peptide for oligonucleotide delivery in solution and as solid formulation. Nucleic Acids Research 2011, 39, 5284-5298.

[33] Andaloussi SE, Lehto T, Mager I, Rosenthal-Aizman K, Oprea, II, Simonson OE, *et al*. Design of a peptide-based vector, PepFect6, for efficient delivery of siRNA in cell culture and systemically *in vivo*. Nucleic Acids Research 2011, 39, 3972-3987.

[34] Brunner S, Sauer T, Carotta S, Cotten M, Saltik M, Wagner E. Cell cycle dependence of gene transfer by lipoplex, polyplex and recombinant adenovirus. Gene Therapy 2000, 7, 401-407.

[35] Sebestyen MG, Ludtke JJ, Bassik MC, Zhang G, Budker V, Lukhtanov EA, *et al*. DNA vector chemistry: the covalent attachment of signal peptides to plasmid DNA. Nature Biotechnology 1998, 16, 80-85.

[36] Zanta MA, Belguise VP, Behr JP. Gene delivery: A single nuclear localization signal peptide is sufficient to carry DNA to the cell nucleus. Proceedings of the National Academy of Sciences USA 1999, 96, 91-96.

[37] van der Aa MA, Koning GA, d'Oliveira C, Oosting RS, Wilschut KJ, Hennink WE, *et al*. An NLS peptide covalently linked to linear DNA does not enhance transfection efficiency of cationic polymer based gene delivery systems. The Journal of Gene Medicine. 2005, 7, 208-217.

[38] Remaut K, Symens N, Lucas B, Demeester J, De Smedt SC. Cell division responsive peptides for optimized plasmid DNA delivery: the mitotic window of opportunity? Journal of Controlled Release 2014, 179, 1-9.

[39] Park TG, Jeong JH, Kim SW. Current status of polymeric gene delivery systems. Advanced Drug Delivery Review 2006, 58, 467-486.

[40] Grandinetti G, Smith AE, Reineke TM. Membrane and nuclear permeabilization by polymeric pDNA vehicles: efficient method for gene delivery or mechanism of cytotoxicity? Molecular Pharmaceutics 2012, 9, 523-538.

[41] Bauhuber S, Hozsa C, Breunig M, Göpferich A. Delivery of nucleic acids via disulfide-based carrier systems. Advanced Materials 2009, 21, 3286-3306.

[42] Klein PM, Wagner E. Bioreducible Polycations as Shuttles for Therapeutic Nucleic Acid and Protein Transfection. Antioxidants & redox signaling. 2013, 21, 804-817.

[43] Akinc A, Thomas M, Klibanov AM, Langer R. Exploring polyethylenimine-mediated DNA transfection and the proton sponge hypothesis. The Journal of Gene Medicine 2005, 7, 657-663.

[44] Ahn CH, Chae SY, Bae YH, Kim SW. Biodegradable poly(ethylenimine) for plasmid DNA delivery. Journal of Controlled Release 2002, 80, 273-282.

[45] Forrest ML, Koerber JT, Pack DW. A degradable polyethylenimine derivative with low toxicity for highly efficient gene delivery. Bioconjugate Chemistry 2003, 14, 934-940.

[46] Kloeckner J, Bruzzano S, Ogris M, Wagner E. Gene carriers based on hexanediol diacrylate linked oligoethylenimine: effect of chemical structure of polymer on biological properties. Bioconjugate Chemistry 2006, 17, 1339-1345.

[47] Troiber C, Wagner E. Nucleic acid carriers based on precise polymer conjugates. Bioconjugate Chemistry 2011, 22, 1737-1752.

[48] Boyer C, Bulmus V, Davis TP, Ladmiral V, Liu J, Perrier S. Bioapplications of RAFT polymerization. Chemical Reviews 2009, 109, 5402-5436.

[49] Lutz J-F, Ouchi M, Liu DR, Sawamoto M. Sequence-Controlled Polymers. Science 2013, 341, 1238149.

[50] Wei H, Pahang JA, Pun SH. Optimization of brush-like cationic copolymers for nonviral gene felivery. Biomacromolecules 2013, 14, 275-284.

[51] Tomalia DA, Baker H, Dewald J, Hall M, Kallos G, Martin S, *et al*. A new class of polymers: starburst-dendritic macromolecules. Polymer Journal 1985, 17, 117-132.

[52] Hartmann L, Krause E, Antonietti M, Borner HG. Solid-phase supported polymer synthesis of sequence-defined, multifunctional poly(amidoamines). Biomacromolecules 2006, 7, 1239-1244.

[53] Buhleier E, Wehner W, Voegtle F. Cascade-chain-like and nonskid-chain-like syntheses of molecular cavity topologies. Synthesis 1978, 155-158.

[54] Lee CC, MacKay JA, Frechet JM, Szoka FC. Designing dendrimers for biological applications. Nature Biotechnology 2005, 23, 1517-1526.

[55] Sonawane ND, Szoka FC, Jr., Verkman AS. Chloride accumulation and swelling in endosomes enhances DNA transfer by polyamine-DNA polyplexes. The Jounal of Biology Chemistry 2003, 278, 44826-44831.

[56] Kukowska-Latallo JF, Bielinska AU, Johnson J, Spindler R, Tomalia DA, Baker JR, Jr. Efficient transfer of genetic material into mammalian cells using Starburst polyamidoamine dendrimers. Proceedings of the National Academy of Sciences USA 1996, 93, 4897-4902.

[57] Hänsler J, Szoka FC, Jr. Polyamidoamine cascade polymers mediate efficient transfection of cells in culture. Bioconjugate Chemistry 1993, 4, 372-379.

[58] Fant K, Esbjörner EK, Jenkins A, Grossel MC, Lincoln P, Nordén B. Effects of PEGylation and acetylation of PAMAM dendrimers on DNA binding, cytotoxicity and *in vitro* transfection efficiency. Molecular Pharmaceutics 2010, 7, 1734-1746.

[59] Nam HY, Nam K, Hahn HJ, Kim BH, Lim HJ, Kim HJ, *et al*. Biodegradable PAMAM ester for enhanced transfection efficiency with low cytotoxicity. Biomaterials 2009, 30, 665-673.

[60] Yu GS, Bae YM, Choi H, Kong B, Choi IS, Choi JS. Synthesis of PAMAM dendrimer derivatives with enhanced buffering capacity and remarkable gene transfection efficiency.

Bioconjugate Chemistry 2011, 22, 1046-1055.

[61] Kono K, Akiyama H, Takahashi T, Takagishi T, Harada A. Transfection activity of polyamidoamine dendrimers having hydrophobic amino acid residues in the periphery. Bioconjugate Chemistry 2004, 16, 208-214.

[62] Santos JL, Oliveira H, Pandita D, Rodrigues J, Pêgo AP, Granja PL, *et al*. Functionalization of poly(amidoamine) dendrimers with hydrophobic chains for improved gene delivery in mesenchymal stem cells. Journal of Controlled Release 2010, 144, 55-64.

[63] Wang M, Liu H, Li L, Cheng Y. A fluorinated dendrimer achieves excellent gene transfection efficacy at extremely low nitrogen to phosphorus ratios. Nature Communication 2014, 5, 3053.

[64] Zhang Q, Li F, Zhuo R-X, Zhang X-Z, Cheng S-X. Self-assembled complexes with dual-targeting properties for gene delivery. Journal of Materials Chemistry 2011, 21, 4636-4643.

[65] Huang RQ, Qu YH, Ke WL, Zhu JH, Pei YY, Jiang C. Efficient gene delivery targeted to the brain using a transferrin-conjugated polyethyleneglycol-modified polyamidoamine dendrimer. The FASEB Journal 2007, 21, 1117-1125.

[66] Kang C, Yuan X, Li F, Pu P, Yu S, Shen C, *et al*. Evaluation of folate-PAMAM for the delivery of antisense oligonucleotides to rat C6 glioma cells *in vitro* and *in vivo*. Journal of Biomedical Materials Research Part A 2010, 93A, 585-594.

[67] Arima H, Yamashita S, Mori Y, Hayashi Y, Motoyama K, Hattori K, *et al*. *In vitro* and *in vivo* gene delivery mediated by lactosylated dendrimer/α-cyclodextrin conjugates (G2) into hepatocytes. Journal of Controlled Release 2010, 146, 106-117.

[68] Ke W, Shao K, Huang R, Han L, Liu Y, Li J, *et al*. Gene delivery targeted to the brain using an Angiopep-conjugated polyethyleneglycol-modified polyamidoamine dendrimer. Biomaterials 2009, 30, 6976-6985.

[69] Lesniak WG, Kariapper MST, Nair BM, Tan W, Hutson A, Balogh LP, *et al*. Synthesis and characterization of PAMAM dendrimer-based multifunctional nanodevices for targeting $\alpha_v\beta_3$ integrins. Bioconjugate Chemistry 2007, 18, 1148-1154.

[70] Kabanov VA, Zezin AB, Rogacheva VB, Gulyaeva ZG, Zansochova MF, Joosten JGH, *et al*. Interaction of Astramol Poly(propyleneimine) Dendrimers with Linear Polyanions. Macromolecules 1999, 32, 1904-1909.

[71] Kim TI, Baek JU, Zhe BC, Park JS. Arginine-conjugated polypropylenimine dendrimer as a non-toxic and efficient gene delivery carrier. Biomaterials 2007, 28, 2061-2067.

[72] Kim KS, Lei Y, Stolz DB, Liu D. Bifunctional compounds for targeted hepatic gene delivery. Gene Therapy 2007, 14, 704-708.

[73] Koppu S, Oh YJ, Edrada-Ebel R, Blatchford DR, Tetley L, Tate RJ, *et al*. Tumor regression after systemic administration of a novel tumor-targeted gene delivery system carrying a therapeutic plasmid DNA. Journal of Controlled Release 2010, 143, 215-221.

[74] Russ V, Gunther M, Halama A, Ogris M, Wagner E. Oligoethylenimine-grafted

polypropylenimine dendrimers as degradable and biocompatible synthetic vectors for gene delivery. Journal of Controlled Release 2008, 132, 131-140.

[75] Denkewalter RG, Kolc J, Lukasavage WJ. US Patent 4289872. 1981.

[76] Okuda T, Sugiyama A, Niidome T, Aoyagi H. Characters of dendritic poly(L-lysine) analogues with the terminal lysines replaced with arginines and histidines as gene carriers *in vitro*. Biomaterials 2004, 25, 537-544.

[77] Luo K, Li C, Li L, She W, Wang G, Gu Z. Arginine functionalized peptide dendrimers as potential gene delivery vehicles. Biomaterials 2012, 33, 4917-4927.

[78] Kuang Y, An S, Guo Y, Huang S, Shao K, Liu Y, *et al*. T7 peptide-functionalized nanoparticles utilizing RNA interference for glioma dual targeting. International Journal of Pharmaceutics 2013, 454, 11-20.

[79] Liu Y, Li J, Shao K, Huang R, Ye L, Lou J, *et al*. A leptin derived 30-amino-acid peptide modified pegylated poly-l-lysine dendrigraft for brain targeted gene delivery. Biomaterials 2010, 31, 5246-5257.

[80] Liu Y, He X, Kuang Y, An S, Wang C, Guo Y, *et al*. A bacteria deriving peptide modified dendrigraft poly-l-lysines (DGL) self-assembling nanoplatform for targeted gene delivery. Molecular Pharmaceutics 2014, 11, 3330-3341.

[81] Plank C, Tang MX, Wolfe AR, Szoka FC, Jr. Branched cationic peptides for gene delivery: role of type and number of cationic residues in formation and *in vitro* activity of DNA polyplexes. Humam Gene Therapy 1999, 10, 319-332.

[82] Wadhwa MS, Collard WT, Adami RC, McKenzie DL, Rice KG. Peptide-mediated gene delivery: influence of peptide structure on gene expression. Bioconjugate Chemistry 1997, 8, 81-88.

[83] Adami RC, Collard WT, Gupta SA, Kwok KY, Bonadio J, Rice KG. Stability of peptide-condensed plasmid DNA formulations. Journal of Pharmaceutical Sciences 1998, 87, 678-683.

[84] Wadhwa MS, Knoell DL, Young AP, Rice KG. Targeted gene delivery with a low molecular weight glycopeptide carrier. Bioconjugate Chemistry 1995, 6, 283-291.

[85] Konstan MW, Davis PB, Wagener JS, Hilliard KA, Stern RC, Milgram LJH, *et al*. Compacted DNA nanoparticles administered to the nasal mucosa of cystic fibrosis subjects are safe and demonstrate partial to complete cystic fibrosis transmembrane regulator reconstitution. Human Gene Therapy 2004, 15, 1255-1269.

[86] McKenzie DL, Collard WT, Rice KG. Comparative gene transfer efficiency of low molecular weight polylysine DNA-condensing peptides. The Journal of Peptide Research 1999, 54, 311-318.

[87] McKenzie DL, Smiley E, Kwok KY, Rice KG. Low molecular weight disulfide cross-linking peptides as nonviral gene delivery carriers. Bioconjugate Chemistry 2000, 11, 901-909.

[88] Read ML, Bremner KH, Oupicky D, Green NK, Searle PF, Seymour LW. Vectors based on reducible polycations facilitate intracellular release of nucleic acids. The journal

of Gene Medicine 2003, 5, 232-245.

[89] Read ML, Singh S, Ahmed Z, Stevenson M, Briggs SS, Oupicky D, *et al*. A versatile reducible polycation-based system for efficient delivery of a broad range of nucleic acids. Nucleic Acids Research 2005, 33, e86.

[90] Chen QR, Zhang L, Stass SA, Mixson AJ. Branched co-polymers of histidine and lysine are efficient carriers of plasmids. Nucleic Acids Research 2001, 29, 1334-1340.

[91] Leng Q, Scaria P, Zhu J, Ambulos N, Campbell P, Mixson AJ. Highly branched HK peptides are effective carriers of siRNA. The journal of Gene Medicine 2005, 7, 977-986.

[92] Wang XL, Jensen R, Lu ZR. A novel environment-sensitive biodegradable polydisulfide with protonatable pendants for nucleic acid delivery. Journal of Controlled Release 2007, 120, 250-258.

[93] Hartmann L, Häfele S, Peschka-Süss R, Antonietti M, Börner HG. Sequence positioning of disulfide linkages to program the degradation of monodisperse poly(amidoamines). Macromolecules 2007, 40, 7771-7776.

[94] Hartmann L, Hafele S, Peschka-Suss R, Antonietti M, Borner HG. Tailor-made poly(amidoamine)s for controlled complexation and condensation of DNA. Chemistry - A European Journal 2008, 14, 2025-2033.

[95] Hartmann L, Börner HG. Precision polymers: monodisperse, monomer-sequence-defined segments to target future demands of polymers in medicine. Advanced Materials 2009, 21, 3425-3431.

[96] Hartmann L. Polymers for control freaks: sequence-defined poly(amidoamine)s and their biomedical applications. Macromolecular Chemistry and Physics, 2011, 212, 8-13.

[97] Mosca S, Wojcik F, Hartmann L. Precise positioning of chiral building blocks in monodisperse, sequence-defined polyamides. Macromolecular Rapid Communications 2011, 32, 197-202.

[98] Wojcik F, Mosca S, Hartmann L. Solid-phase synthesis of asymmetrically branched sequence-defined poly/oligo(amidoamines). Journal of Organic Chemistry 2012, 77, 4226-4234.

[99] Schaffert D, Badgujar N, Wagner E. Novel Fmoc-polyamino acids for solid-phase synthesis of defined polyamidoamines. Organic Letters 2011, 13, 1586-1589.

[100] Salcher EE, Kos P, Frohlich T, Badgujar N, Scheible M, Wagner E. Sequence-defined four-arm oligo(ethanamino)amides for pDNA and siRNA delivery: impact of building blocks on efficacy. Journal of Controlled Release 2012, 164, 380-386.

[101] Schaffert D, Troiber C, Salcher EE, Frohlich T, Martin I, Badgujar N, *et al*. Solid-phase synthesis of sequence-defined T-, i-, and U-shape polymers for pDNA and siRNA delivery. Angewandte Chemie International Edition 2011, 50, 8986-8989.

[102] Fröhlich T, Edinger D, Kläger R, Troiber C, Salcher E, Badgujar N, *et al*. Structure-activity relationships of siRNA carriers based on sequence-defined oligo (ethane amino) amides. Journal of Controlled Release, 2012, 160, 532-541.

[103] Scholz C, Kos P, Wagner E. Comb-like oligoaminoethane carriers: change in topology improves pDNA delivery. Bioconjugate Chemistry 2014, 25, 251-261.

[104] Schaffert D, Troiber C, Wagner E. New sequence-defined polyaminoamides with tailored endosomolytic properties for plasmid DNA delivery. Bioconjugate Chemistry 2012, 23, 1157-1165.

[105] Troiber C, Edinger D, Kos P, Schreiner L, Klager R, Herrmann A, *et al*. Stabilizing effect of tyrosine trimers on pDNA and siRNA polyplexes. Biomaterials, 2013, 34, 1624-1633.

[106] Klein PM, Müller K, Gutmann C, Kos P, Krhac Levacic A, Edinger D, *et al*. Twin disulfides as opportunity for improving stability and transfection efficiency of oligoaminoethane polyplexes. Journal of Controlled Release 2015, 205, 109-119.

[107] Martin I, Dohmen C, Mas-Moruno C, Troiber C, Kos P, Schaffert D, *et al*. Solid-phase-assisted synthesis of targeting peptide-PEG-oligo(ethane amino)amides for receptor-mediated gene delivery. Organic & Biomolecular Chemistry 2012, 10, 3258-3268.

[108] Zhang CY, Kos P, Muller K, Schrimpf W, Troiber C, Lachelt U, *et al*. Native chemical ligation for conversion of sequence-defined oligomers into targeted pDNA and siRNA carriers. Journal of Controlled Release 2014, 180, 42-50.

[109] Kos P, Lächelt U, Herrmann A, Mickler FM, Doblinger M, He D, *et al*. Histidine-rich stabilized polyplexes for cMet-directed tumor-targeted gene transfer. Nanoscale 2015, 7, 5350-5362.

[110] Kos P, Lächelt U, He D, Nie Y, Gu Z, Wagner E. Dual-targeted polyplexes based on sequence-defined peptide–PEG–oligoamino amides. Journal of Pharmaceutical Sciences 2015, 104, 464-475.

[111] An S, He D, Wagner E, Jiang C. Peptide-like polymers exerting effective glioma-targeted siRNA delivery and release for therapeutic application. Small 2015, 11, 5142-5150.

[112] Zhang W, Rödl W, He D, Döblinger M, Lächelt U, Wagner E. Combination of sequence-defined oligoaminoamides with transferrin-polycation conjugates for receptor-targeted gene delivery. The Journal of Gene Medicine 2015, 17, 161-172.

[113] Dohmen C, Edinger D, Frohlich T, Schreiner L, Lächelt U, Troiber C, *et al*. Nanosized multifunctional polyplexes for receptor-mediated siRNA delivery. ACS Nano 2012, 6, 5198-5208.

[114] Kaiser E, Colescott RL, Bossinger CD, Cook PI. Color test for detection of free terminal amino groups in the solid-phase synthesis of peptides. Analytical Biochemistry 1970, 34, 595-598.

[115] Mintzer MA, Simanek EE. Nonviral vectors for gene delivery. Chemical Reviews 2009, 109, 259-302.

[116] Zhang Y, Satterlee A, Huang L. *In vivo* gene delivery by nonviral vectors:

overcoming hurdles? Molecular Therapy 2012, 20, 1298-1304.

[117] Wagner E. Strategies to improve DNA polyplexes for *in vivo* gene transfer: will "artificial viruses" be the answer? Pharmaceutical Research 2004, 21, 8-14.

[118] Sakurai Y, Hatakeyama H, Sato Y, Hyodo M, Akita H, Harashima H. Gene silencing via RNAi and siRNA quantification in tumor tissue using MEND, a liposomal siRNA delivery system. Molecular Therapy 2013, 21, 1195-1203.

[119] De Smedt SC, Demeester J, Hennink WE. Cationic polymer based gene delivery systems. Pharmaceutical Research 2000, 17, 113-126.

[120] Pack DW, Hoffman AS, Pun S, Stayton PS. Design and development of polymers for gene delivery. Nature Reviews Drug Discovery 2005, 4, 581-593.

[121] Son S, Namgung R, Kim J, Singha K, Kim WJ. Bioreducible polymers for gene silencing and delivery. Accounts of Chemical Research 2012, 45, 1100-1112.

[122] Lächelt U, Wagner E. Nucleic acid therapeutics using polyplexes: a journey of 50 years (and beyond). Chemical Reviews 2015, 115, 11043-11078.

[123] Miyata K, Nishiyama N, Kataoka K. Rational design of smart supramolecular assemblies for gene delivery: chemical challenges in the creation of artificial viruses. Chemical Society Reviews 2012, 41, 2562-2574.

[124] Wagner E. Polymers for siRNA delivery: inspired by viruses to be targeted, dynamic, and precise. Accounts of Chemical Research 2012, 45, 1005-1013.

[125] Sun S, Wang M, Knupp SA, Soto-Feliciano Y, Hu X, Kaplan DL, *et al*. Combinatorial library of lipidoids for *in vitro* DNA delivery. Bioconjugate Chemistry 2012, 23, 135-140.

[126] He D, Wagner E. Defined polymeric materials for gene delivery. Macromolecular Bioscience 2015, 15, 600-612.

[127] Boussif O, Lezoualc'h F, Zanta MA, Mergny MD, Scherman D, Demeneix B, *et al*. A versatile vector for gene and oligonucleotide transfer into cells in culture and *in vivo*: polyethylenimine. Proceedings of the National Academy of Sciences USA 1995, 92, 7297-7301.

[128] Kichler A, Leborgne C, Coeytaux E, Danos O. Polyethylenimine-mediated gene delivery: a mechanistic study. The Journal of Gene Medicine 2001, 3, 135-144.

[129] Uchida H, Miyata K, Oba M, Ishii T, Suma T, Itaka K, *et al*. Odd-even effect of repeating aminoethylene units in the side chain of N-substituted polyaspartamides on gene transfection profiles. Journal of the American Chemical Society 2011, 133, 15524-15532.

[130] Zhang W, Rodl W, He D, Doblinger M, Lachelt U, Wagner E. Combination of sequence-defined oligoaminoamides with transferrin-polycation conjugates for receptor-targeted gene delivery. The Journal of Gene Medicine 2015, 17, 161-172.

[131] Lee DJ, Kessel E, Edinger D, He D, Klein PM, Voith von Voithenberg L, *et al*. Dual antitumoral potency of EG5 siRNA nanoplexes armed with cytotoxic bifunctional glutamyl-methotrexate targeting ligand. Biomaterials 2016, 77, 98-110.

[132] Bertrand E, Goncalves C, Billiet L, Gomez JP, Pichon C, Cheradame H, *et al*. Histidinylated linear PEI: a new efficient non-toxic polymer for gene transfer. Chemical Communications 2011, 47, 12547-12549.

[133] Leng Q, Chou ST, Scaria PV, Woodle MC, Mixson AJ. Increased tumor distribution and expression of histidine-rich plasmid polyplexes. The Journal of Gene Medicine 2014, 16, 317-328.

[134] Creusat G, Zuber G. Self-assembling polyethylenimine derivatives mediate efficient siRNA delivery in mammalian cells. Chembiochem 2008, 9, 2787-2789.

[135] Creusat G, Rinaldi AS, Weiss E, Elbaghdadi R, Remy JS, Mulherkar R, *et al*. Proton sponge trick for pH-sensitive disassembly of polyethylenimine-based siRNA delivery systems. Bioconjugate Chemistry 2010, 21, 994-1002.

[136] Yang H, Fung S-Y, Liu M. Programming the cellular uptake of physiologically stable peptide-gold nanoparticle hybrids with single amino acids. Angewandte Chemie International Edition 2011, 50, 9643-9646.

[137] Zeng H, Little HC, Tiambeng TN, Williams GA, Guan Z. Multifunctional dendronized peptide polymer platform for safe and effective siRNA delivery. Journal of the American Chemical Society 2013, 135, 4962-4965.

[138] Harris JM, Chess RB. Effect of pegylation on pharmaceuticals. Nature Reviews Drug Discovery 2003, 2, 214-221.

[139] Kursa M, Walker GF, Roessler V, Ogris M, Roedl W, Kircheis R, *et al*. Novel shielded transferrin-polyethylene glycol-polyethylenimine/DNA complexes for systemic tumor-targeted gene transfer. Bioconjugate Chemistry 2003, 14, 222-231.

[140] Walker GF, Fella C, Pelisek J, Fahrmeir J, Boeckle S, Ogris M, *et al*. Toward synthetic viruses: endosomal pH-triggered deshielding of targeted polyplexes greatly enhances gene transfer *in vitro* and *in vivo*. Molecular Therapy 2005, 11, 418-425.

[141] Neu M, Germershaus O, Behe M, Kissel T. Bioreversibly crosslinked polyplexes of PEI and high molecular weight PEG show extended circulation times *in vivo*. Journal of Controlled Release 2007, 124, 69-80.

[142] Oupicky D, Diwadkar V. Stimuli-responsive gene delivery vectors. Current opinion in molecular therapeutics 2003, 5, 345-350.

[143] Wagner E. Programmed drug delivery: nanosystems for tumor targeting. Expert Opinion on Biological Therapy 2007, 7, 587-593.

[144] Mechtler K, Wagner E. Gene transfer mediated by influenza virus peptides: the role of peptide sequence. New Journal of Chemistry 1997, 21, 105-111.

[145] Leamon CP, DePrince RB, Hendren RW. Folate-mediated drug delivery: effect of alternative conjugation chemistry. Journal of Drug Targeting 1999, 7, 157-169.

[146] Leamon CP, Low PS. Folate-mediated targeting: from diagnostics to drug and gene delivery. Drug Discovery Today 2001, 6, 44-51.

[147] Scholz C, Wagner E. Therapeutic plasmid DNA versus siRNA delivery: Common

and different tasks for synthetic carriers. Journal of Controlled Release 2012, 161, 554-565.

[148] Barz M, Canal F, Koynov K, Zentel R, Vicent MJ. Synthesis and *in vitro* evaluation of defined HPMA folate conjugates: influence of aggregation on folate receptor (FR) mediated cellular uptake. Biomacromolecules 2010, 11, 2274-2282.

[149] Dohmen C, Frohlich T, Lachelt U, Rohl I, Vornlocher H-P, Hadwiger P, *et al*. Defined folate-PEG-siRNA conjugates for receptor-specific gene silencing. Molecular Therapy-Nucleic Acids 2012, 1, e7.

[150] Cotten M, Langle-Rouault F, Kirlappos H, Wagner E, Mechtler K, Zenke M, *et al*. Transferrin-polycation-mediated introduction of DNA into human leukemic cells: stimulation by agents that affect the survival of transfected DNA or modulate transferrin receptor levels. Proceedings of the National Academy of Sciences USA 1990, 87, 4033-4037.

[151] Wagner E. Biomaterials in RNAi therapeutics: quo vadis? Biomaterials Science 2013, 1, 804-809.

[152] He D, Müller K, Krhac Levacic A, Kos P, Lächelt U, Wagner E. Combinatorial optimization of sequence-defined oligo(ethanamino)amides for folate receptor-targeted pDNA and siRNA delivery. Bioconjugate Chemistry 2016, 27, 547-559.

[153] Edinger D, Kläger R, Troiber C, Dohmen C, Wagner E. Gene silencing and antitumoral effects of Eg5 or Ran siRNA oligoaminoamide polyplexes. Drug Delivery and Translational Research 2014, 4, 84-95.

[154] Wagner E. Effects of membrane-active agents in gene delivery. Journal of Controlled Release 1998, 53, 155-158.

8 Publication

Original articles

He D, Müller K, Krhac Levacic A, Kos P, Lächelt U, Wagner E. Combinatorial optimization of sequence-defined oligo(ethanamino)amides for folate receptor-targeted pDNA and siRNA delivery. Bioconjugate Chemistry 2016, 27, 547-559. (Chapter 3.1 and 4.1)

Zhang P, **He D**, Klein P, Liu X, Röder R, Döblinger M, Wagner E. Enhanced intracellular protein transduction by sequence defined tetra-oleoyl oligoaminoamides targeted for cancer therapy. Advanced Functional Materials 2015, 25 (42), 6627–6636.

An S, **He D**, Wagner E, Jiang C. Peptide-like polymers exerting effective glioma-targeted siRNA delivery and release for therapeutic application. Small 2015, 11 (38), 5142-5150.

Liu X, Zhang P, **He D**, Rödl W, Wagner E, Lächelt U. pH-reversible cationic RNase A conjugates for enhanced cellular delivery and tumor cell killing. Biomacromolecules 2016, 17, 173-182.

Zhang W, Rödl W, **He D**, Döblinger M, Lächelt U, Wagner E. Combination of sequence-defined oligoaminoamides with transferrin-polycation conjugates for receptor-targeted gene delivery. The Journal of Gene Medicine 2015, 17 (8-9), 161-172.

Kos P, Lächelt U, **He D**, Nie Y, Gu Z, Wagner E. Dual-targeted polyplexes based on sequence-defined peptide-PEG-oligoamino amides. Journal of Pharmaceutical Sciences 2015, 104 (2), 464-475.

Lee DJ, Kessel E, Edinger D, **He D**, Klein PM, Voith von Voithenberg L, Lamb D, Lächelt U, Lehto T, Wagner E. Dual antitumoral potency of EG5 siRNA nanoplexes armed with cytotoxic bifunctional glutamyl-methotrexate targeting ligand. Biomaterials 2016, 77, 98-110.

Zhang W, Müller K, Kessel E, Reinhard S, **He D**, Klein PM, Höhn M, Rödl W, Kempter S, Wagner E. Targeted siRNA delivery using a lipo-oligoaminoamide nano-core with an influenza peptide and transferrin shell, Advanced Healthcare Materials 2016, *in press*, doi: 10.1002/adhm.201600057.

Kos P, Lächelt U, Herrmann A, Mickler FM, Doblinger M, **He D**, Krhac Levacic A, Morys S, Brauchle C, Wagner E. Histidine-rich stabilized polyplexes for cMet-directed tumor-targeted gene transfer. Nanoscale 2015, 7 (12), 5350-5362.

Review

He D, Wagner E. Defined polymeric materials for gene delivery. Macromolecular Bioscience 2015, 15 (5), 600-612. (Chapter 1)

Manuscripts in preparation

Lee DJ*, **He D***, Kessel E, Padari K, Kempter S, Lächelt U, Rädler J, Pooga M, Wagner E. Tumoral gene silencing by receptor-targeted combinatorial siRNA polyplexes, *submitted*. (*equal contribution, Chapter 3.2 and 4.2)

Meeting abstracts and poster presentations

He D, Müller K, Krhac Levacic A, Kos P, Lee DJ, Wagner E. Conquer the barriers: optimization of sequence-defined multifunctional nanocarriers for folate receptor targeted pDNA and siRNA delivery. 1st LMU-ChAN (Ludwig-Maxmilian-Universität - China Academic Network) Scientific Forum, Munich, Germany, Nov. 13-15, 2015. (Poster)

He D, Krhac Levacic A, Müller K, Kos P, Lee DJ, Wagner E. Sequence defined oligo(ethanamino)amides for folate receptor targeted pDNA or siRNA delivery: optimization and preliminary structure-activity relationship study. Walk and Talk at the Nanoscale, CeNS Workshop, Venice, Italy, Sept. 22-26, 2014. (Poster)

He D, Müller K, Kos P, Lee DJ, Lächelt U, Wagner E. Cargo-specific optimization of sequence-defined non-viral nucleic acid carriers for folate receptor targeted pDNA and siRNA delivery. XX Annual Meeting of German Society for Gene Therapy, Ulm, Germany, Mar. 20-22, 2014. (Poster)

Lee DJ, **He D**, Kessel E, Lächelt U, Wagner E. Combinatorial siRNA Polyplex for Folate

Receptor-Directed Gene Silencing Efficiency and Tumor Targeting. 14th International Congress on Targeted Anticancer Therapies, Mar 21-23, 2016, Washington DC, USA. (Poster)

Lee DJ, Kessel E, **He D**, Klein PM, Lächelt U, Lehto T, Wagner E. Synergistic Antitumoral Potency Mediated by Eg5 siRNA Nanoplexes with Bifunctional Glutamyl-MTX Targeting Ligand. 29th American Association of Pharmaceutical Scientists (AAPS) Annual Meeting, Oct 25-29, 2015, Orlando, USA. (Poster)

Kos P, Lächelt U, Herrmann A, **He D**, Wagner E. Sequence-defined nanocarriers for c-Met receptor-directed gene transfer *in vitro* and *in vivo*. 17th Annual Meeting of the American Society of Gene & Cell Therapy, Washington, USA, May 21-24, 2014. (Poster)

9 Acknowledgements

Once I thought four years was a long time, but everything turned into past just with a blink, leaving only memories and dreams drifting around the campus. After almost four years long march, I finally arrived the finish line of my PhD study, I would like to take this chance to express my sincere gratitude to all the people who supported me during the past years.

First of all, I would like to thank my supervisor Prof. Dr. Ernst Wagner for giving me the opportunity to do my PhD study in this great group. I am very grateful for his professional guidance and scientific support over all these years, and also for his valuable advice and encouragement whenever I have difficulties.

I would like to express my special gratitude to Dr. Ulrich Lächelt for introducing me into the lab work, and also for all the fruitful discussions, suggestions and continuous support and care for my PhD study. Special thanks to Katharina, Ana and Petra, who have spent a lot of time in the cell culture room and the dark FACS room for testing my oligomers. Without your excellent work and support, this thesis will never reach the goal. And many thanks to Petra for showing me the basic technics in cell culture and also help with my first transfection. Especially, I would like to thank Dian-Jang Lee who have been working closely with me for the combinatorial project, and also *in vivo* experiments with Eva. I would also like to thank all “delivery” group members for all the helpful discussions, suggestions and collaborations, and my bachelor student Natalie for helping me with some experiments. I am grateful to Dr. Martina Rüffer for the Christmas party, excursions, the traditional ‘Weißwurst‘ and St. Nicholas’ chocolate, and Andi for the ski trip which was my first ski “experiments”. Many thanks to Wolfgang for solving all the technical problems and always helpful for handling the equipment, as well as Miriam, Ursula, Anna, Olga, Markus and Melinda for keeping the lab running. Thanks also to my lab-mates Philipp K., Innes, Stephan, Claudia, for all the discussions, music and funny times. I would also like to thank Adam for sharing a lot of useful information with me. I would particularly thank my Chinese colleagues, Xiaowen Liu, Peng Zhang, Wei Zhang, for all the discussions in Chinese which is easier for us, and also the numerous lunch time we spent together. In addition, thanks to all AK Wagner members for the nice atmosphere and all the interesting experience.

Particularly gratitude to the China Scholarship Council for providing me the scholarship to

study in Germany, and also the great help from the international office of LMU for adapting my life in Munich.

Furthermore, I would like to thank to all my old friends in China, especially Jian Lei, Yanrui Xie, Jirong Huang, Xi Zhu for all the great old times we spent together, and your sincere care and support sending through internet. I would also like to thank all my new friends in Germany, for all the interesting times we shared in this country, especially my CSC fellowship colleagues for the very beginning settle down in Munich, travelling partners for enjoying the beautiful, historical and also modern Europe, Heilghofstrasse chinese residents for great dinners and leisure time, and also the Sichuan/Chongqing group for our beloved delicious spicy food.

Finally, I would like to acknowledge my big family for their unconditionally love and constant support. My grandpa taught me what is integrity and responsibility, and my grandma showed me a hardworking example, both are model of me since I was a child. Particularly I want to thank my parents, for taking care of me and always being there during the past 28 years, not only the cheerful times we shared, but also the difficult times we went through together. Their silent support gives me courage and confidence to face whatever happened. Without your backup, I would never make it today.

谢谢！